METALLOMICS IN *IN VITRO* TOXICOLOGY RESEARCH

TESI DOCTORAL

Massimo FARINA

Any 2008

FACULTAT DE BIOCIÈNCIES

DEPARTAMENT DE GENÈTICA
I DE MICROBIOLOGIA

Director: Ricard MARCOS DAUDER

Tutor: Enrico SABBIONI

Autor: Massimo FARINA

BELLATERRA, Octubre 2008

This work has been carried out at the Joint Research Centre (JRC), via E. Fermi, 2749, Ispra, Varese, Italy. European Commission, Institute for Health and Consumer Protection (IHCP), European Centre for the Validation of Alternative Methods Unit (ECVAM), (Head of Unit Prof. Thomas Hartung).

ACKNOWLEDGEMENTS

I WOULD LIKE TO THANK

Prof. Ricard Marcos for his essential support and for the help he gave me concerning the training at the Universitat Autònoma de Barcelona and Prof. Amadeu Creus for his availability during such training.

Prof. Thomas Hartung for the possibility he gave me to carry on the laboratory work.

I'm very grateful to Prof. Enrico Sabbioni for his teaching, for the fundamental and unique scientific guide and the pleasure to work with him during this period.

Stefano Bosisio, Francesca Broggi, Riccardo Del Torchio, Salvador Fortaner, Patrick Marmorato, Barbara Munaro, Jessica Ponti, Claire Thomas and Giorgio Tettamanti for the fundamental help during the work, friendship and because it is a pleasure for me to work with them every day.

Dr. Agnieszka Kinsner and Dr. Erwin Van Vliet for their help concerning the brain aggregates and isolated cells.

Last but not least:

Uno speciale ringraziamento va a Chiara e a tutta la mia famiglia per il loro affetto ed incondizionato supporto.

INDEX

INTRODUCTION

This work has been carried out in the context of a research programme of the European Centre for the Validation of Alternative Methods (ECVAM) of JRC-Ispra. The aim of ECVAM is to promote and coordinate the scientific and regulatory acceptance of alternative methods, which are of importance to the biosciences, and which reduce, refine and replace (3Rs) the use of laboratory animals in toxicity testing required by law (Hartung et al., 2004).

In particular, the research executed is a part of the ECVAM key area "omics" aiming at identifying metabolites and biomarkers of toxicity of chemicals by using *in vitro* cell cultures as models of carcinogenicity, reproductive toxicity, toxicokinetics and systemic toxicity (Hartung et al., 2003). The experimental studies here reported are referred to "metallomics" (Szpunar, 2004), a scientific area related to biometals requiring versatile measurement tools that allow for trace detection, identification and measurement of covalent bound metals in proteins or metal-protein complexes. In this context, the aim of this work is to give a mechanistic insight of: (i) cytotoxicity and carcinogenic potential induced in *in vitro* systems by different As, Cd, Cr, Pt and V chemical species which are relevant from environmental and occupational health point of view, (ii) neurotoxic effects induced by As species in brain re-aggregates and their individual cell type constituent and by Mn species in PC12 cells.

Usually, *in vitro* studies by cell cultures are mainly focussed on biochemical/toxicological aspects establishing relation between a biological response (end-point) induced by exposure to xenobiotics and dose exposure, while metabolic pathways (uptake, intracellular distribution, binding to biomolecules and speciation)

are much less considered. This is also due to the severe experimental difficulties concerning the detection and quantification of xenobiotic and its metabolites, into cells and culture medium, almost at *ng-pg* level. These analytical difficulties can be overcome only by using sophisticated and advanced analytical techniques (Sabbioni and Balls, 1995).

Furthermore, since bioavailability and toxicity of the elements depend also on their chemical form, adequate analytical methods for separation of proteins and measurement of metallo-proteins are required for speciation analysis (Suzuki, 2005).

Since major topics in metallomics research includes the study of the distribution of the elements into cells and the chemical speciation of the elements in the biological systems the availability of advanced analytical techniques is of paramount importance.

In our work, peculiar analytical techniques such as nuclear, radioanalytical and advanced spectrochemical techniques have been used in combination with biochemical techniques of protein separation for speciation analysis of different chemical forms of As, Cd, Cr, Pt and V in mouse fibroblasts Balb/3T3 cell line (*in vitro* model for testing the carcinogenic potential of chemicals); of Mn in rat pheochromocytoma cells of the adrenal gland PC12 cell line, of As in and rat brain re-aggregates (*in vitro* models of neurotoxicity).

LITERATURE SURVEY

Hereafter few bibliographic data related to the subjects of the present work are reported. They include few essential on metallomics and speciation studies; the *in vitro* models of carcinogenic potential and neurotoxicity, and the carcinogenicity of metal compounds.

Metallomics and trace element speciation

Metal ions are utilised by fundamental cellular processes. In this context, transcription, translation, proper assimilation and incorporation of the necessary metal to function are regulated by the organism. Thus, the chemistry of a cell needs to be characterized not only by its characteristic genome in the nucleus, in protein context (proteome) but also by the distribution of the metals and metalloids among the different species and cell compartments (**metallome**). Therefore, in analogy with genome and proteome, metallome can be defined as "the entirety of metal and metalloids species within a cell (or tissue) type". In this context, Haraguchi (Haraguchi, 2004) suggested the term "**metallomics**" as a new scentific field in symbiosis with genomics and proteomics, because synthesis and metabolic function of genes (DNA and RNA) and proteins cannot be performed without the aid of various metal ions and metalloenzymes. The metallomic information will comprise the identity of individual metal species and their concentrations. As such, metallomics, referred to cellular biochemistry, can be considered as a subset of speciation analysis understood as the identification and/or quantitation of elemental species (speciation of an element is defined as "distribution of an element among defined chemical species in a system") (Templeton et al., 2000).

Thus, the study of a metallome will inform us of: (i) how an element is distributed among the cellular compartments of a given cell type (ii) in which biomolecule it is incorporated or by which bioligand is complexed (iii) the concentration of the individual metal species present.

In fact, it is now accepted by the scientific community that bioavailability, metabolic pathways, toxicity, bioactivity and detoxifying processes into cells (and therefore the potential impact of toxic elements in the cell) depend on the particular chemical species considered. In this sense, a total element determination of an element in biological samples is absolutely insufficient today to assess its toxicity. In this context, there is an urgent need on additional speciation information to complement total toxic element determinations in toxicological issues. In order to provide such type of information there was an enormous interest in the last years to develop analytical strategies and methods able to tackle this modern challenge of "speciating" trace element concentrations in the different species actually present in the biological samples.

Balb/3T3 cell line

One of the most promising *in vitro* tests used to evaluate the carcinogenic potential of different organic and inorganic compounds is the Balb/3T3 clone A31-1-1 assay (Combes et al, 1999).

Balb/3T3 cells are mouse fibroblasts initially derived from mouse embryo by repeated cell passages and sub sequentially cloned to generate the line A31-1-1 that is typically used in the Cell Transformation Assay (CTA) (Kakunaga, 1973). These cells are contact inhibited and grow at high dilution showing a low saturation density, 50-60% of plating efficiency, hypotetraploydia with telocentric and

acrocentric chromosomes. They growth in monolayer showing a fibroblast-like morphology. The split period is about 16h. Even thought this cell line has some specific characteristic of a transformed cell line (such as heteroploydia, infinite life span, high cloning efficiency, altered morphology in comparison with the primary culture, lacks of anchorage-independent growth when treated with a carcinogenic compound and tumour formation when inoculated in nude mice after treatment) the spontaneous transformation frequency is low (about 10^{-5}foci/dish) (Di Paolo et al., 1980).

The Cell Transformation Assay using Balb/3T3 consists in the estimation of the concurrent cytotoxicity and morphological transformation. The duration of the test is 5 weeks.

The end point of the cytotoxicity is the formation of colony (Colony Forming Efficiency, CFE) and of the neoplastic potential is the presence of foci type III.

Concentrations to be used for the CTA are previously determined by the study of cytotoxicity (80%-50%-20% of CFE). However, there is not a direct relationship between cytotoxicity and morphological transformation. In fact, some compounds could show high cytotoxicity, but no morphological transformation (Kakunuga, 1973).

In Balb/3T3 assay three kind of foci can be induced by chemical exposure:

(i) foci type I, a very low overlapping and piling up of cells.

(ii) foci type II, colony that growth in a multilayer with ramification on the periphery.

(iii) foci type III, colony with all the following characteristics: basophilic, dense multilayered, cells random orientated at focus edge, invasion into the monolayer, cells spindle-shaped.

Only foci type III are considered tumorogenic because it is demonstrated that only they induce neoplastic transformation in nude mice with a frequency of 85% (Saffiotti et al., 1984; IARC/INCI/EPA, 1985).

PC12 cell line

The PC12 clonal cell line was developed from rat pheochromocytoma cells of the adrenal gland (Greene and Tischler, 1976). Clonal cell lines which express neuronal properties are useful model system for studying the neurons systems at the single cell and molecular level (Greene and Tischler, 1976). PC12 cells stimulated by nerve growth factor (NGF) and reduced serum content in the medium differentiate to acquire properties similar to mature sympathetic neurons (Teng et al., 1998). Differentiated PC12 cells are useful for neurotoxicity testing as they have a number of neuronal characteristics, e.g. electrical excitability, polypeptide expression and neurotransmitter receptors (Greene, 1995). The neurotransmitters secreted PC12 cells are dopamine, noradrenaline and Ach (Greene and Tischler, 1976; Leist et al., 1995). By monitoring dopamine metabolism in rat phaeochromocytoma derived PC12 cell cultures during extened treatment with manganese chloride, functional changes occurring in a dopaminergic system during the development of manganese induced damage (Vescovi et al., 1991). The literature describes dopamine alterations in relation with manganese (Stredrick et al., 2004). In PC12 cells, manganese induces complete disappearance of extracellular (free) but not intracellular (vesicles stored) dopamine and its metabolites (Vescovi et al., 1991).

Re-aggregating brain cell cultures

Aggregating brain cells cultures (model for *in vitro* neurotoxcity) are primary, three dimensional cell cultures. The re-aggregated cells are able to migrate within the former structures, and to interact with each other by direct cell-cell contact, as well as through exchange of nutritional and signaling factors. This tissue-specific environment enables aggregating neural cells to differentiate, and to develop specialized structures (e.g. synapses, myelinated axons) resembling those of brain tissue in situ. Aggregating cell cultures are therefore classified as organotypic cultures.

The complexity of *in vitro* neurotoxicity models inversely correlates with the ease of obtaining and maintaining cells and tissues in cultures.

Primary rat-derived neuronal cell cultures, astrocyte primary cultures and oligidendrocytes cultures are the most widely used and extensively characterised, for this mixed primary cultures have been used by a number of investigators for studying receptor-mediated mechanisms.

Some models, such as re-aggregating brain cell cultures from different species, are reported to cover the effects of different cell types and different maturation stages (Honneger and Monnet-Tschudi, 2001). In three-dimensional models, including aggregate cell and brain tissue slice cultures, the interaction of neurons and glia in affecting some types of neurotoxicity end-points are shown for a variety of compounds (Eskes et al., 2002). A benefit of using re-aggregate cultures is that the nervous system cytoarchitecture circuitry and other biochemical processes (e.g. myelination, synaptogenesis) are preserved (Honeger and Matthieu, 1985). Furthermore, the system can be used to detect both acute, chronic and delayed neurotoxic effects in either mature or immature state of the cells (Zurich et al., 2002).

This system can also detect both microglia and astroglial activation which are early markers of neurotoxicity (Monnet-Tschudi et al., 1997). Since primary derived material is currently used, new approaches employing human stem cell derived neuronal and glial cells might overcome this issue in the future

Carcinogenicity of metal compounds

Human exposure to metals is common, with wide use in industry and long-term environmental persistence. Historically, the heaviest metal exposures occurred in the workplace or in environmental settings in close proximity to industrial sources. Among the general population, exposure to a number of metals is widespread but generally at substantially lower levels than have been found in industry.

The existence of relationship between cancer and metals is widely aknowledge by oncologists.

Different agencies, utilising both epidemiological and experimental animal data, classify a compound as carcinogenic if there is an evidence of its potential in humans (International Agency for Research on Cancer, IARC) or place different emphases on the results of animal and genotoxicity studies (U.S. environmental Protection Agency, EPA; Chemical Manufactures Association; European Community). Thus, for assessing human risk from exposure to a compound, several factors are considered to provide a concern in regard to a potential for the induction of human cancer from exposure. Many of these factors are based on the pharmacokinetic and pathological response similarities between humans and the surrogate test species.

Table A summarises the IARC classification of metal compounds according to evidence of carcinogenic effects IARC (IARC, 1990).

Table A. IARC classification of metal compounds

Compound	IARC classification	
	Group	**Evidence**
Aluminium[a]	1. Carcinogenic	Sufficient[b] in human
Arsenic[a]		
Beryllium[a]		
Cadmium[a]		
Chromium[a]		
Iron[a]		
Nickel[a]		
Cisplatinum	2A. Probably carcinogenic	Limited[c] in human, sufficient in animal
Antymony trioxide	2B. Possible carcinogenic	Limited in human
Cobalt[a]		
Lead[a]		Inadequate[d] in human
Methylmercury		
Metallic nickel		Sufficient in human
Manganese[a]	3. Not carcinogenic	-
Antimony trisulfoxide		
Organolead[a]		
Metallic mercury		
Inorganic mercury[a]		
Selenium[a]		
Titanium dioxide		
-	4. Probably not carcinogenic	Inadequate in human and in animal

a: element and its compounds
b: there is a causal relationship between the agent or agents and human cancer
c: there is a credible causal interpretation, but alternative explanations such as chance, bias and confounding variables could not completely be excluded
d: one or three conditions prevailed:

- there are few pertinent data
- the available studies, while showing evidence of association, don't exclude change, bias or confounding variables
- studies are available, but they don't show evidence of carcinogenicity.

Among the metal compounds considered in our work, only V is not included in the IARC list. Moreover, Pt in the list concerns only cis-Pt.

For comprehensive reviews on health, toxic and carcinogenic effects of the metals considered in the present work see: WHO-224, 2001 and Styblo et al., 2002 (As), O'Brien et al., 2004 (Cr), Ravindra et al., 2004 (Pt) and WHO-29, 2001 (V).

Neurotoxicity of metal compounds

Metals are inextricably bound to many aspects of modern life. While some are biologically essentials (e.g. Cu,Se,Zn), others are not and are considered toxic (e.g. Cd, Hg and Pb). Among toxic metals, several have a primary target action on the nervous system. These groups of metals are referred as neurotoxic metals. The most noticeable neurotoxic metals are Al, As, Cd, Hg, Mn and Pb together with organometals such as methylmercury, alkyl leads, trimethyltin and triethyltin which are known as potent neurotoxicants. The damage by most neurotoxic metals is unlikely to be solely ascribed to generation of excessive reactive oxygen species (ROS).The toxicity of each metal is distinctive and involves a characteristic range of morphological and biochemical abnormalities. Catalysis of generation of ROS may represent a final common path induced by metal-containing chemicals. Table B groups metals by classes believed to involve mechanisms underlying their prooxidant potential.

Table B. Neurotoxic metals according their potential for inducing oxidative events

Different oxidation state	Sulfhydryl affinity	Excitation by mimicking calcium	Unknown
Cu	As	Pb	Al
Fe	Cd	Sn	
Mn	Hg		
V	Tl		

In our work attention has been paid to manganese. There is increasing evidence for the role of oxidative stress in Parkinson Disease. In this context, catecholaminergic pathways seem particularly susceptible to metal-catalysed oxidative damage. This is especially true of dopamine auto-oxidation, and such a mechanism may be related to “manganism” (Donaldson et al, 1991).Injury to the catecholamine neurons seems

caused by the free radicals and quinones formed as a result of Mn-catalysed auto-oxidatio of dopamine. (Stredrick et al, 2004).

Manganese is transition metal that can exist in different oxidation states, the most common in biological systems being +2 and +3, +4. Therefore, metallomics is of particular interest in the study of metabolic patterns and toxicity of this element in biological systems.

OBJECTIVES

An emerging area of bioinorganic analysis of the distribution of metals and metalloids among different species concern metallomics and cell compartments, metallome.

The objectives of this study are linked to metallomics. In particular, the experimental work of this thesis are:

- to complete previous investigations related to the setting of a database of the carcinogenic potential of metal compounds in mouse fibroblasts Balb/3T3 cell line. In particular, the metallomics study here carried out represents the 4^{th} step of a research that involves: the determination of basal cytotoxicity at fixed-dose exposure; the setting of dose-effect relationship in order to establish the IC_{50} values and suitable ranges of exposure dose to be used in the final morphological transformation assay; the identification of metal compounds inducing neoplastic morphological transformation (Mazzotti, 2001).

- to start a research on metabolic pathways and biotransformation of inorganic As(III) and Mn(II) and Mn(VII) in whole rat brain re-aggregates, individual cell type constituents of such aggregates (microglia, neurons and astrocytes) or rat pheochromocytoma cells of the adrenal gland PC12.

Figures A, B and C outline the experiments carried out and the objectives of the present experimental work.

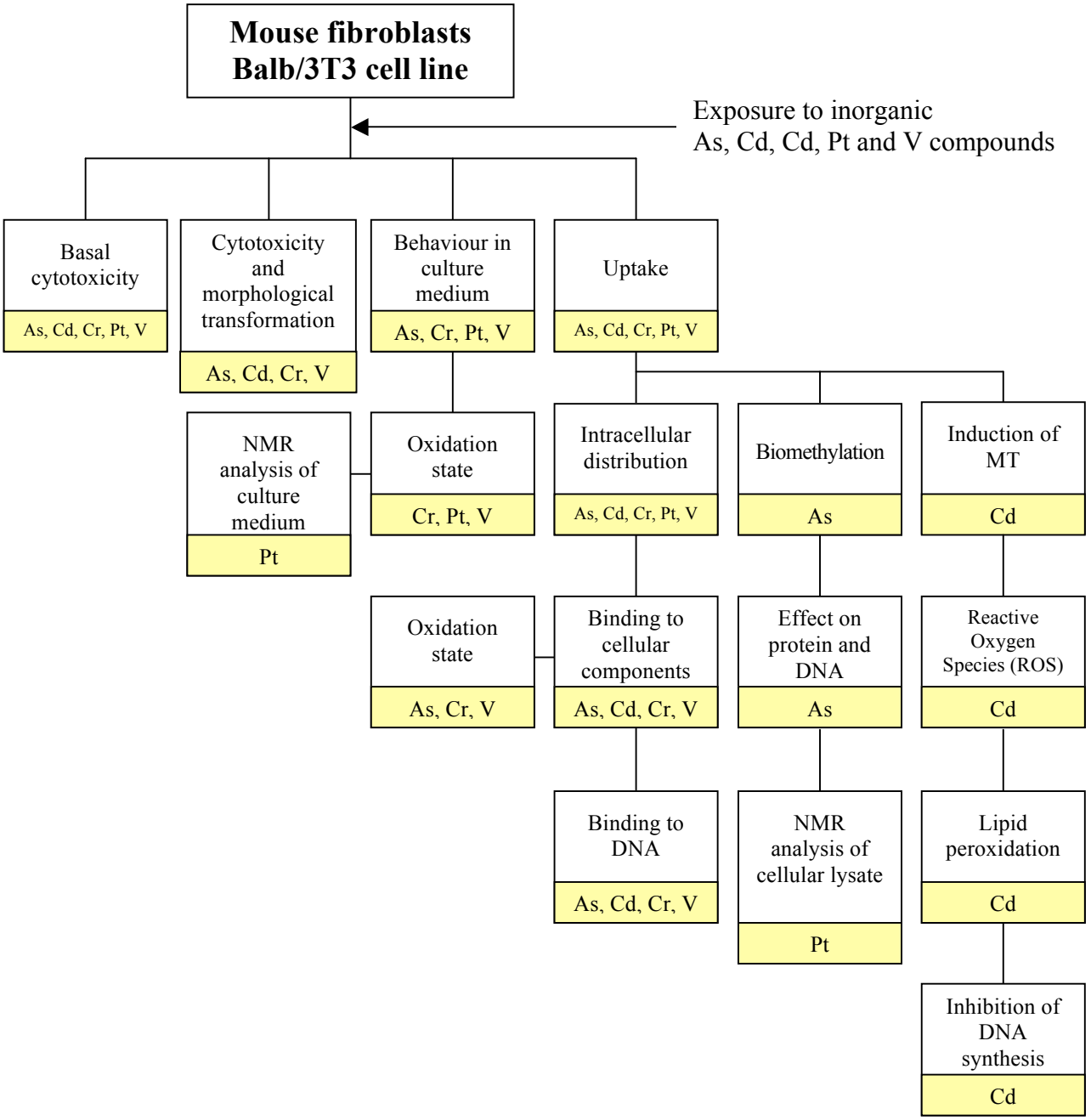

Figure A. Objectives of the present research on Balb/3T3 cell line.

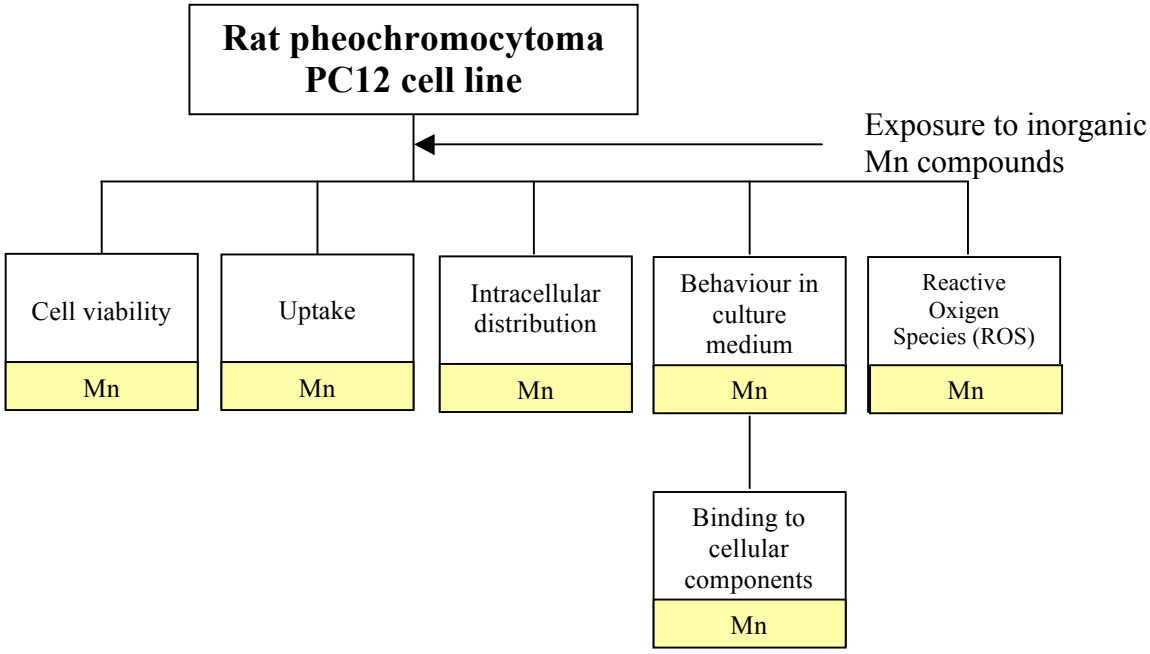

Figure B. Objectives of the present research on PC12 cell line.

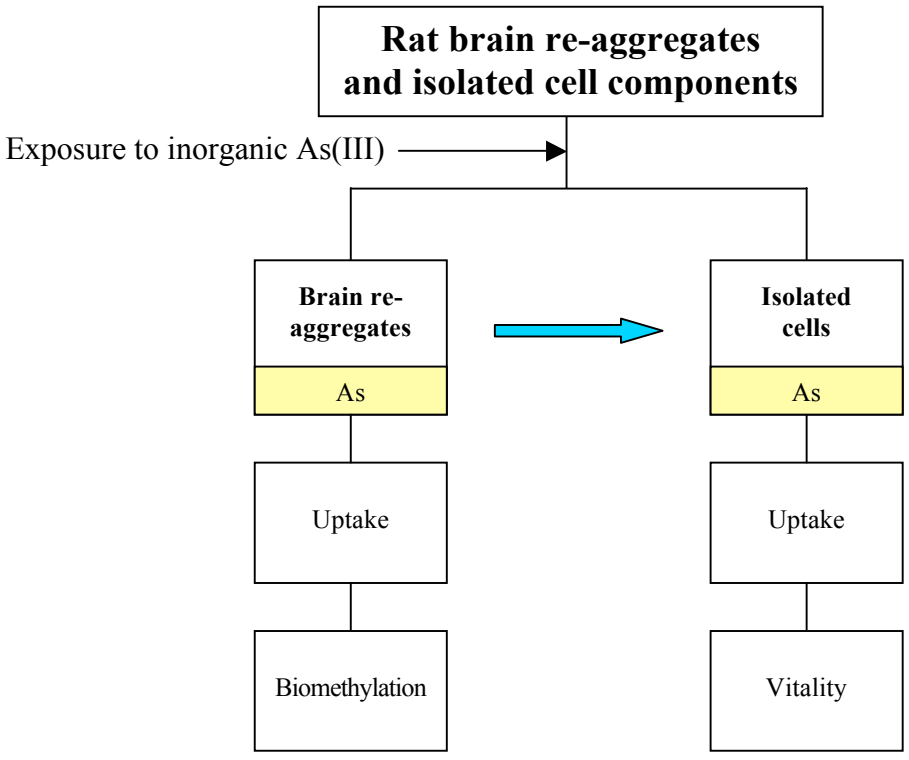

Figure C. Objectives of the present research on whole rat brain re-aggregates and their individual cell type constituents.t

MATERIALS AND METHODS

1. Chemicals

All chemicals used were of the highest analytical purity available.

Sodium(meta)arsenite(III) ($NaAsO_2$, CAS 7784-46-5, hereafter named As(III)) and sodiumarsenate(V)dibasic heptahydrate ($Na_2HAsO_4 \cdot 7H_2O$, CAS 10048-95-0, hereafter named As(V)) were supplied by Sigma Aldrich (Milan, Italy); sodium hexafluoroarsenate(V) ($NaAsF_6$, CAS 12005-86-6, hereafter named AsF) was supplied by Alfa Aesar (Cologno Monzese, Milan, Italy); tetraphenylarsonium(V) chloride ($(C_6H_5)_4AsCl$, CAS 507-28-8, hereafter named Ph_4As) and triphenylarsine(III) ($(C_6H_5)_3As$, CAS 603-32-7, hereafter named Ph_3As) were supplied by Sigma Aldrich (Milan, Italy); tetramethylarsenic iodide ($(CH_3)_4AsI$, CAS 5814-20-0, hereafter named TMAI), arsenocholine ($[(CH_3)AsCH_2CH_2OH)]^+Br^-$, CAS 39895-81-3, hereafter named AsCh), arsenobetaine ($[(CH_3)AsCH_2COOH]^+Br^-$), CAS 64436-13-1, hereafter named Asβ), trimethylarsine oxide ($(CH_3)_3AsO$, CAS 4964-14-1, hereafter named TMAO), methylarsonic(V)acid ($CH_3AsO(OH)_2$, CAS 124-58-3, hereafter named MMA(V)) and dimethylarsinic(V)acid ($(CH_3)_2AsO(OH)$, CAS 76-60-5, hereafter named DMA(V)) were supplied by Trichemical Laboratory (Osaka-fu, Japan); monomethyl arsenic(III) ($CH_3As(OH)_2$, was a gift of Prof. Styblo M., (Triangle Park, North Carolina University, USA). It was prepared according to Cullen synthesis (Cullen et al., 1984, hereafter named MMA(III)),.

Cadmium chloride(II)bihydrated ($CdCl_2 \cdot 2H_2O$, CAS 654054-66-7, hereafter named Cd(II)) was supplied by Sigma Aldrich (Milan, Italy).

Sodium chromate(VI)tetrahydrate ($Na_2CrO_4 \cdot 4H_2O$, CAS 10034-82-9, hereafter named Cr(VI)) and chromium(III)chloride hexahydrate ($CrCl_3 \cdot 6H_2O$, CAS 10025-73-7, hereafter named Cr(III)) were supplied by Alfa Aesar (Cologno Monzese, Milan, Italy).

Manganese chloride(II)hydrated ($MnCl_2 \cdot 4H_2O$, CAS 73913-06-1, hereafter named Mn(II)) was supplied by Sigma Aldrich (Milan, Italy), potassium permanganate(VII) ($KMnO_4$, CAS 7722-64-1, hereafter named MnO_4^-) was supplied by Alfa Aesar (Cologno Monzese, Milan, Italy).

Sodium hexachloroplatinate(IV) (Na_2PtCl_6, CAS 16919-58-7), sodium tetrachloroplatinate(II) (Na_2PtCl_4, CAS 13820-41-2), platinum(IV)chloride ($PtCl_4$, CAS 13454-96-1), platinum(II)dichloride ($PtCl_2$, CAS 10025-65-7) were supplied by Sigma Aldrich (Milan, Italy).

Sodium metavanadate(V) ($NaVO_3$, CAS 13718-26-8, hereafter named V(V)) and vanadium(IV)oxide sulfate pentahydrate ($VOSO_4 \cdot 5H_2O$, CAS 123334-20-3, hereafter named V(IV)) were supplied by Sigma Aldrich (Milan, Italy).

Buthioine sulfoximine ($C_8H_{18}N_2O_3S$, CAS 83730-53-4, hereafter named BSO), diethylmaleate ($C_2H_5OCOCH{=}CHCOOC_2H_5$, CAS 141-05-9, hereafter named DEM) and 2'-7' dichlorofluorescein diacetate ($C_{24}H_{14}Cl_2O_7$, CAS 2044-85-1, hereafter named DCFH-DA) were supplied by Sigma Aldrich (Milan, Italy).

2. Radiochemicals

In this work the following radiotracers of high specific radioactivity were used:

(i) ^{73}As, purchased by Los Alamos National Laboratory (Los Alamos, USA).

(ii) ^{51}Cr, purchased by Amersham, Perkin Elmer Life Sciences (Boston, USA).

(iii) ^{109}Cd, purchased by Amersham, Perkin Elmer Life Sciences (Boston, USA).

(iv) ^{54}Mn, purchased by Amersham, Perkin Elmer Life Sciences (Boston, USA).

(v) ^{52}Mn, produced at the JRC-Cyclotron by (p, xn) nuclear reaction on metallic Cr foil (Bonardi, private communication).

(vi) ^{56}Mn, produced by (n, γ) reaction of $Mn(CH_3COO)_2$ at the Triga Mark II reactor of the Radiochemical and Activation Analysis Center of the Pavia University (Fortaner, private communication).

(vii) ^{191}Pt, produced at the JRC-Cyclotron by (α, n) nuclear reaction on metallic Os powder (Birattari et al., 2001).

(viii) ^{48}V, produced at the JRC-Cyclotron by (α, n) nuclear reaction on metallic Sc foil (Sabbioni et al., 1989).

(ix) ^{14}C-aminoacids cocktail, purchased by Amersham, Perkin Elmer Life Sciences (Boston, USA).

(x) ^{35}S-cysteine, purchased Amersham, Perkin Elmer Life Sciences (Boston, USA).

(xi) ^{3}H-thymidine (^{3}H-TdR), purchased Amersham, Perkin Elmer Life Sciences (Boston, USA).

The characteristics of the radioisotopes are summarized in Table 1. They were used for the labelling of As, Cd, Cr, Mn, Pt and V compounds at different concentrations ranging from 0.01 to 1000μM. For this purpose, aliquots of radiotracers were added

to the corresponding aqueous solutions containing appropriate amounts of the non radioactive stable compound in the same chemical form. Before the use, such solutions were equilibrated at room temperature for 15min. Table 2 reports the radiolabelled final chemical forms of the compounds used in the present work which were prepared and tested for the chemical form as previously described.

Table 1. Radiochemical characteristics of the radiotracers.

Isotopes	Characteristic					
	Specific radioactivity (mCi/µg)	Radiochemical purity (%)	Radioactive concentration (mCi/mL)	Mode of decay	Half life ($T_{1/2}$) (days)	Principal γ or β ray emitted (KeV)
Inorganic radiochemicals						
^{73}**As** (0.1M HCl)	1.6	>99.5	2.2	EC[a]	80.3	53.4
^{109}**Cd** (0.5M HCl)	0.0034	99.8	22	EC[a]	462.6	22 - 88
^{51}**Cr** (Saline solution)	0.45	99	5	EC[a]	27.7	320
^{52}**Mn** (0.1M HCl)	0.031	>98	0.6	EC[a]	5.6	744 – 935 - 1434
^{54}**Mn** (0.1M HCl)	51	99.9	2.3	EC[a]	312.3	834.9
^{56}**Mn** (0.1M HCl)	15	>99	40	EC[a]	0.11	847 - 1811 - 2120
^{191}**Pt** (0.1M HCl)	4.6	>99.9	0.4	β^-	3	96 - 624
^{48}**V** (0.1M HNO_3)	1	>99.8	0.5	EC[a], β^-	16.1	983 - 1311
Organic radiochemicals						
[^{14}C] Amoniacids[b]	50mCi/Matom Carbon		0.1	β^-	5730years	0-156.4
[1-^{35}S] Cysteine[b]	1075Ci/mmol	>95	0.01	β^-	87.4	0-166.8
[^{3}H] Thymidine[b]	6.7Ci/mmol	>97	1	β^-	12.43years	0-18.6

a: EC = Electron Capture
b: aqueous solution

Table 2. Radiolabelled chemical species.

Original chemical form of the radiotracers	Chemical form prepared	REF
^{73}As (0.1M HCl)	$Na^{73}AsO_2$ $Na_2{}^{73}HAsO_4$	(Sabbioni et al., 1987)
^{109}Cd (0.5M HCl)	$^{109}CdCl_2$	(Sabbioni et al., 1987)
$^{51}CrO_4^{2-}$	$^{51}CrCl_3$ $Na_2{}^{51}CrO_4$	(Sabbioni et al., 1987)
^{52}Mn	$MnCl_2$	(Bonardi, private communication)
^{54}Mn (0.1M HCl)	$MnCl_2$ $KMnO_4$	(Fortaner, private communication)
^{56}Mn	$MnCl_2$	(Fortaner, private communication)
^{191}Pt (0.1M HCl)	$Na_2{}^{191}PtCl_6$ $Na_2{}^{191}PtCl_4$	(Birattari et al., 2001)
^{48}V (0.1M HNO_3)	$Na^{48}VO_3$ $^{48}VOSO_4$	(Sabbioni et al., 1989)

Hereafter are reported the γ-ray spectra regarding the radioisotopes used in this work.

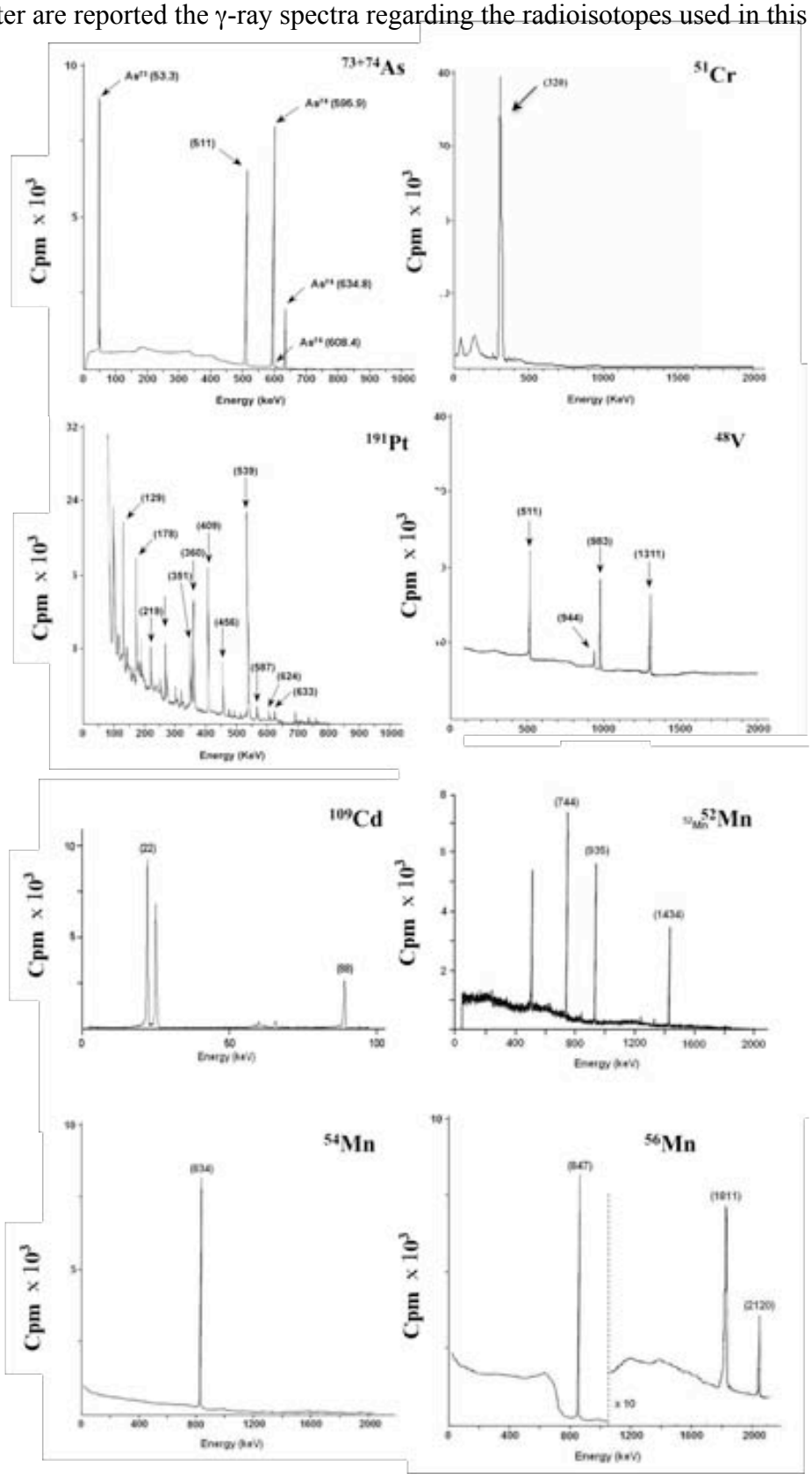

Figure 1. γ-spectra of $^{73+74}$As, ^{51}Cr, ^{109}Cd, ^{52}Mn, ^{54}Mn, ^{56}Mn, ^{191}Pt and ^{48}V.

3. Analytical techniques

The following analytical nuclear and spectrochemical techniques were used: Neutron Activation Analysis (NAA), Inductively Coupled Plasma Mass Spectrometry (ICPMS) and Graphite Furnace Atomic Absorption (GFAAS).

3.1 Neutron Activation Analysis (NAA)

In this work NAA has been used to determine: (i) the element impurities in salts to which cells have been exposed, (ii) the background level in culture medium and in unexposed cells, (iii) to study the uptake of AsF and organic As compounds by Balb/3T3 cells.

NAA is a high specific and very sensitive multielemental and absolute nuclear technique widely used in biological sciences for the analysis of trace elements in the range of mg-ng (Sabbioni, 1978). Due to the peculiar characteristics of this nuclear technique we shortly report here its basic principle. It is based on the radioactive isotope generation by neutron interaction with stable isotopes. These isotopes are detected and measured by γ-spectrometry. The most common nuclear reaction used is (n,γ) reaction:

$$ {}^{A}_{Z}X + n \rightarrow \left[{}^{A+1}_{Z}X \right] + \gamma \downarrow \beta^{-}/\gamma \ decay $$

where X is the stable isotope bombarded by neutron n; $\left[{}^{A+1}_{Z}X \right]^{*}$ is the resulting radioisotope in highly excited state; A and Z are the mass and atomic number; γ is a prompt radiation (decay times in the order of 10^{-12} - 10^{-15}s) which has no practical use.

The highly excited radioisotope decay to sable state by β^- and γ emission. This latter radiation is used for the detection and measurements of the element. In spite, NAA is an absolute technique (it should be possible to determine the quantity of the element simply using nuclear constant), for practical purpose a comparative method based on the irradiation of a standard with well know element concentration under the same experimental conditions is used:

$$m_X = \frac{m_{st} \cdot A_{st}}{A_c}$$

where: A_{st}= standard radioacivity

A_c= sample radioactivity

m_{st}= standard mass

m_x= sample mass

After neutron activation, standards and samples were directly counted for their γ-rays (Instrumental NAA) or submitted to radiochemical separation to eliminate strong interfering radionuclides such as ^{24}Na, ^{82}Br and ^{32}P (Radiochemical NAA) (Pietra et al., 1986).

3.2 Counting of the radioactivity

Hereafter are reported the counting systems used for the determination of the γ-ray emission from single radiotracers or neutron irradiated samples.

3.2.1 Low resolution integral γ-counting

This technique has been employed in the experiments when individual radiotracers were used.

In this case, the radioactivity was counted using an automatic integral γ-counter Wizard Wallac 1480 3" (Perkin Elmer-Wallac, Sweden) equipped with NaI(Tl)

crystal (3”x3.5”). The integral γ-counting was acquired using appropriate acquisition software.

3.2.2 Computer-based high resolution γ ray spectrometry

Such counting has been used to detect the γ rays from neutron irradiated salts, culture media and cells.

The radioactivity measurement has been carried out by means of a system involving a γ-spectrometer equipped with a high purity germanium crystal (Ge) detector, photomultiplier, amplificator, multichannel analyzer and autosampler (Figure 2). The acquisition and analysis of the spectra has been carried out by specific software (Nuclear Elements Digital Analysis, NEDA, Ascom, Milano).

Figure 2. γ-spectrometry system with Ge crystal and autosampler.

The measures of the radioisotopes are expressed in counts for minute (cpm). At any time such measurements have been interpreted in terms of concentration of the corresponding element for comparison with standard solutions of the radioisotopes of well known specific radioactivity.

3.2.3 Computer-based β spectrometry

The β emitters ^{3}H, ^{14}C and ^{35}S radioisotopes were measured by Liquid Scintillation Counting using a Wallac 1414 WinSpectral Liquid Scintillation Counter (PerkinElmer Life Sciences, Finland).

0.2mL liquid sample (i.e.chromatographic fractions from gel filtration or from NucleoSpin for the isolation of DNA) was diluted at 0.5mL with ultrapure water and mixed with 1.5mL of the commercial scintillation mixture (Flo-ScintII, PerkinElmer, USA). The quenching effect was compensate by the instrument using ^{152}Eu internal standard.

In samples with double label (^{109}Cd and ^{35}S-cysteine, ^{109}Cd and ^{14}C-aminoacid cocktail) all measured were corrected for the contribution due to the ^{109}Cd radioactivity.

Additionally, the fractions of interest were pooled and wet-ashed in a Teflon bomb and the ^{35}S or ^{14}C radioactivity was measured following selective radiochemical separation of ^{35}S or ^{14}C from ^{109}Cd by cation exchange resin AG 50-x8 (0.7x3cm column) (Sabbioni and Marafante, 1975).

3.3 Inductively Coupled Plasma Mass Spectrometry (ICPMS)

This advanced spectrochemical technique has been used to complement the analysis carried out by NAA of salts, culture medium and cells.

The instrument used was an ICPMS SCIEX ELAN DRC II (Perkin Elmer, Turhill, Ontario, Canada) equipped with a Dynamic Reaction Cell (DRC) able to eliminate the interferences. The gas for the instrument were Argon 99.99% (Air Liquide) and anhydrous NH_3 99.99% (Sigma Aldrich, Milan, Italy) (for the DRC). The determinations have been executed in HNO_3 2-3%. Before the instrumental analysis,

samples have been mineralized in microwave oven (CEM-MSD 2000) with HNO_3 50% (Farina, 2003). The aim was to have homogeneous solution. In order to correct the matrix effect due to the different source of the samples and standards in the analysis of the biological samples (DMEM and products for cellular cultivations) the internal standard method was used. The internal standards (In, Rh and Re) were added to samples, blank and standards at concentrations of 1-5 ppb (Farina, 2003).

3.4 Graphite Furnace Atomic Absorption Spectrometry (GFAAS)

Atomic Absorpion Spectrometry is an analytical technique widely used in toxicological studies. It was used in combination with ICPMS and NAA (Minoia et. al., 1992). The instrument used was a SIMAA 6000 (Perkin Elmer, Monza, Italy) equipped with a graphite furnace and Zeeman longitudinal effect for the interference correction. Lamps used were hallow cathode lamps type HCL or EDL, depending on specific element to be analysed (Perkin Elmer, Monza, Italy). The protocols and analysis conditions was those made by Perkin Elmer.

3.5 Nuclear Magnetic Resonance (NMR)

This technique was used to study the interaction of manganese and platinum compounds with culture medium components and Na2PtCl6 with cellular lysate in the within of a contract study named “In vitro cellular biotransformation and interaction of metal compounds”. The instrument used was a NMR Bruker Avance 6000 (Bruker BioSpin S.r.l., Milano, Italy), operating with magnetic field of 14.1T (600.13MHz). The instrument was located and the analyses were performed at the Dipartimento di Genetica, Biologia e Biochimica, Sezione Biologia, Turin University (Italy).

The analyses were conducted on culture medium or cellular lysate after addition of and 50µL of D2O (necessary to obtain the field frequency lock) to 550µL of sample.

4. Biochemical techniques

The biochemical techniques used for speciation analysis included ion exchange chromatography, high-pressure liquid chromatography, gel filtration differential centrifugation, NucleoSpin and ultrafiltration.

4.1 Chromatographic techniques for speciation analysis

Hereafter are shown several chromatographic techniques used for the speciation analysis of As, Cd, Cr, Mn, Pt and V compounds in culture medium and cellular cytosol fraction.

4.1.1 Tam's method (TAM) and solvent extraction

This method was used to study the ^{73}As(III) and ^{73}As(V) biomethylation in Balb/3T3 cells involving the determination of As metabolites in cytosol and culture medium in Balb/3T3 cells and in brain aggregates exposed to both inorganic arsenic species. The biomethylated arsenic metabolites were separated by an ion exchange resin AG 50-X4 (Tam et al, 1978) (Figure 3). The ^{73}As(III) and ^{73}As(V) in eluate were separated by solvent extraction with diethylditiocarbamate (DTTC) in chloroform.

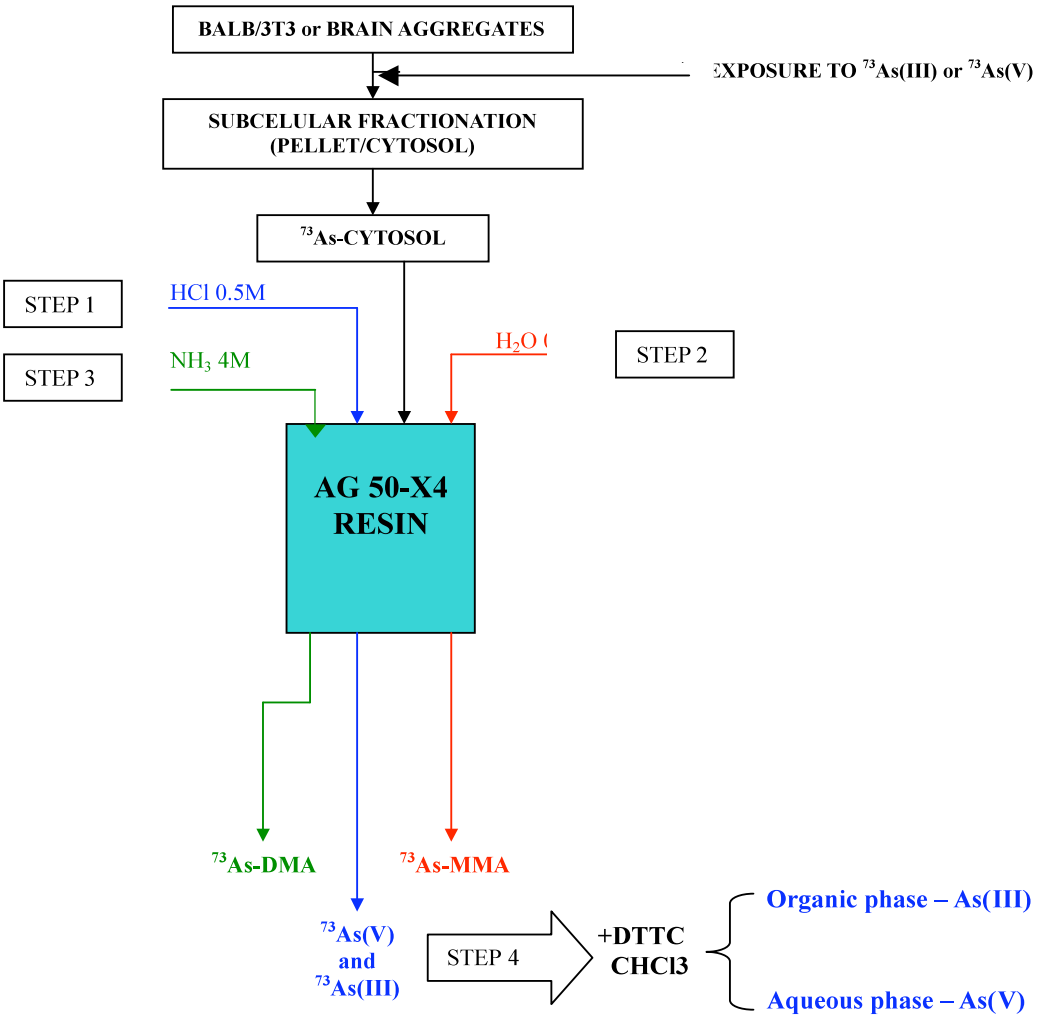

Figure 3. Tam's method and solvent extraction procedures for speciation of As in Balb/3T3 cells or rat brain aggregates exposed to ^{73}As inorganic species. DTTC: diethyldithiocarbamate.

4.1.2 Sabbioni's method

This method was used in the study of Balb/3T3 cells exposed to ^{48}V(V) or ^{48}V(IV), which allowed the determination of the oxidation state of V in the cytosol of the cell and in culture medium. The method was based on the use of Chelex 100 resin (0.8x4.0cm, BioRad) (Figure 4). After equilibration of the resin with 10mM CH_3COOH, pH=5.0, sample was absorbed on the column (0.8x4.0cm). V(IV) was retained on the resin and eluted by 0.1M NaOH. V(V) was recovered in the eluate.

The method was developed and validated in combination with EPR technique (Sabbioni, unpublished) that is able to distinguish between V(IV) and V(V).

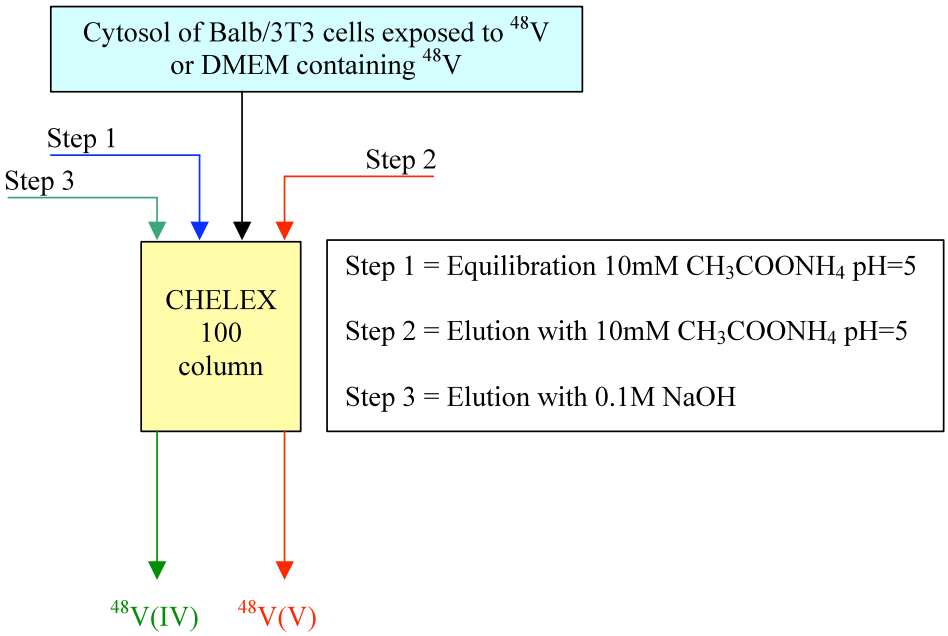

Figure 4. Method of speciation of V in Balb/3T3 cells exposed to ^{48}V(V) and ^{48}V(IV) species.

4.1.3 Minoia's method

This method, based on solvent extraction and the use of liquid anion exchanger resin Amberlite LA1 (Minoia et al., 1983) was used for the study oxidation states of Cr in ^{51}Cr-containing cytosol of Balb/3T3 at the end of exposure to ^{51}Cr(III) or ^{51}Cr(VI). The Cr(VI) was extracted in the organic phase while Cr(III) was recovered in the aqueous phase (Figure 5).

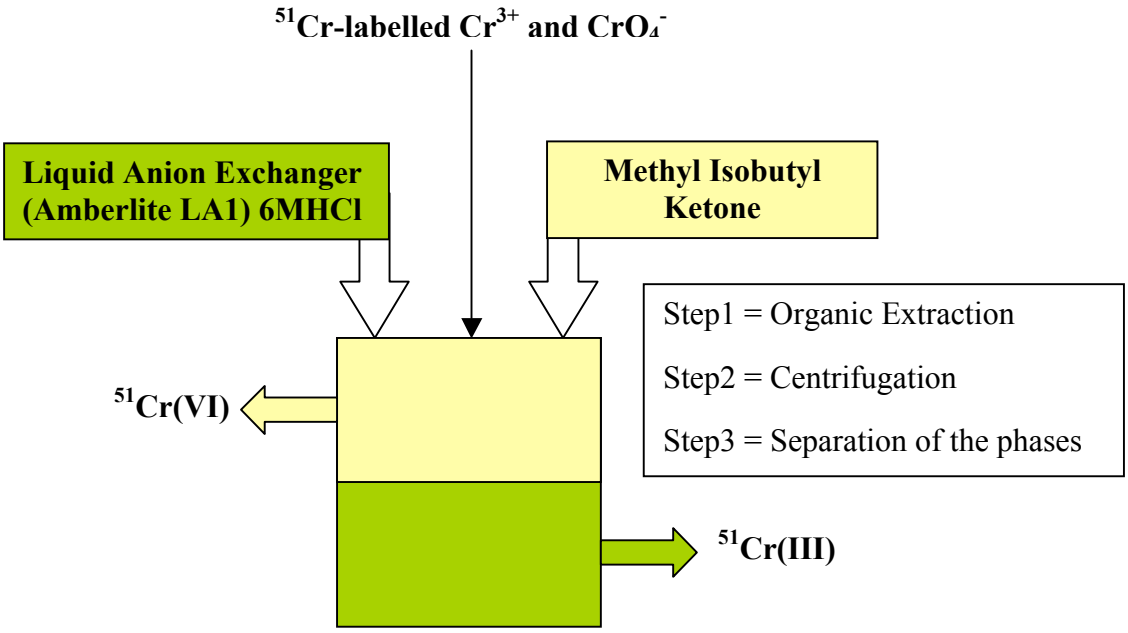

Figure 5. Method of speciation of Cr in Balb/3T3 cells exposed to $^{51}Cr(III)$ or $^{51}Cr(VI)$.

4.1.4 HPLC

This technique, coupled with ICPMS as detector (Section 3.3), was used for the on-line study of As and Pt speciation in culture medium (DMEM). The instrument used was a SERIES 200 (Perkin Elmer, Monza, Italy). Two different columns and conditions were used:

(i) arsenic species were separated by using an anionic exchange resin HAMILTON PRP-X100 (25cm x 4.1mm, resin size=10µm) under the following conditions: eluent A=$NH_4H_2PO_4$ (0.25mM) - pH=9.0 - 2%MeOH; eluent B= $NH_4H_2PO_4$ (20mM) - pH=8.8 - 2%MeOH. The eluents were degased with helium at 0.7psi (Table 3).

(ii) platinum species were separated by using a TEKNOKROMA NUCLEOSIL 100-CN resin (25cm x 4.0mm, resin size=5µm) and the following conditions: eluent A= $NaNO_3$ 50mM; eluent B= CH_3COOH 10 mM; eluent C= H_2O MilliQ. The eluents were degased with helium at 0.7psi (Table 4).

Table 3. Elution program for As speciation in culture medium (DMEM) and rat brain aggregates exposed to As(III) or As(V).

Step	Time (min)	Flow (ml/min)	%A	%B	Curve
0	7.0	1.00	100.0	0.0	0.0
1	10.0	1.00	100.0	0.0	0.0
2	20.0	1.00	0.0	100.0	0.0

Table 4. Elution programe for Pt speciation in culture medium (DMEM).

Step	Time (min)	Flow (ml/min)	%A	%B	%C	Curve
0	6.0	0.3	0.0	0.0	100.0	0.0
1	8.0	0.3	0.0	10.0	90.0	0.0
2	16.0	0.3	50.0	0.0	50.0	0.0
3	6.0	0.3	50.0	50.0	0.0	0.0

4.1.5 Gel filtration

This technique was used for: (i) the fractionation of the culture medium and the determination of the biochemical pools of As, Cd, Cr, Mn, Pt and V in the cytosol from Balb/3T3 cells exposed to ^{73}As, ^{109}Cd, ^{51}Cr, ^{52}Mn, ^{54}Mn, ^{56}Mn, ^{191}Pt and ^{48}V compounds; (ii) the study of the binding of Cr and V to DNA from Balb/3T3 cells.

It is based on the separation of molecules of different molecular weight and steric dimension by the well known Sephadex, Sephacryl and Superdex resins. The high molecular weight components (hereafter named HMWC) are moving into the resin faster than low molecular weight components (hereafter named LMWC): the HMWC don't penetrate the pores of the resin and hence them exit from the column before LMWC.

The results of the chromatography are expressed in terms of Ve/Vo (Ve=eluted volume, Vo=column void volume). The elution volumes are a linear function of the logMW (Figure 6). By means of protein with a known MW it is possible to establish

a calibration curve to determine the MW of the unknown components in the eluate (Wood and Cooper, 1970). Blu Dextrane (MW=200KDa) was used to determine Vo.

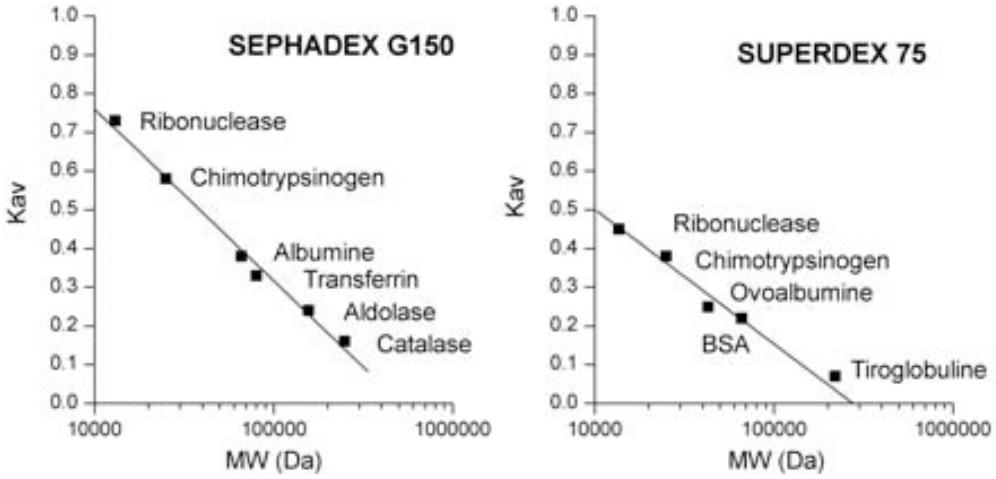

Figure 6. Calibration curves of Sephadex G150 and Superdex-75 resins by standard molecular weight protein kit.

The gel filtration was carried out by an automatic system involving a biocompatible low pressure and high flux chromatography apparatus FPLC (Pharmacia, Uppsala, Sweden) (Figure 7) specific for the proteins and peptide purification. This system is faster than classical gel filtration chromatography.

Figure 7. Fast Protein Liquid Chromatography system (FPLC)

4.2 Differential ultracentrifugation

This technique was used for the subcellular fractionation of Balb/3T3 and PC12 cell line and in the study on Brain aggregates (Sabbioni and Marafante, 1976). It is based on the sequential sedimentation of the cellular organelles by means of increasing of centrifugal force by a cooled ultracentrifuge OPTIMAMAX 130.000rpm (Beckman, USA) (Table 5).

Table 5. Subcellular fractionation of Balb/3T3 cells by differential ultracentrifugation.

Subcellualr fractions	Applied centrifugal force (xg)	Time (min)
Nuclei and Membrane	700	10
Mitochondria	9000	15
Lysosomes	30000	25
Microsomes/Cytosol	105000	90

4.3 NucleoSpin for the isolation of DNA

Table 6 reports the NucleoSpin procedure for the separation of DNA from Balb/3T3 cells.

Table 6. Isolation of highly pure DNA from Balb/3T3 cell line: NucleoSpin protocol.

Sample preparation
Homogenisation of Balb/3T3 cells (2.5mL, 10mM cacodilate buffer, pH 7.4)
Pre-lysis[a]
Add 180µL buffer T1 and 25µL proteinase K solution to 0.5mL homogenate (in 1.5mL ultracentrifuga tube). Incubate (56°C, 2h).
Lysis[a]
Vortex, add 200µL buffer B3 and incubate (10min, 70°C).
Adjust DNA binding conditions
Add 210µL ethanol (100%). Vortex vigorously.
Bind DNA
Place a Nucleospin Tissue column into a 2mL collecting tube, apply the sample (from the previous step) to the column, centrifuge (1min, 11000xg), discharge flow-through and place the column back into the collecting tube.
Wash silica membrane
1st wash Add 500µL buffer BW, centrifuge (1min, 11000xg), discharge flow-through and place the column back into the collecting tube.
2nd wash Add 600µL buffer B5 to the column, centrifuge (1min, 11000xg), discharge flow-through and place the column back into the collecting tube.
Dry silica membrane
Centrifuge the column (1min, 11000xg) to remove residual ethanol.
Elute pure DNA[a]
Place a Nucleospin Tissue column into a 1.5mL ultracentrifuge tube. Add 100µL prewarmed elution buffer BE (70°C). Incubate (20°C, 1min). Centrifuge (1min, 11000xg). DNA determination (A_{260nm}) and ^{51}Cr counting.

a: The composition of T1, BW, B5 e BE buffers is not known, being covered by commercial patent (Macherey-Nagel).

4.4 Ultrafiltration

In order to establish if Cr was bound to protein this technique has been applied to ^{51}Cr-containing medium and to the ^{51}Cr-containing peaks from gel filtration of Balb/3T3 cells exposed to $^{51}Cr(VI)$ (Section 4.1.5). Ultrafiltration is a separation

process using membranes, with well defined pore size, mainly polysulphone and cellulose acetate. Typically, it removes high molecular weight substances, colloidal materials and polymeric molecules which allows the separation of unbound metal ions species from protein-bound metals. In our study, ultrafiltration of 1-2mL ^{51}Cr-containing culture medium and ^{51}Cr-cytosol was carried out on Centricon (YM-1) Centrifugal Filter Devices (Amicon, Millipore, nominal molecular weight cut off 1KDa). Sample in the Filter Device was by centrifuged at 100xg for 30min.

In addition, ultrafiltration experiments were carried out also in cadmium experiments on ^{109}Cd-^{14}C amino acids-DNA solution loaded onto Ultrafree Microcon Filter Units at 30K nominal molecular weight limit (NMWL).

5. Biological systems

Mouse fibroblasts Balb/3T3 cell line, rat brain re-aggregates (brain aggregates) as whole or as individual cell components such as granule cells (neurons), mixed primary glial cells (astrocytes) and microglia cells were used.

5.1 Balb/3T3 cell line and culturing

The cellular line of immortalized mouse fibroblasts Balb/3T3 (clone A31-1-1) has been supplied to ECVAM from Istituto Zooprofilattico Sperimentale of Lombardia and Emilia (IZS), Laboratorio Centro Substrati of Brescia (Balb 3T3, step n°76-78).

Cells were maintained in culture under standard conditions (37°C, 5%CO_2, 95% of humidity, in an incubator HERAEUS, Germany) and counted using a "Bürker"

chamber 0.0025mm^2 (Blau-Brand, Germany) and Trypan blue solution (Sigma, Milano, Italy). The number of cells/mL was calculated using the formula:

$$N=(a/b)\cdot 10^4 \cdot DF$$

where: N = number of cells
a = number of cells counted in minimum 3 squares
b = number of squares considered (minimum 3)
10^4 = conversion factor of chambers volume
DF = dilution factor

All cells have been certified free of bacteria, mycoplasma and fungi from by the supplier. Figures 8A and 8B show the cells morphology as obtained by optical microscope (Figure 8A) or by SEM (Figure 8B).

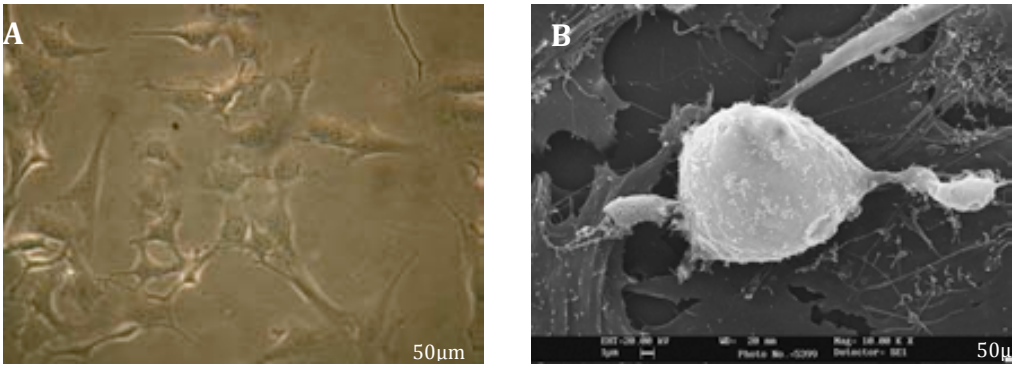

Figure 8. Balb 3T3 cells morphology: optical microscope (A); Scanning Eletron Microscope (SEM) (B).

Table 7 summarizes the cultures procedures concerning growth and maintenance of the cells.

Table 7. Balb/3T3 cell line: mainteinance and freezing protocols[a].

Culture medium	
• Dulbecco's Modified Eagle Medium (1X), liquid 1000mgL^{-1} D-Glucose, with L-Glutamine and Sodium Piruvate, (hereafter named DMEM low Glucose)	GIBCO, Invitrogen Corporation
• 10% of Foetal Clone III serum, Bovine serum products (hereafter named FCIII)	HYCLONE, CELBIO, Milano
• 4.8mM of L-Glutamine 200mM (100X)	GIBCO, Invitrogen Corporation
• 1% of Fungizone liquid (250µg/mL)	GIBCO, Invitrogen Corporation
• 0.6% of Penicillin/Streptomycin solution, liquid, 5000UmL^{-1} Penicillin and Steptomycin 5000µg/mL (hereafter named P/S)	GIBCO, Invitrogen Corporation
Maintenance	
1. Seed 4X10^5 cells in 75cm^2 flask with 15mL DMEM to get an 80% confluent culture in 4 days as follow	
1st day	
2. Wash cells twice with 10mL of Phosphate Buffer Solution (PBS) (1X) without Ca, Mg and sodium bicarbonate (GIBCO, Milano)	
3. Replace PBS solution with 0.5mL of trypsin/EDTA (1X), liquid, 0.5g/L trypsin (1:250) and 0.2g/L EDTA·4Na in Hank's BSS (GIBCO, Invitrogen Corporation)	
4. Harvest cells (10mL of fresh medium)	
5. Count and seed (15mL of fresh medium)	
2nd day	
6. Change culture medium	
Freezing	
1. Add DMSO (10%) and FCIII (10%) to culture medium (80%)	
2. Store at –80°C (24h) and then in liquid nitrogen	

a: Mazzotti et al., 2001

5.2 PC12 cell line and culturing

The rat pheochromocytoma PC12 clonal cell line (Figure 9) were purchased by Clontech Laboratories (Mountain View, CA, USA) and cultivated under standard conditions (37°C and 5%CO_2 in an incubator HERAEUS, Germany). Due to the poor adherence of PC12 cell line, these cells were grown on collagen Vitrogen 100 coated tissue culture flasks and dishes for at least 3h at 37°C before using flasks for cells maintenance or treatment.

Table 8 summarizes the cultures procedures concerning growth and maintenance of the PC12 cells.

Table 8. PC12 cells: maintenance protocol.

Coating solution

- 1%v/v Vitrogen 100 — GIBCO, Invitrogen Corporation
- 1% BSA 10% — GIBCO, Invitrogen Corporation
- 98% HBS: pH=7.5
  - 122mM NaCl
  - 2.67mM KCl
  - 9.4mM glucose
  - 14mM NaH_2PO_4
  - 20mM Hepes

Culture medium

- RPMI 1640 (1X), liquid 2000mg/L D-Glucose, with Sodium Piruvate, (hereafter named RPMI) — GIBCO, Invitrogen Corporation
- 10% of Horse serum — HYCLONE, CELBIO, Milano
- 5% Foetal Calf Serum — GIBCO, Invitrogen Corporation
- 1% of Penicillin/Streptomycin solution, liquid, 10000U/mL Penicillin and Steptomycin 10000µg/mL (hereafter named P/S) — GIBCO, Invitrogen Corporation

Maintenance

1. Seed $1X10^6$ cells in $75cm^2$ "coated" flask with 10mL culture medium to get an 80% confluent culture in 4 days.

   2^{st} day

2. Wash cells twice with 10mL of Phosphate Buffer Solution (PBS) (1X) without Ca, Mg and sodium bicarbonate (GIBCO, Milano)
3. Replace PBS solution with 0.5mL of trypsin/EDTA (1X), liquid, 0.5/L trypsin (1:250) and 0.2g/L EDTA·4Na in Hank's BSS (GIBCO, Invitrogen Corporation)
4. Harvest cells (10mL of fresh medium)
5. Count and seed (15mL of fresh medium)

   3^{nd} day

6. Change culture medium

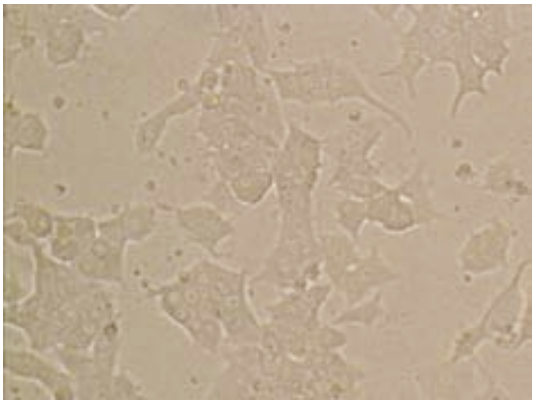

Figure 9. PC12 cells morphology by optical microscope.

5.3 Brain re-aggregating and culturing

The brain re-aggregating cultures (Figure 10) were prepared from 16-day old foetal rat telencephalon at the Insubria University (Varese, Italy) as previously described (Honegger and Monnet-Tschudi, 2001). The dissected tissue was mechanically dissociated using nylon sieves with 200 and 115μM pores.

Cells were cultivated under standard conditions (37°C and 10%CO_2 in an incubator HERAEUS, Germany).

Table 9 summarizes the cultures procedures concerning growth and maintenance of the brain aggregates.

Table 9. Brain aggregates: maintenance protocol.

Culture medium

- DMEM (1X), liquid 25mM D-Glucose (hereafter named DMEM high Glucose)
- 0.8µM Insulin
- 30nM Triiodothyroidine
- 20nM Hydrocortisone-21-phosphate
- 1µg/mL Transferrin
- 4µM Bioin
- 1µM Vitamin B12
- 10µM Linoleate
- 1µM Lipoic Acid
- 10µM L-Carnitine

Cell culture maintenance

1. Re-suspension of cells at a density of $7.5 \cdot 10^6$ cells/mL in culture medium
2. Maintainance in 15ml flasks under initial gyratory shaking speed of 68rpm, which was increased over the days *in vitro* to a constant speed of 80rpm, at 37ºC in an atmosphere of 10%CO_2.
3. Replacement of culture medium at intervals of three days up to day 14 and every other day thereafter (5ml replaced of 8ml total).

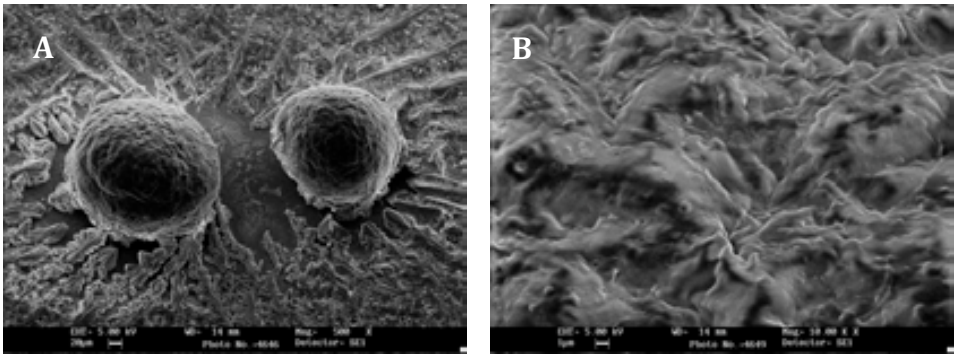

Figure 10. Brain aggregates microphotography by SEM: whole aggregates (A); details of surface (B).

5.4 Isolation and culture of primary neurons, astrocytes and microglia

Tables 10, 11 and 12 show the protocols concerning isolation and culturing of primary cerebellar granule cells (neurons), mixed primary glial cells (containing 85% of astrocytes) and microglial cells, respectively (Figures 11, 12 and 13).

Table 10. Neurons: protocol of preparation[a].

Culture medium

• 100mL DMEM high Glucose	GIBCO, Invitrogen Corporation
• 5mL Foetal Bovine Serum	GIBCO, Invitrogen Corporation
• 5mL Horse serum	EuroClone
• 0.8mL of 1.66M D(+)glucose stock: 30 g D(+)glucose in 100ml of DMEM	Sigma
• 0.5ml of 1M Hepes	GIBCO, Invitrogen Corporation
• 1mL of of Glutammine (200 mM): 292mg of Glutammine in 10ml sterile water	GIBCO, Invitrogen Corporation
• 2mL of KCl (1M) stock: 3.728g KCl in 50mL DMEM	Sigma
• 20µl of Gentamicin (50mg/mL)	GIBCO, Invitrogen Corporation

PBS glucose

• 500mL PBS	GIBCO, Invitrogen Corporation
• 3.03mL of 1.66M D(+)glucose stock	Sigma
• 3.85mL of P/S	GIBCO, Invitrogen Corporation

Coating solution

• Poly-L-Lysine solution 1:10 in sterile water	Sigma

Coating

1. Add the coating solution to wells (Kinsner at al., 2005)
2. Incubate 30min at room temperature in the flow hood
3. Remove the coating solution
4. Wash 1x with sterile water (150mL)
5. Wash 1x with PBS/glucose (100mL)
6. Add complete medium to wells (0.5mL – 24-well plates; 70µL – 96-well plates; 200µl – chamber slides). Leave the plates in the incubator overnight.

Isolation

7-8 days old rat pups are sacrified by decapitation.

1. Remove the brains and place in sterile PBS supplemented with 0.6% D(+)glucose in a Petri dish
2. Isolate the structure (cerebella) and place them in a sterile 50-ml tube with PBS/0.6%D (+)glucose. The tube with the material must be kept on ice during the isolation.
3. Cut the cerebella into small pieces on a Petri dish; place the pieces in a sterile 50mL tube containing 7mL of 1:5000 Versene (pre-warmed at 37°C).
4. Incubate the tissue for 5min at 37°C.
5. After incubation triturate the tissue 7-10 times using a fire polished, large bored glass Pasteur pipette. Allow large pieces of tissue to settle, remove the cells suspension and place it into a sterile 50ml/tube.

6. Add 5mL of Versene to the remaining tissue.
7. Again triturate the tissue 7-10 times using a fire polished, small bored glass Pasteur pipette. Allow large pieces of tissue to settle, remove the cell suspension and add it to the first.
8. Repeat the procedure until the tissue is fully dissociated.
9. Centrifuge the collected cell suspension for 6min, 900rpm at 40°C.
10. Discard the supernatant and add 10mL of medium.
11. Pass the cell suspension through a 40µm cell strainer.
12. Count the cells and plate at a density 250000cells/cm^2.

Inhibition of glial cell proliferation

If necessary, after 24 hours the cells can be treated with 10µM cytosine-D-arabinoside hydrochloride (Ara-C) (Kinsner et al., 2005) to inhibit proliferation of glial cells.

a: Kinsner et al., 2005.

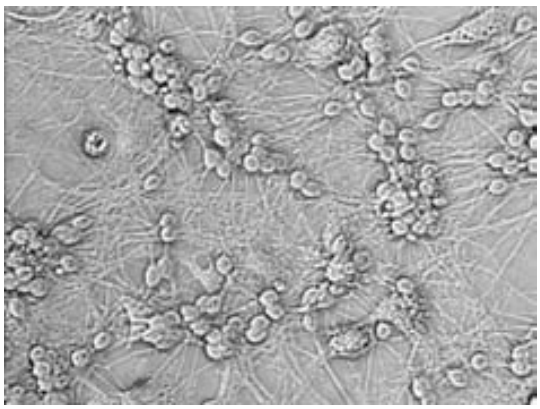

Figure 11. Morphology of cerebellar granule neurons observed under the phase-contrast microscope.

Table 11. Astrocytes: protocol of preparation[a]

Culture medium	
• 100mL DMEM high Glucose	GIBCO, Invitrogen Corporation
• 11.4mL Foetal Bovine Serum	GIBCO, Invitrogen Corporation
• 2.3mL of P/S	GIBCO, Invitrogen Corporation
PBS glucose	
• 500mL PBS	GIBCO, Invitrogen Corporation
• 3.03mL of 1.66M D(+)glucose stock	Sigma
• 3.85mL of P/S	GIBCO, Invitrogen Corporation
DNA-se	
• 50ml of EBSS	GIBCO, Invitrogen Corporation
• 2mg DNA-se	Sigma
• 150mg of BSA	Sigma
Trypsin	
• 25ml of EBSS/ DNA-se/ BSA solution	GIBCO, Invitrogen Corporation

- 6.25mg trypsin Sigma

Coating solution

- Poly-L-Lysine solution 1:20 in sterile water Sigma

Coating

1. Add the coating solution to flasks: -75cm^2 flasks: add 7mL of coating solution/flask
   -25cm^2 flasks: add 2.5mL of coating solution/flask
2. Incubate 30 minutes at room temperature under the flow hood
3. Remove the coating solution
4. Wash 1x with sterile water (7ml/T75 flask; 2.5ml/T25 flask)
5. Wash 1x with PBS/glucose (7ml/T75 flask; 2.5ml/T25 flask)
6. Add complete medium to flasks (7ml/T75 flask; 2.5ml/T25 flask)
7. Leave the flasks in the incubator overnight.

Isolation

7-8 days old rat pups are sacrified by decapitation. The cortex is isolated from the brains removed from the scull.

1. Cut the isolated cortex in small pieces in a Petri dish.
2. Add 15mL EBSS/DNA-se/Trypsin and put into a 50mL tube.
3. Incubate for 15 min at 37°C.
4. Add an equal volume of DMEM to neutralise the trypsin.
5. Centrifuge at 900rpm, 7min, 4°C.
6. Discard the supernatant, add 10mL of EBSS/DNA-se and triturate the pellet using glass Pasteur pipettes with big hole.
7. Allow the tissue to settle for 1min and remove the supernatant to a sterile 50mL tube.
8. Add 10mL of EBSS/DNA-se to the tissue and triturate the pellet using Pasteur pipettes with small hole.
9. Allow the tissue to settle for 1min and remove the supernatant and add it to the first.
10. Repeat the procedure until the tissue is fully dissociated.
11. Centrifuge the collected supernatant at 900rpm, 7min, 4°C.
12. Discard the supernatant and add 3mL of DMEM to the pellet.
13. Gently disperse the pellet and resuspend the tissue completely by triturating with a glass Pasteur pipette.
14. Make the volume up to 30mL with DMEM.
15. Filter the cells through the 100μm and than 40μm mesh.
16. Count the cells and plate at a cell density 3x10^{4}cells cm^{-2}.

a: Kinsner et al., 2005.

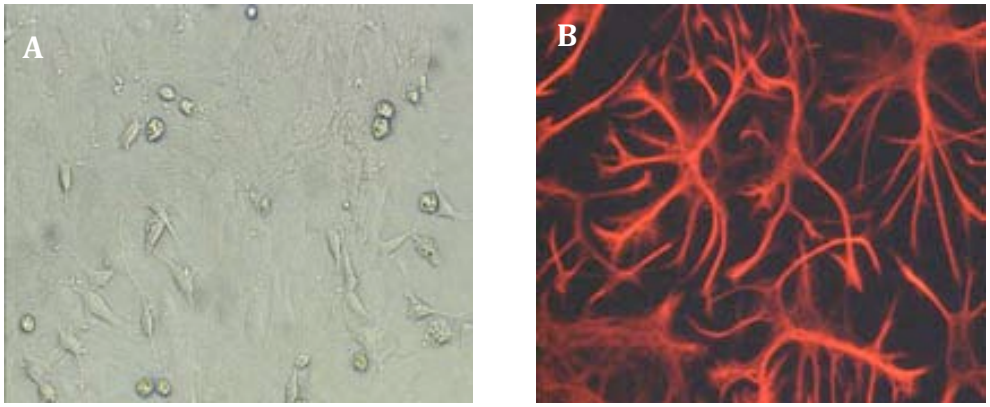

Figure 12. Astrocytes morphology: optical (A) and fluorescent (B) microscope.

Table 12. Microglia: protocol of preparation[a]

Culture medium

• 100mL DMEM high Glucose	GIBCO, Invitrogen Corporation
• 10% Foetal Bovine Serum	GIBCO, Invitrogen Corporation
• 1% of P/S	GIBCO, Invitrogen Corporation

Hank's balanced salt solution (HBSS)

• 0.25% trypsin	GIBCO, Invitrogen Corporation
• 0.02mg/mL DNA-se I	GIBCO, Invitrogen Corporation
• 1% of BSA	Sigma

Isolation

Primary, mixed glial cultures were prepared as described before from the cerebral cortex of 7-day-old rats.

1. Briefly, the cells isolated from cerebral hemispheres were dissociated in Hank's balanced salt solution (HBSS).
2. Cells were plated at a cell density of $1x10^4$cells/cm in 75cm^2 culture flasks (Costar, Corning).
3. All flasks and plates were coated with poly-L-lysine (see above).
4. Cells were grown in a humidified incubator at 37°C in 5% CO_2 in air. Medium was changed every 3 days.
5. At confluence (14-16 days in vitro) the primary mixed glial cultures were used to isolate microglial cells.
6. The cultures were shaken for 2h to dislodge microglia that were loosely attached to the astrocytes.
7. Isolated microglia were seeded into 6-well or 12-well plates (Costar, Corning) at a density of 2.0 x 10^5cells/cm^2 and maintained in astrocyte-conditioned medium (medium collected from astrocytic cultures and spun down) mixed 1:1 (v/v) with fresh culture medium. The purity of microglial cultures was determined immunocytochemically with anti-GFAP antibody (astrocytic marker) and anti-OX-42 antibody (microglial marker).

a: Kinsner et al., 2006.

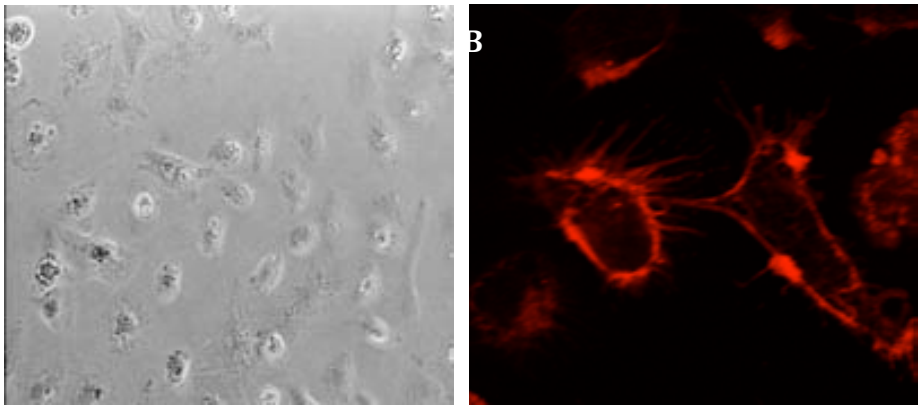

Figure 13. Microglia morphology: optical (A) and confocal (B) microscope.

6. Studies on Balb/3T3 cell line

This section reports the studies carried out on As, Cd, Cr, Pt and V compounds in Balb/3T3 cell line. In addition, procedures concerning specific studies related to biomethylation of inorganic As species, their effects on protein and nucleic acids content and the determination of the oxidation state of Cr and V in the cytosol of exposed cells, are reported.

6.1 Basal cytotoxicity

Hereafter is reported the screening of the basal cytotoxicity induced by As, Cd, Cr, Pt and V compounds considered in this study in Balb/3T3 cells as determined by Colony Forming Effciency assay (CFE).

According to a previous reported protocol (Mazzotti, 2001), 200cells/4mL of complete medium were seeded in 60x15mm culture dish (Falcon, Italy) using 6 culture dishes for every treatment and control (complete medium) (Table 13).

After 24h the culture medium was replaced with fresh medium solution containing metal compounds to be tested at the appropriate concentration.

After 2h or 72h of exposure the metal-containing medium was replaced with fresh complete medium (without the metal compound) that was changed twice/week.

Seven days later the culture medium was removed, cells were washed with 4mL PBS/dish for 10min., fixed with 4mL/dish of a 10% in PBS formaldehyde 37% solution Formalin (Sigma) for 20min. and stained with 4mL/dish of a 10% in MilliQ H_2O Giemsa stain stock solution (0.4%) for 30min. Dishes were rinsed with MilliQ H_2O and let to dry.

Colonies with more than 50 cells were counted using a stereo Wild Heerbrugg (Switzerland) microscope. Results have been expressed as relative Colony Forming Efficiency (CFE), assuming the number of colonies in metal treated plates as percentage of viability of control (100%).

6.2 Concurrent cytotoxicity (CFE) and Morphological Transformation Assay

Cytotoxicity and carcinogenic potential of metal compounds were evaluated in Balb/3T3 cells using concurrent CFE and morphological transformation assay (Mazzotti, 2001). The protocol (Table 13) consists of two steps:

(i) evaluation of cytotoxicity (CFE).

(ii) evaluation of induction of foci TypeIII.

The results concerning the morphological transformation were elaborated considering the following parameters:

- plating efficiency (mean of colonies in CFE dish x 100/200 cells seeded in every dishes)
- total number of seeded cells (number of dishes for morphological transformation x 10000 cells seeded in every dishes)

- surviving cells ((total number of cells seeded x plating efficiency) / 100)
- transformation frequency (total number of foci type III per treatment / surviving cells)

The significance of transformation efficiency was calculated using Fisher analysis (Ponti et al., 2007).

Table 13 summarizes the protocols used in CTA assay.

Table 13. Balb/3T3 concurrent cytotoxicity and morphological transformation assay: protocol[a].

Reagents	**Source**
• DMEM low Glucose	SIGMA, Milano, Italy
• Formaldehyde solution (37%)	SIGMA, Milano, Italy
• Giemsa solution 0.4%	GIBCO, Milano, Italy
• Phosphate Buffer Solution (1X) without calcium, magnesium and sodium bicarbonate (PBS)	SIGMA, Milano, Italy

Protocol

1st day

1. Seed 200cell/dish 60x15mm in 4mL of fresh medium (6 dishes per treatment) for CFE and 10^4cells dish 60x15mm in 4mL of fresh medium (20 dishes per treatment) for morphological transformation assays

2nd day

2. Replace te medium with 4mL of treatment solution containing the metal compound for 72h

5th day

3. Replace the treatment solution with 4mL of fresh complete medium

8th day

4. Change the medium (4mL)

11th day (end of CFE)

5. Fix the colonies with 4mL/dish of formaldehyde solution 10% in PBS for 20min.
6. Stain colonies with 4mL/dish of Giemsa filtered solution 10% in H_2O MilliQ for 30min.

11th day (morphological transformation)

7. Change the medium (4mL) and culture cells for 4 weeks changing medium every 3 days

40th day (end of morphological transformation)

8. Fix the cells with 4mL/petri dish 60x15mm of formaldehyde solution 10% in PBS for 20min.
9. Stain the cells with 4mL/petri dish 60x15mm of Giemsa filtered solution 10% in H_2O MilliQ for 30min.
10. Count of the foci type III and estimate transforming frequency

a: Mazzotti, 2001.

In the cases of As(V), Cd(II) and V(V) further transformation assays were carried out by exposing Balb/3T3 to of Na_2HAsO_4, $CdCl_2$ or $NaVO_3$ alone or to of the same compounds in the presence of 3μM diethylmaleate (DEM), a cellular glutathione (GSH)- depleting agent.

6.3 Behaviour in culture medium

The behaviour of ^{51}Cr and ^{48}V compounds in DMEM were investigated by Minoia's and Sabbioni's methods and by Chelex 100 (0.8x4.0cm) followed by gel filtration on Sephacryl S200 (1.6x40cm). The corresponding studies on As were carried out by HPLC (Section 4.1.2) and on Pt by HPLC (Section 4.1.4) and by NMR (section 3.5). In the case of Cr, the ^{51}Cr-cell-free medium was also ultrafiltered on Centricon (YM-1) Centrifugal Filter Devices (Section 4.4).

6.4 Uptake

Table 14 summarizes the protocol of the study related to the uptake of ^{73}As, ^{109}Cd, ^{51}Cr, ^{191}Pt and ^{48}V in Balb/3T3 cells exposed to different concentrations of the radiolabelled species.

Table 14. As, Cd, Cr, Pt and V in Balb/3T3 cells: protocol of uptake.

1. Seed $5x10^5$cells in $75cm^2$ flasks (CORNING) with 10mL of DMEM.

1^{st} day

0. Replace the medium with 10mL of fresh DMEM containing the metal compound of interest and incubation for 4h, 24h or 72h
3. Remove DMEM
4. Wash three times cells with 10mL of PBS
5. Add 1mL of Trypsin-EDTA (1X)
6. Harvest the cells using 10mL of DMEM
7. Count the cells by using a Bürker chamber
8. Wash twice the pellet with PBS (290xg, 10min)
9. Determinate the incorporation of metal into cells (by counting the radiotracer or by NAA).

6.5 Intracellular distribution

The intracellular distribution of ^{73}As, ^{109}Cd, ^{51}Cr, ^{191}Pt and ^{48}V incorporated into cells has been studied by differential ultracentrifugation (Section 4.2). Cells, after exposure to the compound, have been washed three times with PBS, treated with trypsin, resuspended in 2mL of cacodilate buffer 10mM, pH=7.5 containing 0.25M sucrose and homogenised using a Potter-Elvehjem supplied of Teflon pestle (1000rpm). The homogenate has been submitted to differential centrifugation by means of cooled miniultracentrifuge 100 TL (Beckmann, Milan, Italy) at increasing centrifugal force (g) in order to sediment organelles (Sabbioni and Marafante, 1976) (Section 4.2, Table 5). The subcellular fractions were counted by the radioactivity content.

6.6 Distribution of elemets among cytosol components

0.5mL of a cytosol fraction obtained by ultracentrifugation of the homogenates from Balb/3T3 cells exposed to $^{73}As(III)$, ^{109}Cd, $^{51}Cr(VI)$, $^{191}Pt(IV)$ as chloroplatinate and $^{48}V(V)$ compounds were chromatographed on Sephacryl S200 (1.6x40cm) previously equilibrated with Hepes buffer, pH=7.2. UV absorption of the eluate was monitored continuously at 280nm using a Lambda 25 spectrophotometer (Perkin Elmer, Monza, Italy) and the collected fractions were counted for the radioactivity content by integral γ-counting (Section 3.2.1).

$PtCl_2$ was also analysed by NMR (Section 3.5) to detect the interaction of platinum with cellular lysate components. The lysate was obtained by suspending in PBS, iced-homogenates and centrifuged at 4°C for 10min the cells from uptake (Section 6.4). The supernatant was ultracentrifuged at 100000xg for 90min.

6.7 Binding of metals to DNA

Two kind of experiments were carried out on DNA isolated by NucleoSpin method:

(i) isolation of DNA from Balb/3T3 cells exposed to ^{73}As(III), ^{109}Cd, ^{51}Cr(VI) and ^{48}V(V) species. 5÷10x10^{6}cells were exposed for different times to 10÷20μCi of each radiolabelled compound at different concentrations. DNA was isolated by NucleoSpin protocol (Section 4.3) and UV and radioactivity monitored in the DNA fraction. Then, ^{51}Cr- ^{109}Cd- and ^{48}V-containing DNA fractions were chromatographed on Sephadex G25 resin (1.6x40cm) previously equilibrated with 10mM Hepes, pH=7.2. UV and radioactivity were monitored in the collected fractions.

(ii) incubation of ^{109}Cd or ^{48}V(V) with DNA previously isolated from Balb/3T3 cells. DNA was isolated from unexposed 5÷10x10^{6}cells by NucleoSpin. Then, the nucleic acid was incubated with 5μM V(V) or 1μM Cd(II) spiked with 5μCi ^{48}V or 2μCi ^{109}Cd, respectively. The DNA was subsequently chromatographed as at the point (i).

In order to asses the stability of the Cd-amino acid(s)-DNA complex isolated from 109Cd-treated cells preincubated with ^{14}C-amino acids, each fresh DNA sample was incubated with 10mMTris, pH=7.8 and 20mM EDTA for 30 min at room temperature. Following each incubation, the sample was loaded onto filtered Ultrafree-MC (30000 NMWL, Millipore) filter units and centrifuged at 1000g for 5 min at room temperature. Each sample was washed 5 times with 10mM Tris, pH=7.8 and 20mM EDTA and the released ^{14}C-amino acid residues and ^{109}Cd radioactivities were determined in the washings as described in the Section 3.2.3.

6.8 Binding to DNA and cross linking of Cd

The cross linking of aminoacids to DNA was studied by isolating the nucleic acid by proteinase K method (Nucleo Spin, Section 4.3) that yield deproteinated DNA and aminoacid associated to DNA, (Lin et al., 1994), from cells treated with 1 and 5µM $^{109}CdCl_2$ for 72h pre-treated or not with 20µCi ^{14}C-aminoacid cocktail. Then, ^{14}C and ^{109}Cd were counted as reported in Section 3.2.

6.9 Biomethylation of As(III), As(V) and AsF

The biomethylation of ^{73}As(III), As^{73}(V) and AsF in Balb/3T3 cell line was studied by TAM method (Section 4.1.1). The presence of ^{73}As-biomethylated form of arsenic was determined in culture medium after exposure of cells to inorganic ^{73}As species and in the cytosol from intracellular distribution (Section 4.2) by γ-counting of ^{73}As in the different chromatographic fractions. In the case of AsF the determination of As in the fraction was carried by NAA (Section 3.1).

6.10 NCG, cellular protein, DNA and RNA after exposure to As(III)

Table 15 summarizes the protocol concerning the determination of cellular protein, DNA and RNA.

Table 15. Determination of protein , DNA and RNA in Balb/3T3 cell line: protocol.

Culture medium (Table 7, Section 5.1)

Cell culture and treatment

1. Seed 1X10^4 cells in 10cm^2 flask with 15mL in DMEM complete medium in order to get an 80% confluent culture in 5 days as follow

   1st day

2. Determination of cell number and plating efficiency
3. Exposure to chemicals

   5nd day

4. Determination of Nt and NCG for all the dishes
5. Determination of total DNA, total RNA and total protein

6.11 Oxidation state of Cr and V in the cytosol

The emerging ^{51}Cr- or ^{48}V-containing peaks from gel filtration on Sephacryl S200 were submitted to Minoia's or Sabbioni's methods (Sections 4.1.3 and 4.1.2) (Figures 4 and 5) in order to determine the oxidation state of the metal. The ^{51}Cr and ^{48}V radioactivity were measured by integral γ-counting (Section 3.2.1).

6.12 Induction of Cd-BP by Cd

In order to confirm the protein nature of the 6KDa ^{109}Cd- and ^{35}S- containing peak (Cd-BP, Figure 30C), two "ad hoc" experiments were carried out.

1. An aliquot of the cytosol from cells exposed to ^{35}S-cysteine and 1μM of $^{109}CdCl_2$ was also chromatographed by FPLC after heating for 1min at 80°C followed by cooling in an ice-bath.
2. The second study concerned the UV absorption characteristic of the 6KDa component. In this context, the fractions eluted from FPLC arising from the last heating experiment were spectrophotometrically analysed for their absorbance both at 280 and 254nm.

6.13 Reactive oxygen species (ROS) induced by Cd

To determine the rate of Balb/3T3 ROS generation induced by Cd(II), the fluorescent probe 2'-7' dichlorofluorescein diacetate (DCFH-DA) was added to cell incubation mixture. DCFH-DA diffuses through the cell membrane readily and is enzymatically hydrolised by intracellular esterases to non-fluorescent dichlorofluorescein (DCFH), which, in presence of ROS, is rapidly oxidised to high fluorescent dischlorofluorescein (DCF) which effluxes the cells (Pourahmad et al., 2003). The

DCF intensity is parallel to the amount of ROS formed intracellularly. The stock DCFH-DA (2mM) was prepared in absolute ethanol and kept at -70°C in the dark.

Cells collected from culture flasks using a cell scraper were washed twice with PBS prior to the analysis. Cells (10^6cells/mL) were suspended in 10mL DMEM and were incubated with 1, 3 and 5μM Cd(II) at 37°C for 15, 30 and 60min. After centrifugation (50xg, 1min), the cells were resuspended in PBS, adjusted to pH=7.4 with 50mM Tris-HCl and dichlorofluorescein by incubating with 2μM DCFH-DA for 30min at 37°C.

The fluorescent intensity of the ROS product was measured using a Perkin Elmer LS55 fluorescence spectrophotometer (Perkin Elmer, Monza, Italy). Excitation and emission wavelengths were 500 and 520nm respectively. The results were expressed as fluorescent intensity/10^6cells.

6.14 Lipid peroxidation by Cd

In order to estimate the lipid peroxidation effect in Balb/3T3 cells exposed to different Cd(II) concentrations (ranging from 1 to 5μM) the amount of thiobarbituric acid-reactive substances (TBA-RS), formed during the decomposition of lipid hydroperoxides, were determined (Smith et al., 1982). After incubation of $5 \cdot 10^6$cells with Cd(II) for 72h, cells were collected by a cell scraper, washed with 1mL PBS and resuspended (10^6cells/mL) in 0.5mL of PBS with trichloroacetic acid (70%w/v) (SigmaAldrich, Milan, Italy). The suspension was boiled with thiobarbituric acid (0.8%w/v) (SigmaAldrich, Milan, Italy) for 30min. After cooling, 1.5mL of butylated hydroxytoluene (BHT) was added (0.05%w/v) in order to prevent artifactual formation and/or degradation of hydroperoxides. After centrifugation the

absorbance of the butanol phase was recorded at 532nm in a Perkin Elmer LS55 fluorescence spectrophotometer (Perkin Elmer, Monza, Italy). The concentration of TBA-RS was then calculated using a molar extinction coefficient of $1.56 \cdot 10^5$/M·cm (Buege and Aust, 1978).

6.15 Inhibition of DNA synthesis by Cd

Balb/3T3 cells were exposed for 72h to 1, 3 and 5μM Cd(II) as reported in the Section 10.2.10. Then, the medium was discarded, the cells trypsinised and the survived cells in each flask were counted, aliquotated into three duplicate tubes (10^6cells/mL in each tube), 5μCi/mL ^{3}H-TdR was added to each tube and then incubated in water bath at 37°C for 24h. After incubation the cells were extracted to glass-fiber membranes, rinsed in 5% thrichloroacetic acid and 5mL ethanol, then stored at 50°C until fully dry, placed in scintillation liquid and measured for ^{3}H radioactivity by β^- counting (Section 3.2.3). Triplicates were prepared for each concentration.

6.16 Determination of glutathione inducedd by Cd

The spectrophotometric/microplate reader assay method for glutathione (GSH) involves oxidation of GSH by the sulfhydryl reagent 5,5′-dithio-bis(2-nitrobenzoic acid) (DTNB) to form the yellow derivative 5′-thio-2-nitrobenzoic acid (TNB), measurable at 412nm. The glutathione disulfide (GSSG) formed can be recycled to GSH by glutathione reductase in the presence of NADPH. Levels of total glutathione (reduced form (GSH) plus disulfide form (GSSG)) were determined according to the microplate assay as previously described (Baker et al, 1990). Following treatment with Cd(II) cells were scrapped, suspended in 0.01M HCl and homogenized by

sonication at 50W for 15sec. Protein was precipitated by adding sulfosalicilic acid (2.5%v/v) and incubating the samples at 0ºC for 30min. Following centrifugation to remove precipitate (1000g, 10 min), a 0.8mL portion of the acid-soluble fraction from each sample was drawn off and neutralized by the addition of 80µL 50% aqueous triethanolamine. Then, 0.1mL of the neutralized extract was transferred to a 96-well microplate and assayed for the glutathione. The final assay mixture contained 0.1mL extract, 0.15mL of 150mM phosphate buffer (pH=7.2), 100µg 5,5′-dithiobis-(2 nitrobenzoic acid), 50µg NADPH and 0.1unit of glutathione reductase. Following the addition of the enzyme, the increase in absorbance at 405nm was monitored over a period of 5min:

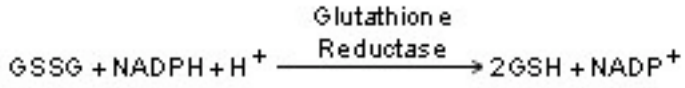

Each experiment included a set of internal standards containing known amounts of reduced glutathione (Sigma, Milan, Italy). Total protein in the original homogenate was determined using Protein Assay Kits (BioRad). Results were calculated as nmol GSH per mg protein.

7. Studies on Mn in PC12 cell line

This section reports the studies carried out on Mn compounds in PC12 cell line. Procedures concerning specific studies related to the cell viability (MTT assay), behaviour in culture medium, uptake, intracellular distribution, interaction of Mn with cellular components and expression catecholamine were performed.

7.1 Cell viability by MTT assay

Cell viability has been determined by MTT assay (Mosmann, 1983) (Table 16). In such assay, the tetrazolium salt, 3-(4,5 dimethylthiazol-2-yl)-2-5 diphenyltetrazolium bromide (MTT), is actively absorbed into cells and reduced in a mitochomdrial-dependent reaction to yield a formazan product, which accumulates within the cell since it cannot pass through the cell membrane. Upon addition of RPMI the product is solubilised and liberated and it is readily quantified colorimetrically. The ability of cells to reduce MTT provides an indication of mitochondrial integrity and activity which is interpreted as a measure of cell viability.

Cells were plated in 96 well plates (Costar, Milan, Italy) previously treated with 100µL 1%v/v collagen Vitrogen 100 (Section 5.3).

After 24h, the medium was removed and the solution of Mn(II) or Mn(VII) was added to each well and incubated for 72h at the selected concentrations ranging from 1 to 500µM.

Thereafter, 100µL MTT solution (1mg/mL HBSS) was directly added to each well and incubated for 2h at 37°C, 5%CO_2. The medium was discarded and 200µL of MTT Desorb solution (50% DMSO and 50% ethanol) were added to cells in order to solubilise the formazan crystals. Then, the plate was put on shaker for 15min until the black spots disappeared. The optical density of the solution obtained was read at 550 and 620nm (wavelengths of reference) (Spectra Max 250µL plate reader, Molecular Devices, Sunnyvale, CA, USA).

Table 16. MTT assay used to determine cell viability in PC12 exposed to Mn compounds: protocol.

1st day
1. Incubation of PC12 with Mn compounds
2. Addition of MTT[a] stock solution to incubating medium (HBSS) for 2h to 37°C
3. Remove medium and replace with 50% RPMI – 50% ethanol
4. Shake for 15min
5. Read absorbance at 550nm and 620nm against blank

7.2 Behaviour in culture medium

The behaviour of ^{54}Mn in RPMI was investigated by gel filtration on Sephacryl S200 (1.6x40cm) (Section 4.1.5) and by NMR (section 3.5).

7.3 Uptake

Table 17 summarizes the protocol of the study related to the uptake of ^{54}Mn, ^{52}Mn and ^{56}Mn in PC12 cells exposed to different concentrations of the radiolabelled Mn(II).

Table 17. ^{54}Mn, ^{52}Mn and ^{56}Mn in PC12 cells: protocol of uptake.

Seed 5x10^{5}cells in previously "coated" 75cm^2 flasks (CORNING) with 10mL of complete RPMI.
1st day
1. Replace the medium with 10mL of fresh RPMI containing the ^{54}Mn of interest and incubation for 24h
2. Add ^{52}Mn or ^{56}Mn for 3h (first experiment)
3. Add ^{56}Mn for 3h (second experiment)
4. Remove RPMI
5. Wash three times cells with 10mL of PBS
6. Add 1mL of Trypsin-EDTA (1X)
7. Harvest the cells using 10mL of RPMI
8. Count the cells by using a Bürker chamber
10. Wash twice the pellet with PBS (290xg, 10min)
11. Determinate the incorporation of different isotoper of the metal into cells (by counting the radiotracers or by NAA)

7.4 Intracellular distribution

The intracellular distribution of ^{54}Mn incorporated into cells has been studied by differential ultracentrifugation (Section 6.5).

7.5 Reactive oxygen species (ROS)

The determination of the rate of the ROS generation induced by Mn(II) and Mn(VII) in PC12 grown in RPMI 1640 medium was studied as reported in Section 6.13.

8. Studies on As in aggregating rat brain cell cultures and isolated brain cells (neurons, microglia and astrocytes)

In this work we have studied the uptake and biometylation of As(III) in rat brain aggregates and some of their cell components (neurons, microglia and astrocytes).

8.1 Uptake of As by brain aggregates

Table 18 summarize the protocol concerning the uptake of As(III) on Brain aggregates.

Table 18. Uptake of As in Brain aggregates: protocol.

Pooling of Re-aggregating brain cell cultures and distribution over six well plates (Nunc, Milan, Italy). Each well contained approximately 40 aggregates in 2ml of culture medium containing As(III).
4^{th} day
1. Remove medium
2. Wash twice the cells with 10mL of PBS
3. Harvest the cells using 10mL of complete medium
4. Count the aggregates by microscope
5. Count ^{73}As incorporated into Brain aggregates

8.2 Uptake of As by neurons, astrocytes and microglia cells

Table 19 summarizes the protocol concerning the uptake of As in neurons, astrocytes and microglia cells. In the same experiments, cell viability was estimated using the Alamar Blue assay (Al-Nasiry, 2007).

Table 19. Uptake of As in neurons, astrocytes and microglia cells: protocol.

Seed $1x10^6$ Neurons or Astrocytes or Microglial cells in 6-well plates coated with poly-L-lysine (Costar) with 2.5mL of culture medium containing As(III).

4^{th} day

1. Remove medium
2. Wash twice the cells with 10mL of PBS
3. Add 1mL of Trypsin-EDTA (1X)
4. Harvest the cells using 10mL of complete medium
5. Count the cells using a Bürker chamber
6. Wash twice the pellet with PBS (290xg, 10min)
7. Determination of the metal incorporated into cells (by counting ^{73}As)

8.3 Biomethylation studies

After exposure to As(III) (Table 19) the biomethylation of As(III) in rat brain aggregates was studied by their homogenisation and ultracentrifugation at 105000xg for 90min. Then, the extract was submitted to ion exchange chromatography according to the Tam's method (Section 4.1.1).

RESULTS

9. Elemental analysis of salts, culture media and cells

Tables 20 and 21 report the analytical data concerning the determination of impurities of As, Cd, Cr, Pt and V salts used for carcinogenicity studies, of the complete DMEM and of Balb/3T3 cells as determined by ICPMS, GFAAS or NAA (Section 3).

The following conclusions can be drawn:

(i) the impurities of more than 30 elements of the 14 compounds analysed ranged from a minimum of 0.0001 to 32.8ng/g for Cs and Fe in $NaAsO_2$ and $VOSO_4 6H_2O$ respectively (Table 20). The same Table reports detailed analytical data for elements, which are of particular interest in order to avoid artifacts in carcinogenicity studies (As, Cd, Cr, Pt and V) (Farina, 2003).

(ii) the quantitative baseline of background concentrations of As, Cd, Cr, Pt and V in the incubation DMEM medium were 6.2, 0.05, 16, 0.03 and 0.1µg/L respectively (Table 21). The corresponding values of such elements in unexposed Balb/3T3 cells were <0.03, <0.1, 0.3, <0.02 and 0.06fg/cell. The other elements tested in DMEM ranged from 0.0005 to 78µg/L for Ir and Zn respectively, while the corresponding values of Balb/3T3 cells were 0.00002 (Ir) and 36 (Zn) fg/cell[1].

Table 20. Elemental impurities of As, Cr, Pt and V salts used for carcinogenicity studies in Balb/3T3 cells.

Compounds	Concentration (ng·/g)						
	Max	Min.	As	Cd	Cr	Pt	V
$Na_2HAsO_4 \cdot 7H_2O$	0.5 (Al)	0.0005 (La)	-	0.03	-	-	0.3
$NaAsO_2$	6.4 (Al)	0.0002 (Cs)	-	0.15	1.72	<0.05	-
Asrsenocholine	24.1 (Fe)	0.008 (La)	-	<0.06	0.03	<0.04	<0.02
Arsenobetaine	14.3 (Fe)	0.001 (Cs)	-	<0.06	0.05	<0.01	0.04
Tetraphenylarsonium chloride	7.2 (Zn)	0.0002 (Rh)	-	1.9	4.9	0.002	0.42
$CdCl_2 \cdot 2H_2O$	18.6 (As)	0.0004 (La)	15.5	-	0.07	0.002	0.4
$Na_2CrO_4 \cdot 4H_2O$	9.3 (Fe)	0.0004 (Rh)	0.03	0.004	-	<0.002	1.2
$PtCl_2$	27.6 (Zn)	0.02 (Ce)	-	-	8.9	-	-
$PtCl_4$	12.4 (Zn)	0.001 (Be)	-	0.8	0.02	-	3.3
$(NH_4)_2PtCl_4$	3.3 (Mo)	0.0002 (In)	0.9	0.007	0.06	-	0.07
$(NH_4)_2PtCl_6$	3.9 (Zn)	0.003 (Sb)	0.6	0.008	0.03	-	0.09
$VOSO_4 \cdot 5H_2O$	32.8 (Fe)	0.0005 (Pd)	2.1	2.45	0.03	0.006	-
NH_4VO_3	23.5 (Fe)	0.0004 (Lu)	1.4	1.7	0.02	0.005	-

a: mean of 3 determinations, RSD<15%

Concerning the neurotoxicity studies on PC12 cell line, the content of Mn in unexposed cells and complete RPMI was 1.9fg/cell and 4.3µg/L respectively.

Table 21. Baseline concentrations of trace elements in Balb/3T3 cells and in complete DMEM culture medium[a].

Element	Balb/3T3 (fg/cell)	DMEM (µg/L)	Element	Balb/3T3 (fg/cell)	DMEM (µg/L)
As	**<0.03**	**6.2**	La	0.0007	0.001
Cd	**< 0.1**	**0.05**	Lu	0.0001	-
Cr	**0.3**	**16.0**	Mn	0.9	2.52
Pt	**< 0.02**	**0.03**	Mo	0.21	0.34
V	**0.06**	**0.1**	Ni	0.07	-
			Pb	0.2	0.34
Ag	0.05	0.11	Rb	0.6	4.8
Au	0.0013	0.08	Sb	0.002	0.43
Ba	< 6	5.99	Sc	0.0004	-
Ce	0.0025	0.01	Se	0.63	7.00
Co	0.06	9.40	Sn	< 0.6	0.03
Cs	0.044	0.02	Sr	<1.7	-
Cu	0.8	6.4	Ta	0.0009	0.03
Eu	0.0003	0.001	Tl	< 0.05	0.06
Fe	16.6	-	Rh	<0.0003	-
Ga	0.003	-	U	< 0.2	0.01
Hf	0.0009	0.002	W	0.002	0.002
Hg	0.08	0.06	Zn	36	78
Ir	0.00002	0.0005	Zr	< 0.05	0.08

a: Mean of 3-5 determinations, RSD<30%.

10. Studies on Balb/3T3 cell line

Hereafter are reported the results concerning the studies carried out on As, Cd, Cr, Pt and V compounds in Balb/3T3 cell line.

10.1 Arsenic

Results presented concern different As compounds. In particular, they are related to the following studies: cytoxicity, morphological neoplastic transformation, behaviour in culture medium, uptake, intracellular repartition, binding to biomolecules, biomethylation of inorganic As species , effect of trivalent inorganic As on number of cell generations (NGC), protein and nucleic acids content.

10.1.1 Cytoxicity assay (CFE)

Figures 14 and 15 illustrate the results of the Colony Forming Efficiency assay (CFE) carried out to estimate the cytotoxic effect induced in Balb/3T3 cells exposed for 72h to inorganic/organic As species.

The following remarks can be drawn:

(i) inorganic As(III) and As(V), but not AsF, inhibited CFE of cultured Balb/3T3 cells in a dose-dependent relationship (Figure 14A). Complete inhibition for As(III) and As(V) was reached at 20 and 50µM respectively (IC_{50}=1.5 and 5µM respectively).

(ii) phenylated organic As species such as Ph_3As and Ph_4As displayed a complete different cytotoxic response. Ph_3As did not induce a CFE inhibition at all doses tested (0.1 to 100µM) while Ph_4As inhibited CFE in a obvious dose-dependent relationship (IC_{50}=5µM) (Figure 14B).

(iii) MMA(V), DMA(V), TMAO did not cause a significant CFE inhibition also at high dose exposure (1000µM) (Figure 15A). No CFE inhibition was also

observed for Asβ, AsCh and TMAI (Figure 15B). On the contrary MMA(III) species induced a complete CFE inhibition already at 1µM exposure (IC_{50}=0.03µM) (Figure 15A).

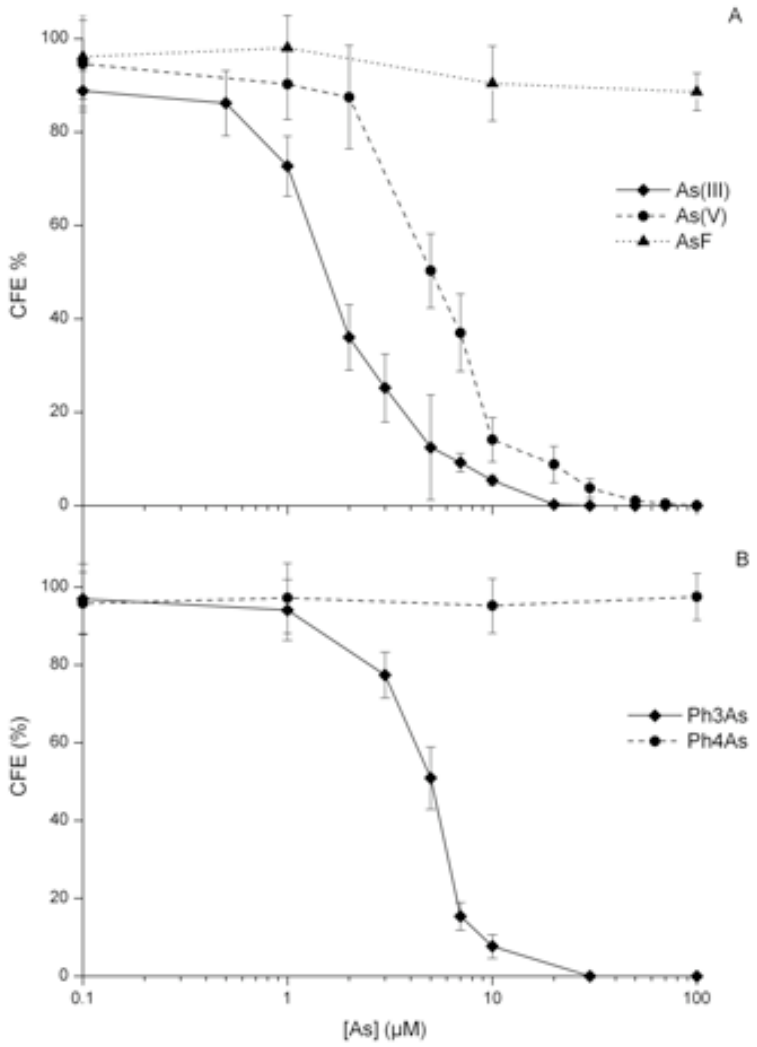

Figure 14. CFE response in Balb/3T3 cells exposed for 72h to different concentrations of inorganic As species (A) or to phenylated organoarsenic species (B).

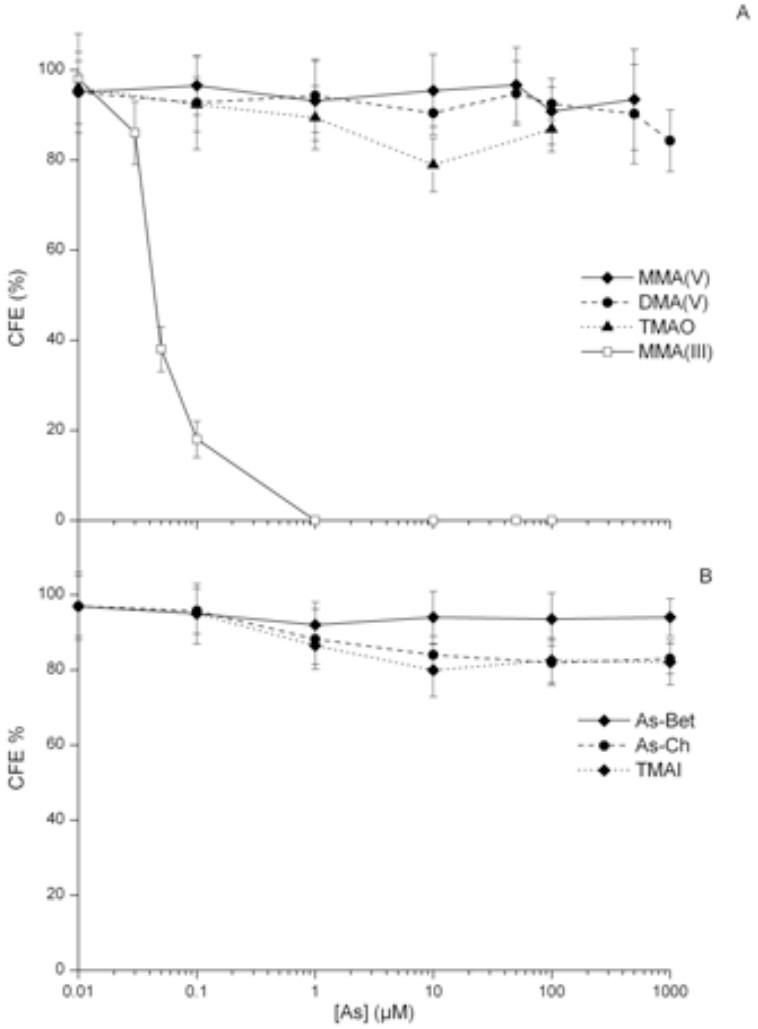

Figure 15. CFE response in Balb/3T3 cells exposed for 72h to different concentrations of methylated organoarsenic species considered As metabolites in mammals (A) or related to "seafood arsenic" (B).

10.1.2 Morphological transformation assay

Table 22 summarizes the analytical data of the concurrent cytotoxicity and morphological transformation assay carried out on Balb/3T3 cells exposed to inorganic (As(III), As(V) and AsF) or organic As (MMA(V), MMA(III), DMA(V), TMAO, Asβ, AsCh and Ph_4As) compounds.

The following remarks can be drawn:

(i) among the 3 inorganic As species tested, As(III) and As(V) were found positive in the transformation assay, inducing type III foci (Figure 16) in a dose-dependent fashion. On the contrary AsF failed in inducing the formation of any type III foci.

(ii) among the 7 organic As compounds tested only the phenylated Ph_4As species was found positive inducing a dose-dependent morphological transformation. No biomethylated organic As species were able to induce neoplastic transformation also at high concentration of exposure (500μM). The same results was also obtained for the MMA(III) compound tested for morphological transformation which was tested at low concentrations of 0.1 and 0.3μM (Table 22) being very toxic (Figure 15A).

The results of the concurrent cytotoxicity and transformation assays of As on Balb/3T3 cells exposed to 10, 20 and 30μM of As(V) alone or in combination with 3μM of DEM are shown in Table 23.

The following remarks can be drawn:

(i) As(V) alone was significantly positive in the transformation assay at doses of 20 and 30μM.

(ii) compared to the control, the transformation frequency was significantly lower in cells simultaneously exposed to the same As(V) concentrations and 3μM of DEM (Tf=2.6 and 7.8 at 20 and 30μM) than in cells exposed to As(V) alone (Tf=1.1 and 1.7 at 20 and 30μM).

Table 22. Cytotoxicity and morphological transformation of As species in Balb/3T3 cell line.

Exposure		CFE (%) ± SD	N° type III foci / N° dishes	N° type III foci positive dishes / N° dishes	Transformation frequency (T_f)	*p*
As chemical form	Dose (μM)					
H_2O biol.	**0.1% v/v**	100	1 / 20	1 / 20	0,03	N.S.
B*(a)*P[a]	**0.1**	10.5 ± 3	13 / 20	9 / 20	13.1	< 0.001
			INORGANIC As COMPOUNDS			
As(III)	**1**	78 ± 6	0 / 18	0 / 18	0.0	–
As(III)	**3**	28 ± 4	2 / 18	2 / 18	0.6	< 0.005
As(III)	**5**	12 ± 2	5 / 18	4 / 18	2.3	< 0.005
As(III)	**6**	5 ± 2	9 / 18	6 / 18	5.7	< 0.005
As(V)	**10**	53 ± 2	0 / 18	0 / 18	0.0	–
As(V)	**20**	28 ± 3	9 / 18	7 / 18	2.6	< 0.005
As(V)	**30**	11 ± 3	9 / 18	8 / 18	7.8	< 0.005
AsF	**20**	92 ± 4	0 / 18	0 / 18	0.0	–
			ORGANIC As COMPOUNDS			
Asβ	**100**	90 ± 6	0 / 18	0 / 18	0.0	–
Asβ	**500**	94 ± 3	0 / 18	0 / 18	0.0	–
AsCh	**100**	95 ± 3	0 / 18	0 / 18	0.0	–
AsCh	**500**	92 ± 5	0 / 18	0 / 18	0.0	–
MMA(V)	**100**	99 ± 6	0 / 18	0 / 18	0.0	–
MMA(V)	**500**	93 ± 5	0 / 18	0 / 18	0.0	–
MMA(III)	**0.1**	53 ± 5	0 / 18	0 / 18	0.0	–
MMA(III)	**0.3**	12 ± 4	0 / 18	0 / 18	0.0	–
DMA(V)	**100**	94 ± 6	0 / 18	0 / 18	0.0	–
DMA(V)	**500**	90 ± 8	0 / 18	0 / 18	0.0	–
TMAO	**100**	89 ± 2	0 / 18	0 / 18	0.0	–
Ph4As	**7**	37 ± 5	11 / 18	6 / 18	1.5	<0.01

a: α-benzopyrene, positive control

Table 23. Cytotoxicity and morphological tansformation of BALB/3T3 induced by As(V) alone or in presence of diethylmaleate (DEM).

Exposure		CFE (%) ± SD	N° type III foci / N° dishes	N° type III foci positive dishes / N° dishes	Transformation frequency (Tf)	*p*
As chemical form	Dose(μM)					
H_2O biol.	**0.1%v/v**	100	1 / 20	1 / 20	0,03	N.S.
B*(a)*P	**0.1**	10.5 ± 3	13 / 20	9 / 20	13,1	<0.001
As(V)	**10**	53 ± 2	0 / 18	0 / 18	0.0	–
As(V)	**20**	28 ± 3	9 / 18	7 / 18	2.6	<0.005
As(V)	**30**	11 ± 3	9 / 18	8 / 18	7.8	<0.005
As(V)+DEM	**20**	49 ± 5	5 / 18	3 / 18	1.1	<0.02
As(V)+DEM	**30**	26 ± 4	6 / 18	4 / 18	1.7	<0.01
DEM	**3**	88 ± 6	1 / 18	1 / 18	0.05	N.S.

a: α-benzopyrene, positive control

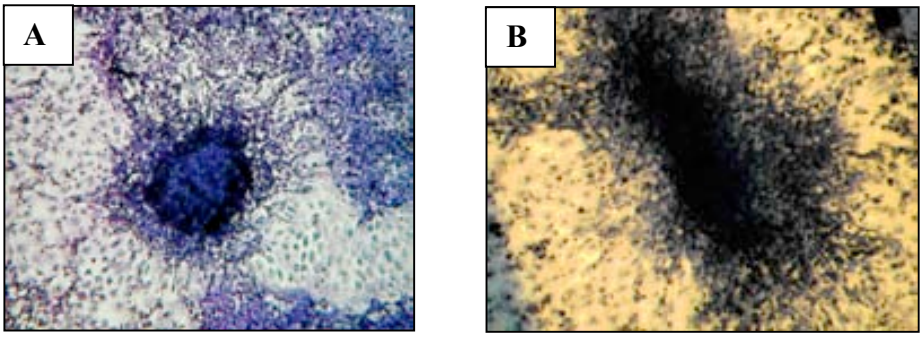

Figure 16. TypeIII foci induced in Balb/3T3 exposed to As(III) (A) or As(V) (B).

10.1.3 Behaviour in culture medium

Figure 17 illustrates the chromatograms of As(III), As(V), MMA(V), DMA(V), Asβ and AsCh after incubation for 72h with complete DMEM as obtained by HPLC-ICPMS. Compared to the chromatogram obtained at T=0, after 72h all chemical As species tested were eluted with the same retention time (Rt) and unchanged peak area.

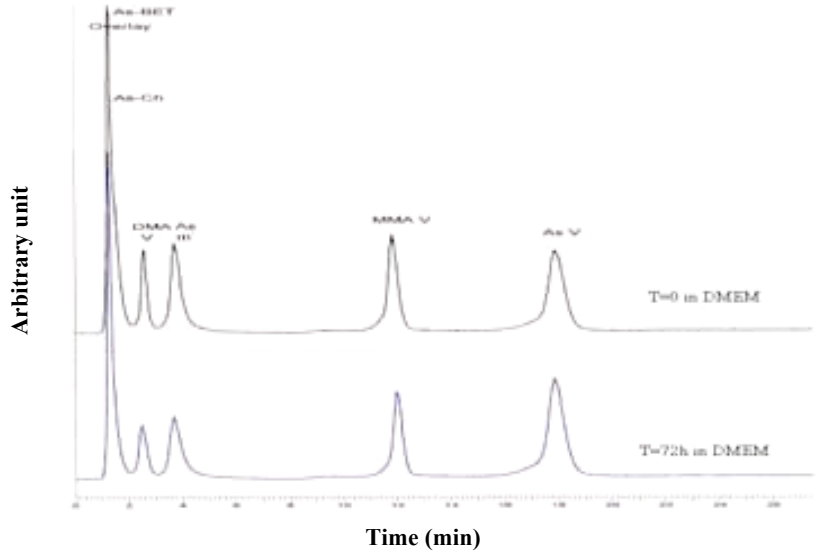

Figure 17. Stability of organic and inorganic As species after incubation for 72h in DMEM.

10.1.4 Uptake

Table 24 summarizes the analytical results of the uptake of As by Balb/3T3 cells, expressed as fgAs/cell, exposed for 24h to organic As (MMA(V), DMA(V), TMAO, Asβ, AsCh, Ph_4As) or inorganic (As(III), As(V), AsF) species, while Figures 18 and 19 show the corresponding curves expressed as pmol/10^6cells/h.

The following remarks can be drawn:

(i) the uptake of As in Balb/3T3 cells after incubation with inorganic As(III), As(V) and AsF was dose-dependent. Exposure to equimolar concentrations of the three As compounds resulted in about 4-fold higher incorporation of As in cells exposed to As(III) compared to As(V) and AsF (Figure 18).

(ii) the uptake of As by cells after incubation with organic As compounds was also linear with the dose. At high dose exposure (500μM) the As content ranged from 50.8 to 104.8fgAs/cell for TMAO and AsCh respectively. Concerning the organic As species present in "seafood", in the concentration range tested the cellular uptake of As (on average) was 2.8-fold higher for AsCh than Asβ. Exposure to the organic compound that was found transforming (Ph_4As) led to an uptake of 1.11fgAs/cell which was about 10 and 3-times lower compared to the transforming activity of As(III) and As(V) respectively.

Table 24. Uptake of As by Balb/3T3 cells exposed for 24h to different concentrations of various As species .

Dose exposure (µM)	Uptake (fgAs/cell)[a]								
	As(III)	As(V)	AsF	MMA(V)	DMA(V)	TMAO	Asβ	AsCh	Ph_4As
0.1	0.67	0.16	0.24	0.020	0.03	0.032	0.013	0.058	0.034
0.5	2.75	0.58	-	0.11	0.12	0.065	0.077	0.17	-
1	4.51	1.19	1.42	0.16	0.22	0.12	0.11	0.52	0.43
3	13.7	3.42	-	-	0.68	0.43	-	-	1.11
5	20.1	6.32	7.91	1.01	0.83	0.72	0.86	2.57	1.46
7	-	-	-	-	-	-	-	-	1.89
10	40.7	11.0	-	2.38	1.62	1.53	1.76	4.23	-
20	60.5	15.1	14.0	-	-	-	-	-	-
50	-	-	-	-	8.70	5.76	5.77	13.3	-
100	-	-	-	17.3	12.5	10.6	8.60	21.6	-
500	-	-	-	80.5	72.9	50.8	58.9	104.8	-

a: **MMA(III)** has been tested only at 1.0µM dose exposure leading to an uptake of 5.71fgAs/cell
Mean of 3 determinations, RSD<15%

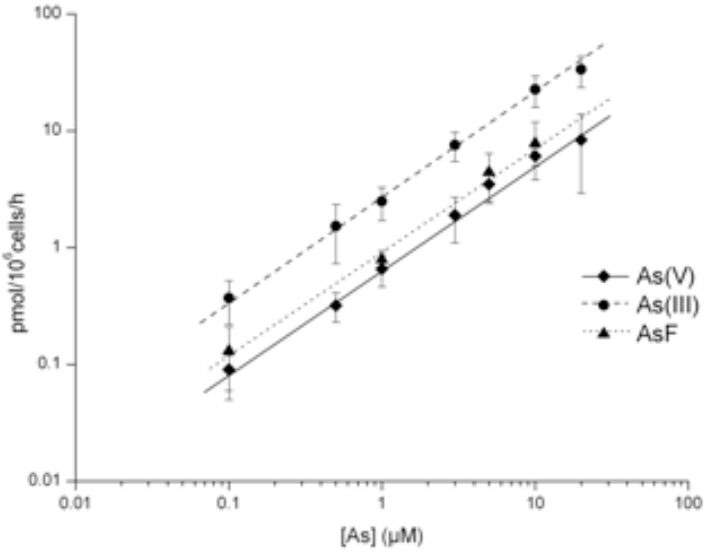

Figure 18 Uptake of As by Balb/3T3 exposed for 24h to inorganic As compounds.

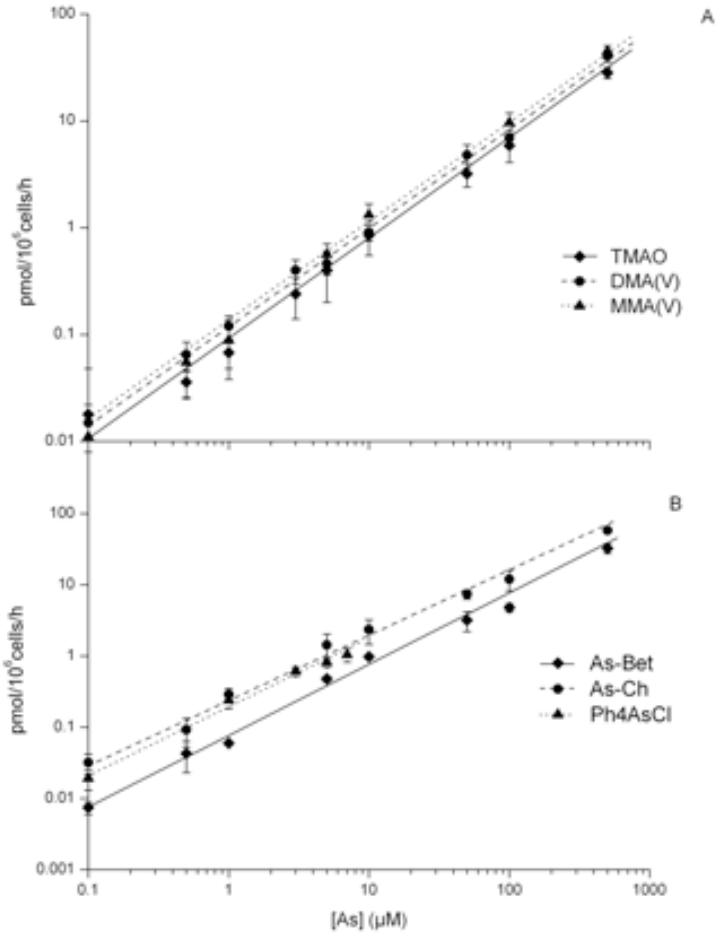

Figure 19. Uptake of As by Balb/3T3 exposed for 24h to organic As compounds.

10.1.5 Intracellular distribution and binding to biomolecules

Table 25 reports the intracellular repartition of As in Balb/3T3 cells exposed for 1, 24 and 72h to 0.1 and 3µM of As(III), to 3 and 30µM of As(V) and to 20µM AsF.

At non-toxic doses of exposure (0.1µM for As(III), 3µM for As(V) and 20µM for AsF) 92-98% of cellular As was present in the cytosol. At toxic doses these percentages decreased to 78-85% (As(III)) and to 81-94% (As(V)).

Table 26 and Figure 20 show the results of the experiments concerning the nature and the binding of As incorporated into cytosol as determined by ^{73}As radiotracer, Tam's method coupled with solvent extraction procedure (Section 4.1.1) and gel filtration (Section 4.1.5).

The following remarks can be drawn:

(i) in the cytosol of Balb/3T3 exposed for 72h 0.1µM ^{73}As(III) or 3µM ^{73}As(V), ^{73}As was recovered in the different Tam's fractions including those corresponding to the biomethylated forms as MMA(V) and DMA(V) (Table 26). Such organic species were not detected in the case of AsF as determined by NAA of the Tam's fractions. Interestingly, exposure to As(III) did not lead to appreciable amount of As(V) (1.1%) while in cell exposed to As(V) 86.5% of As was in trivalent state.

(ii) gel filtration of the ^{73}As-cytosol on Sephacryl S200 resin after exposure of Balb/3T3 cells to 0.1 and 0.5µM of ^{73}As(III) shows two peaks of As in the eluate: a first small in association with high molecular weight components (about 10% of the cytosolic As) and a second major peak emerging in the region of low molecular weight components (Figure 20).

Table 25. Intracellular repartition of As in Balb/3T3 cells exposed to inorganic ^{73}As(III), ^{73}As(V) or AsF species.

Exposure (h)	As content (% of the total homogenate)[a]									
	As(III)				As(V)				AsF	
	0.1µM		3µM		3µM		30µM		20µM	
	Pellet	Cytosol	Pellet	Cytosol	Pellet	Cytosol	Pellet	Cytosol	Pellet	Cytosol
1	5	95	22	78	3	97	6	94	3	97
24	4	96	19	81	3	97	10	90	7	93
72	8	92	15	85	2	98	19	81	5	95

a: Mean of 3-5 determinations, RSD<30%.

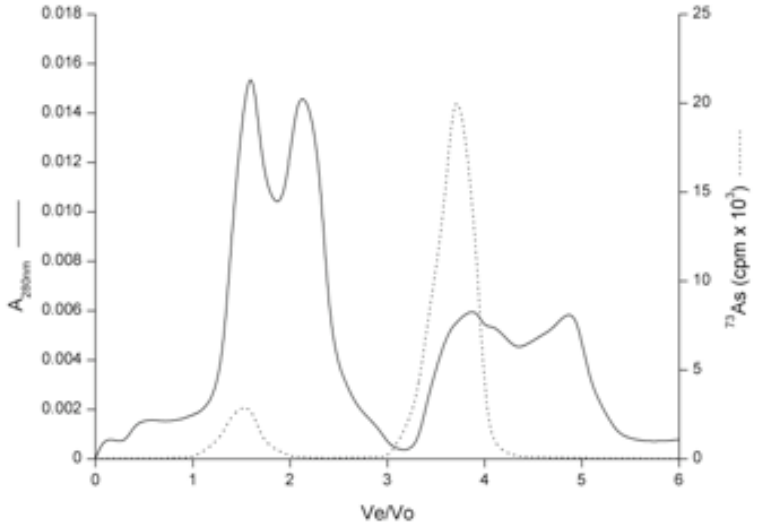

Figure 20. Gel filtration on Sephacryl S-200of the cytosol from Balb/3T3 cells exposed to 0.1 and 0.5µM of ^{73}As(III).

10.1.6 Biomethylation

Table 26 summarizes the data on the speciation of As (Tam's method and solvent extraction, Section 4.1.1) in cell-containing medium and in the cytosol of Balb/3T3 cells exposed for 72h to 0.1, 3 and 20µM As(III), As(V) and AsF respectively.

The following remarks can be drawn:

(i) As(III) exposure: more than 94% of As was present in the organic phase of the DTTC extraction (As(III) fraction). Less than 5% was eluted in H_2O and NH_4OH fractions (biomethylated forms).

(ii) As(V) exposure: the As repartition in the different fractions of the cytosol were similar to that of As(III). In cell-containing medium 12,6% of As appeared in the fraction corresponding to As(III).

(iii) AsF exposure: less than 2,5% were extracted in the organic phase from DDTC solvent extraction. No significant As was detected in the fractions corresponding to biomethylated forms.

Table 26. Speciation of As: (i) in the cytosol of Balb/3T3 cells exposed for 72h to 0.1µM ^{73}As(III), 3µM ^{73}As(V) and 20µM AsF (ii) in cell-containing culture medium.

Fraction	As species	As species (% whole samples)[a]	
		Cytosol	Cell-containing medium
	^{73}As(III)		
Whole cytosol or cell-containing medium		100	100
0.5M HCl	As(III)+As(V)	96.2	98.2
DDTC[b] organic phase	As(III)	94.6	96.7
DDTC[b] aqueous phase	As(V)	1.6	1.5
H_2O	MMA(V)	2.1	0.4
4M NH_4OH	DMA(V)	1.7	1.4
	^{73}As(V)		
Whole cytosol or cell-containing medium		100	100
0.5M HCl	As(III)+As(V)	94.5	97.6
DDTC[b] organic phase	As(III)	92.8	12.6
DDTC[b] aqueous phase	As(V)	1.7	85.0
H_2O	MMA(V)	3.4	0.8
4M NH_4OH	DMA(V)	2.1	1.6
	AsF		
Whole cytosol or cell-containing medium		100	100
0.5M HCl	As(III)+As(V)	100	100
DDTC[b] organic phase	As(III)	2.1	1.2
DDTC[b] aqueous phase	As(V)	97.9	98.8
H_2O	MMA(V)	ND	ND
4M NH_4OH	DMA(V)	ND	ND

a: mean of 3 determinations, RSD<30%
b: DDTC=diethyldithiocarbamate

10.1.7 Effect of As(III) on NCG, protein and nucleic acid

Figures 21-24 show the curves concerning the effect of exposure of Balb/3T3 cells to 0.4, 1 and 3µM As(III) on NGC, protein, DNA and RNA content.

The following remarks can be drawn:

(i) there is a clear inhibition of cell proliferation for all the doses tested (Figure 21).

(ii) a gradual increase of total protein can be observed from 0.35mg/10^6cells in unexposed cells to 1mg/10^6cells in cell exposed to 3µM of As(III) (Figure 22).

(iii) the RNA content increased from 80µg/10^6cells at 0.4µM As(III) to 185µg/10^6cells at 3µM, while the total DNA was double compared to control values for exposed cells at all the dose studied (Figure 23). The ratio RNA/DNA increased linearly as a function of the dose (Figure 24).

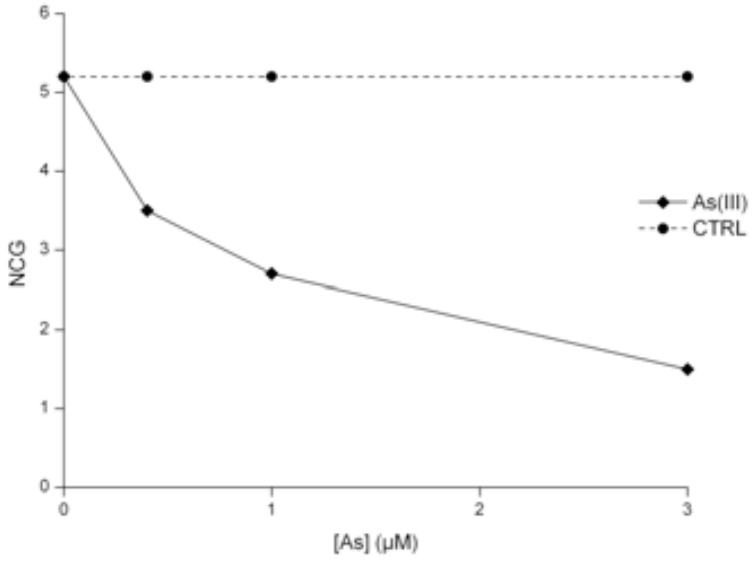

Figure 21. Number of Cell Generation (NCG) of Balb/3T3 cells exposed to different concentrations of As(III). Basal mean value=5.2NGC.

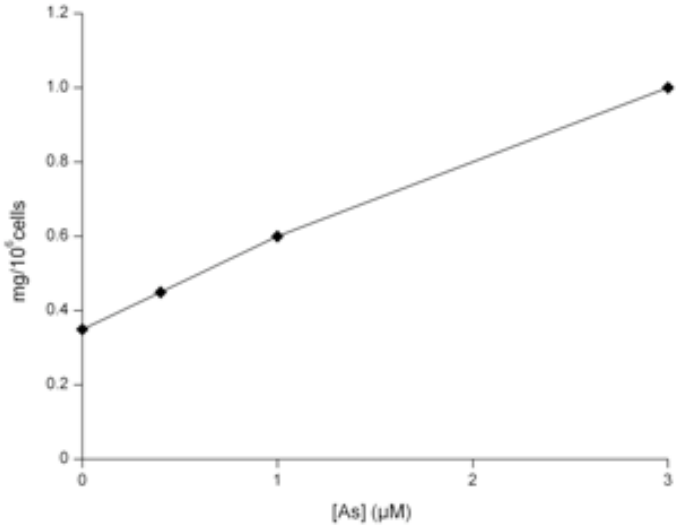

Figure 22. Total cell protein in Balb/3T3 cells exposed to different concentrations of As(III). Basal mean value=0.35mg/10^6cells.

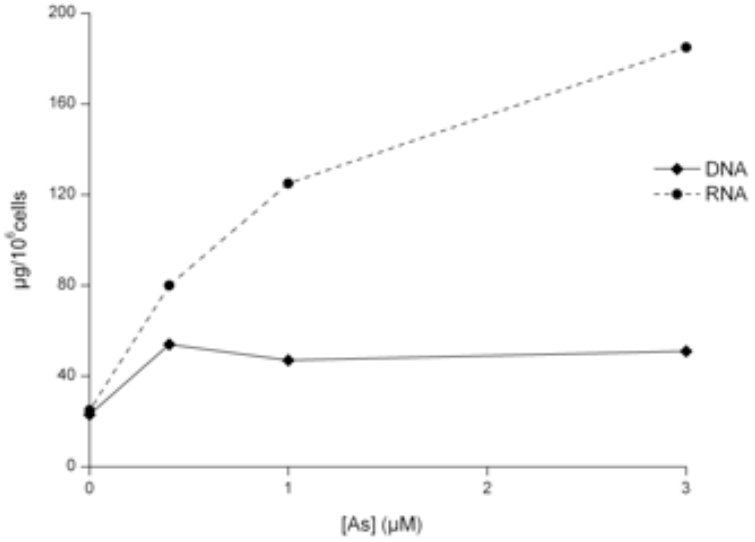

Figure 23. Total DNA and RNA of Balb/3T3 cells exposed to different concentrations of As(III). Basal mean values: DNA=27µg/10^6cells; RNA=2523µg/10^6cells.

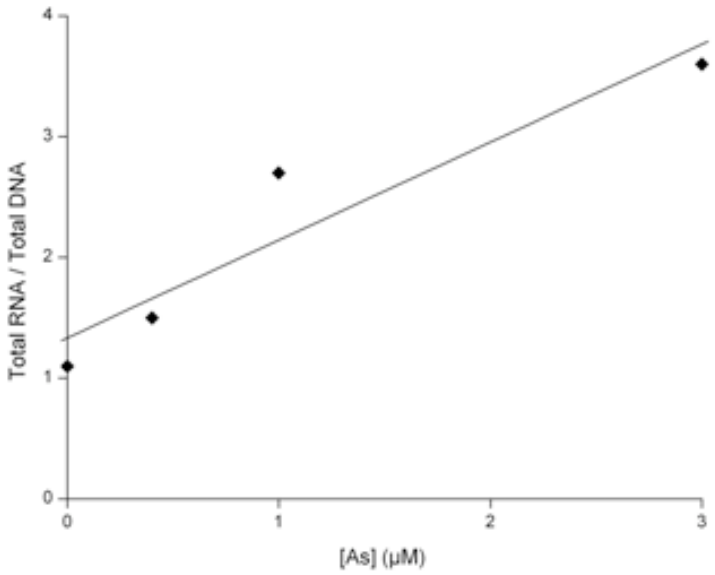

Figure 24. Ratio DNA/RNA for Balb/3T3 cells exposed to different concentrations of As(III).

10.1.8 Binding of As(III) to DNA

Table 27 reports the results of the As incorporated into DNA from Balb/3T3 cells after exposure for 72h to 0.5µM ^{73}As(III) as determined by NucleoSpin method (Section 4.3) while Table 28 summarizes the data concerning the ultrafiltration of a solution obtained *in vitro* by incubating 0.5µM ^{73}As(III) with DNA previously isolated from Balb/3T3 cells.

The following remarks can be drawn:

(i) no significant As content (<0.005ngAs) was found in DNA fraction isolated from Balb/3T3 after exposure to ^{73}As(III) (Table 27).

(ii) no significant As content was found retained on the ultrafiltration membrane(Table 28).

Table 27. Incorporation of As into DNA isolated from Balb/3T3 exposed to 0.5µM ^{73}As(III) for 72h.

Fraction	As content[a]	
	ngAs/fraction	%
Homogenate	7.2	100
Eluate	6.3	86.4
Washings	0.9	13.6
DNA fraction	<0.005	~0.0004

a: mean of 3 determinations, RSD<15%

Table 28. Ultrafiltration of DNA, previously isolated from Balb/3T3 cells, incubated *in vitro* with 0.5µM ^{73}As(III).

Fraction	As content[a]	
	ngAs/fraction	%
Incubation mixture	38	100
Ultrafiltrate	27.4	72.2
Washings	10.6	27.8
Membrane	~0.007	~0.0005

a: mean of 3 determinations, RSD<10%

10.2 Cadmium

Results reported are related to the exposure of cells to $CdCl_2 \cdot 2H_2O$ (Cd(II)). They concern: cytotoxicity, morphological transformation (including the influence of the glutathione (GSH) depletion), uptake, intracellular distribution, binding to cytosolic biomolecules (metallothionein) as well as to DNA and aminoacid cross-linking.

10.2.1 Cytotoxicity assay (CFE)

The cytotoxicity induced in Balb/3T3 cells exposed for 3, 24 and 72h to increasing Cd(II) concentrations ranging from 0.5 to 20µM was analysed by CFE. The CFE decreased gradually for the different exposure times with the increase of Cd(II) concentrations indicating that the induced cell toxicity is time and dose-dependent. The IC_{50} values drawn from the graphics of Figure 25 were 15, 7 and 4µM at 3, 24 and 72h, respectively.

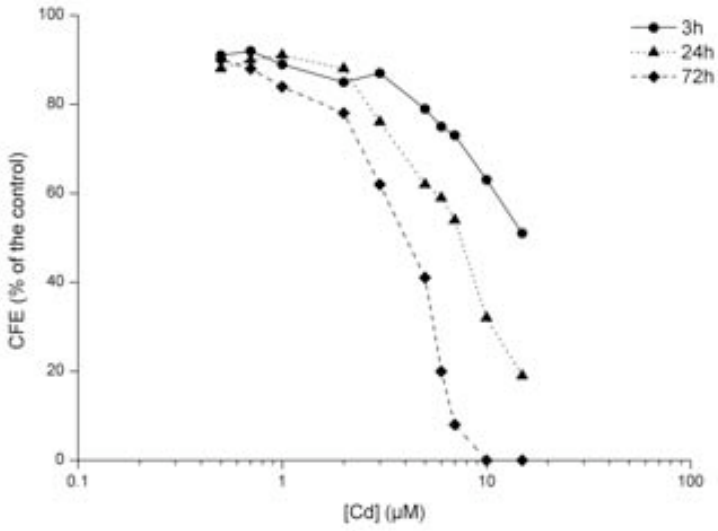

Figure 25. CFE response in Balb/3T3 cells exposed to different concentrations of Cd(II).

In order to study the effect of GSH depleting agents on Cd(II) cytotoxicity, experiments were carried out by exposing Balb/3T3 for 12h to increasing concentrations of Cd(II) alone or in combination with 1µM buthionine-S-R-

sulfoximine (BSO) or 10µM diethylmaleate (DEM). The concentrations of the two depleting agents were selected after an "ad hoc" study on the determination of their cytotoxic effects in Balb/3T3 cells as measured by CFE (Figure 26, derived IC_{50} at 72h were 2.3 and 18 µM for BSO and DEM, respectively).

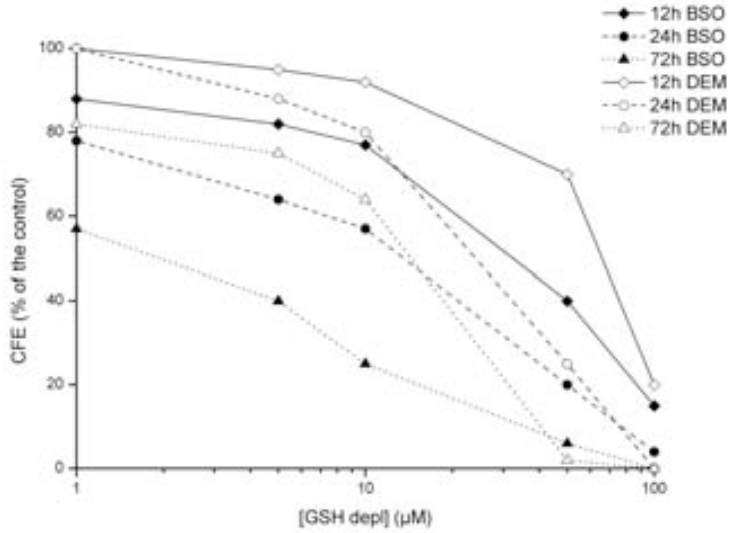

Figure 26. CFE response in Balb/3T3 cells exposed at different times to increasing concentrations of two GSH- depleting agents (BSO and DEM).

Figure 27 shows how the inhibition of CFE was significantly higher when the cells were simultaneously incubated with Cd(II) and BSO or Cd(II) and DEM in comparison to the corresponding value concerning the exposure to metal alone. The inhibition level was higher in Cd-exposed cells in presence of 10 µM DEM than of 1µM BSO. The derived IC_{50} in cells exposed to Cd(II) alone was 8.3µM, while this value decreased to 6 and 3.5µM in presence of BSO and DEM, respectively.

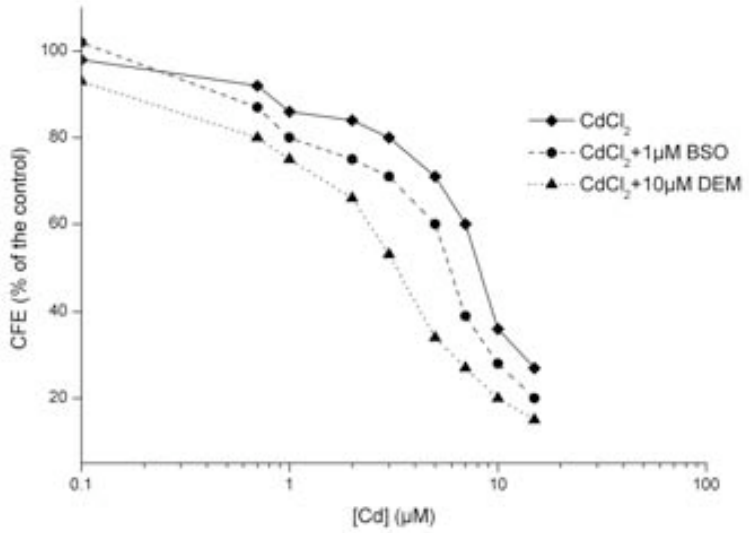

Figure 27. CFE response in Balb/3T3 cells exposed for 12h to different concentrations of Cd(II) alone or in combination with 1µM BSO or 10µM DEM.

10.2.2 Morphological transformation assay

Table 29 summarizes the results of the concurrent cytotoxicity and morphological transformation assays carried out on Balb/3T3 cells exposed to Cd(II) alone or in presence of 3µM DEM. The DEM concentration was drawn from the CFE data of the exposure of Balb/3T3 for 72h to this GSH-depleting agent (Figure 26).

The following remarks can be drawn:

(i) morphological features of the cells changed in a consistent manner after transformation. Differently from the non-transformed cells that grew in a monolayer the Cd-transformed cells showed morphological changes including invasiveness, disoriented criss-cross organization, multilayer growth, piling and foci formation

(ii) the transformation frequency was dose-dependent for the tested Cd(II) concentrations. Compared to the controls, the transformation frequency (Tf) was significantly and consistently higher in Balb/3T3 cells simultaneously exposed to

Cd(II) and 1μM DEM compared to the corresponding values in cells exposed to Cd(II) alone (Figure 28). However, exposure to Cd alone led to no statistically significant difference in the formation of foci type III up to 2μM while in the simultaneous exposure to Cd and 3μM DEM a statistical significant difference was achieved at 1μM (Table 29).

Table 29. Concurrent cytotoxicity and morphological transformation induced in Balb/3T3 cell line by exposure to Cd(II) alone or in presence of 3μM DEM.

Exposure		CFE (%) ± SD	N° type III foci / N° dishes	N° type III foci positive dishes / N° dishes	Transformation frequency (T_f)	*p*
Cd chemical form	**Dose (μM)**					
H_2O biol.	**0.1% v/v**	100	0 / 20	0 / 20	0.00	N.S.
B*(a)*P[a]	**0.1**	10.5 ± 3	13 / 20	9 / 20	13.1	<0.001
			Cd(II)			
$CdCl_2$	**0.7**	91±5	1 / 20	1 / 20	0.15	N.S.
	1	85±7	4 / 20	3 / 20	0.40	N.S.
	2	80±5	2 / 20	2 / 20	0.48	N.S.
	3	67±8	9 / 20	7 / 20	1.80	$1.4 \cdot 10^{-3}$
	5	48±6	18 / 20	15 / 20	3.50	$1.77 \cdot 10^{-6}$
	6	24±6	13 / 20	12 / 20	4.60	$5.08 \cdot 10^{-7}$
	7	12±8	8 / 20	7 / 20	7.60	0.0025
	10	0	0 / 20	0 / 20	-	-
			Cd(II) + 3μM DEM			
$CdCl_2$	**0.7**	80±4	2 / 20	2 / 20	0.39	N.S.
	1	72±7	4 / 20	3 / 20	0.81	0.038
	3	41±3	11 / 20	10 / 20	5.00	0.001
	5	26±4	16 / 20	14 / 20	9.30	$2.3 \cdot 10^{-7}$
	7	5±2	10 / 20	9 / 20	14.00	$1.76 \cdot 10^{-11}$
	10	0	0 / 20	0 / 20	-	-

a: α-benzopyrene, positive control

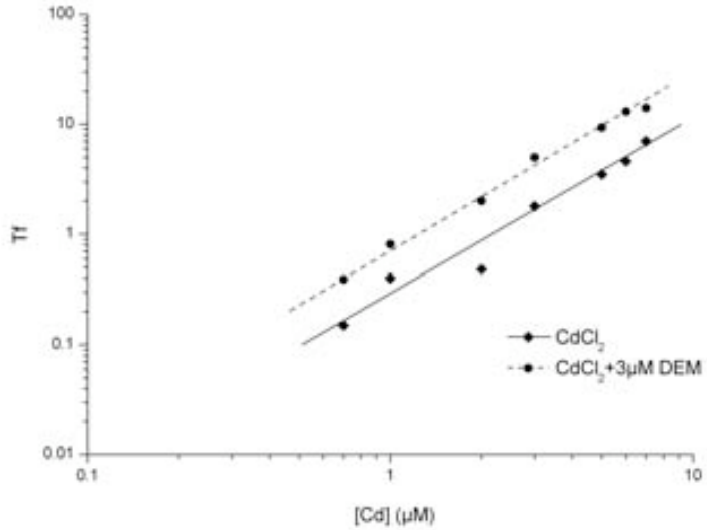

Figure 28. Transformation frequency from studies on in Balb/3T3 cell line by exposure to Cd(II) alone or Cd(II)+3μM DEM.

10.2.3 Uptake

Cadmium uptake was investigated in cells exposed to increasing Cd(II) concentrations ranging from 0.5 to 10μM for 3, 24 and 72h.

Cadmium uptake by cells, expressed as nmolCd/10^6cells, was a concentration-dependent process (Figure 29). The accumulation increased linearly up to 2μM at 3h post-exposure and to 5μM at 24 and 72h post-exposure, then the Cd taken up by cells leveled off or slightly decreased. Interestingly, the uptake of Cd at 72h in presence of 1μM DEM was similar to that of cells exposed to Cd(II) alone.

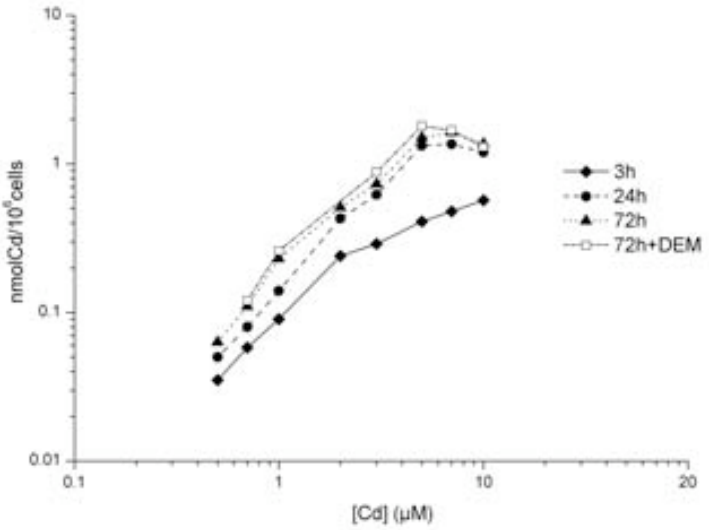

Figure 29. Uptake of Cd by Balb/3T3 cells exposed to Cd(II) alone or in presence of DEM

10.2.4 Intracellular disribution

Table 30 reports the time course intracellular repartition between cells organelles and cytosol of the accumulated Cd examined after 24 and 72h cells exposure to increasing Cd(II) concentrations.

At both times considered and up to 3μM Cd(II) exposure, the element was consistently recovered into cytosol (from 98.4 to more than 99% of the cell-associated Cd) and only 2-3% was recovered associated to cell organelle. At higher doses (5 and 7μM) a decreasing of the metal in the cytosol of the order of 10% was observed which was matched by an increase of the element in cell organelles.

Table 30. Intracellular repartition of Cd between cytosol and cell organelles (pellet) of Balb/3T3 cells exposed for 24 and 72h to Cd(II), and association of cytosolic Cd to cadmium-binding protein (Cd-BP).

Dose (μM)	ngCd/10^6cells					
	24h			72h		
	Pellet	Cytosol		Pellet	Cytosol	
		Whole	Cd-BP		Whole	Cd-BP
0.5	0.03	5.6	5.6	0.12	7.0	7.0
0.7	0.03	9.1	9.1	0.16	12.3	12.3
1	0.40	15.3	15.3	0.51	25.2	25.2
2	0.90	47.2	47.2	1.7	55.4	55.4
3	1.4	68.0	68.0	3.3	78.4	78.4
5	10.4	138.6	116.2	15.1	153.1	120.5
7	16.7	135.5	114.0	21.9	160.7	124.2

a: mean of 3 determinations, RSD<10%

10.2.5 Distribution among cellular components

Analysis of $^{109}CdCl_2$ content in Superdex-75 eluates after application of the 110000xg supernatant (cytosol) showed that, after 72h of exposure to 1μM Cd, the metal was bound only to a low molecular weight component (Cd-BP) eluted at Ve/Vo=2.2÷2.6 (molecular weight of 6KDa) (Figure 30C). However, at dose exposure of 5μM Cd, two other small but obvious peaks of ^{109}Cd emerged in the chromatogram in association with UV absorbing material: the first was eluted after the void volume (Ve/Vo=1, high molecular weight components), approximately accounting for 3% of the total cytosolic Cd; the second (approximately 7% of the cytosolic Cd) appeared in the region of molecular weight components <3KDa (Figure 30D).

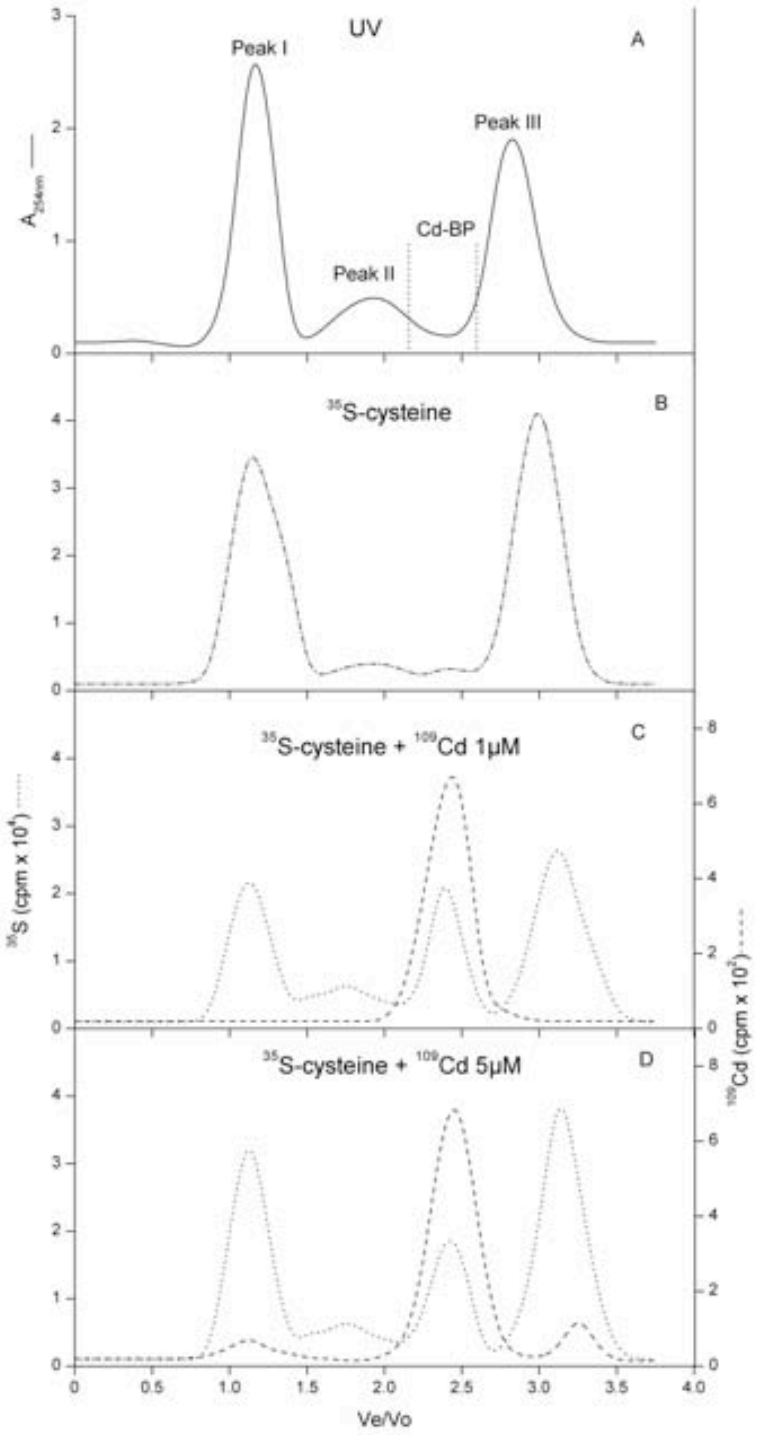

Figure 30. Superdex-75 elution profiles of cytosol from Balb/3T3 cells exposed to 1µM and 5µM ^{109}Cd(II) and ^{35}S-cysteine for 72h.

10.2.6 Induction of Cd-BP

To further investigate whether Cd accumulation in the cytosol corresponded to enhanced synthesis of Cd-BP, Balb/3T3 cells were exposed or not to $^{109}CdCl_2$ in presence of ^{53}S-cysteine. This doubly radiolabelling technique had the advantage of being able to simultaneously follow the incorporation of sulfur and Cd into cellular components. Figure 30 displays UV, ^{35}S and ^{109}Cd radioactivity profiles of the eluates of Balb/3T3 cytosols of unexposed cells or of cells exposed to ^{35}S-cysteine alone or in presence of 1 and 5μM $^{109}CdCl_2$.

Three UV absorbing peaks were eluted from the column (Figure 30A): the first peak appeared in the void volume and thus had a molecular weight >300KDa (peak I, high molecular weight components); the second peak (peak II) emerged in the region of 75÷80KDa as determined by a molecular weight calibration curve (Figure 6), whereas a third UV absorbing peak (peak III) was eluted in the chromatographic region of low molecular weight (<3KDa).

Figure 30B shows the ^{35}S radioactivity distribution in the cytosol of cells exposed to ^{35}S-cysteine but not to $^{109}CdCl_2$. Three ^{35}S peaks emerged from the column in association with UV-absorbing peaks I, II and III. The repartition of ^{35}S among the three peaks was of the order of 43, 2 and 55% of the total ^{35}S in the cytosol. A very small ^{35}S peak was also present in the chromatogram at Ve/Vo=2.2÷2.6, corresponding to the region of 6KDa.

Figures 30C and D show the ^{35}S and ^{109}Cd distribution in the cytosol of cells exposed to ^{35}S-cysteine and 1 or 5μM $^{109}CdCl_2$. In cells exposed to 1μM of $^{109}CdCl_2$ the radioactivity was totally recovered in one peak, eluted in the region at Ve/Vo=2.2÷2.6 (Cd-BP region), in association with a obvious ^{35}S peak (Figure 30C).

The ^{35}S associated to Cd-BP peak accounted for about 30% of the total ^{35}S incorporated into cytosol.

Differently, in the cytosol of cells exposed to ^{35}S-cysteine and 5μM $^{109}CdCl_2$ a small but significant amount of ^{109}Cd radioactivity appeared in the chromatogram, being distributed in the peaks I and II, which accounted for about 5 and 10% of the total ^{109}Cd in the cytosol, respectively.

In order to confirm the protein nature of the 6KDa ^{109}Cd- and ^{35}S- containing Cd-BP (Figure 30C), two "ad hoc" experiments were carried out:

(i) heat stability. Figure 31 shows that were no significant change of ^{109}Cd and ^{35}S associated with 6KDa component after heat treatment (Figure 31A) compared to the non-heated component (Figure 31B) (section 6.11). However, there was a significant decrease in the amount of ^{35}S recovered in the void volume peak I. This decrease was accompanied by an increase of the ^{35}S associated with the low molecular weight components, peak III (Figure 31C).

(ii) UV absorption. Figure 32 shows the spectrophotometric analysis concerning the ultraviolet absorbance of the chromatographic fractions derived from the gel filtration shown in Figure 31C. The results of this analysis indicate that the 6KDa molecular weight component (Cd-BP) absorbed at 254nm but had a poor absorbance at 280nm (Section 6.12). In contrast, fractions corresponding to peak I (high molecular weight components) showed absorbance at both wavelengths.

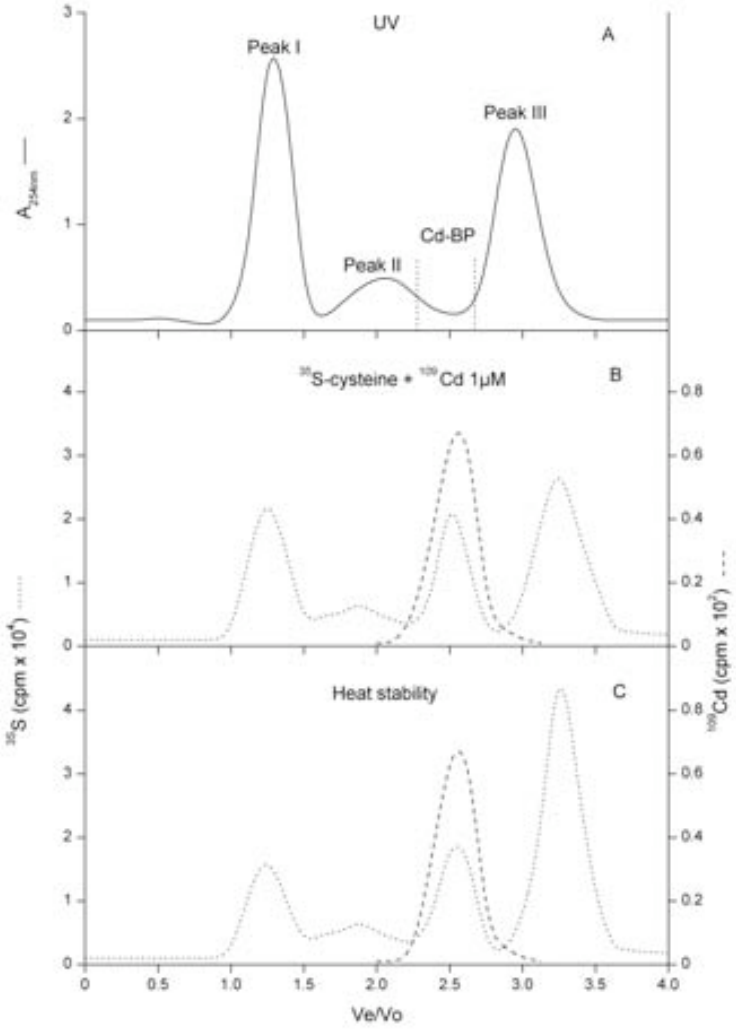

Figure 31. Superdex-75 elution profiles of cytosol heated (Figure 29C) or not (Figure 29B) from Balb/3T3 cells exposed to 1µM ^{109}Cd(II) and ^{35}S-cysteine for 72h)

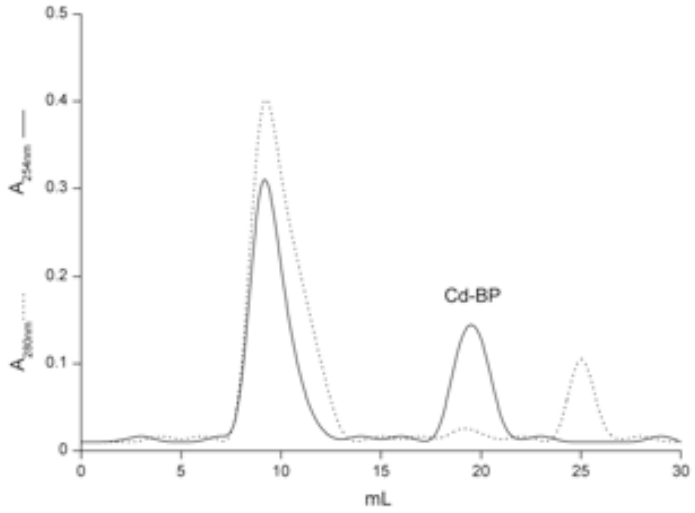

Figure 32. Ultraviolet absorbance of the chromatographic Gel filtration at 280 and 254nm of DMEM arising from Balb/3T3 cells exposure to 1µM Cd(II)

We can reasonably conclude that the 6KDa (Cd-BP) component in Balb/3T3 cells exposed to $CdCl_2$ is a metallothionein-like protein. Thus, from gel filtration of the cytosols of ^{109}Cd-exposed cells (from 0.5 to 7μM) and the measure of ^{109}Cd profiles in the eluates, it was possible to detect the proportion of Cd bound to Cd-BP compared to the total Cd incorporated into the cytosol (Table 30). The results show that up to 3μM of Cd exposure the metal in the cytosol was associated only to the Cd-BP component, while at 5 and 7μM a significant amount, ranging from 17% (exposure to 5μM $CdCl_2$ for 24h) to 22.8% (7μM for 72h) was recovered in components other than Cd-BP, in agreement with the results of Figures 30C and D.

Interestingly, the enhancement of the amount of Cd-BP, estimated by the incorporation of ^{109}Cd, tended to be of the same order of magnitude in Cd-treated cells at 24 and 72h post-exposure (Table 30).

Table 31 reports the results concerning the time course effects of BSO and DEM treatment on Cd-induced levels of ^{35}S-cysteine incorporation into Cd-BP fraction. In 1μM Cd-exposed cells, Cd significantly induced accumulation of ^{35}S-cysteine into Cd-BP at 6, 12, 24 and 72h post-exposure. BSO and DEM treatment had a different effect on Cd-induced ^{35}S-cysteine incorporation into Cd-BP: BSO significantly enhanced Cd-induced ^{35}S-cysteine incorporation at 6 and 12h post-exposure. The increases were of the order of 30% compared to the ^{35}S-cysteine incorporation in cells exposed to Cd alone. On the contrary, DEM decreased the ^{35}S-cysteine incorporation into Cd-BP (about 35% for 10μM DEM at 72h).

Table 31. Incorporation of ^{35}S into Cd-BP of Balb/3T3 cells exposed at different times to Cd(II) in presence or not of BSO and DEM

Treatment	^{35}S incorporated into Cd-MT (cpm x 10^3 ± SD)			
	6h	12h	24h	72h
Unexposed cells(Ctrl)	0.43	0.72	0.84	0.88
1µM $CdCl_2$	73±6	142±11	153±16	157±18
1µM $CdCl_2$ + 1µM BSO	96±8	181±14	-	-
1µM $CdCl_2$ + 10µM DEM	49±7	108±8	-	-
1µM $CdCl_2$ + 3µM DEM	-	-	112±21	103±9

10.2.7 Binding to DNA and aminoacids cross-links

Figure 33 displays the elution profiles from gel filtration on Sephadex G-25 resin of (i) a solution of 1µM $^{109}CdCl_2$ incubated *in vitro* for 1h with DNA previously isolated from Cd-unexposed Balb/3T3 cells (Figure 33A) (ii) a solution of DNA isolated by NucleoSpin from Balb/3T3 cells previously exposed for 72h to 1 or 5µM of $^{109}CdCl_2$ (Figure 33B) (iii) a solution of DNA isolated from Balb/3T3 cells previously exposed for 72h to 1 or 5µM $^{109}CdCl_2$ and simultaneously to a cocktail of ^{14}C-aminoacids (Figure 33C).

The following remarks can be drawn:

(i) a small peak of ^{109}Cd was found associated to DNA previously isolated from Balb/3T3 cells. The ratio was 0.01ngCd/µgDNA (Figure 33A).

(ii) a peak of ^{109}Cd was eluted in association to DNA fraction isolated from ^{109}Cd-treated cells. The ratios measured were 0.92 and 1.75ngCd/µgDNA in cells exposed to 1 and 5µM $^{109}CdCl_2$, respectively (Figure 33B). These latter values didn't change significantly when Cd-exposed cells were simultaneously exposed to a cocktail of ^{14}C-aminoacids. Interestingly, a marked presence of ^{14}C

radioactivity was also associated to the UV absorbing peak of DNA to which ^{109}Cd radioactivity was bound.

In order to verify the stability of the complex ^{109}Cd- ^{14}C- DNA, a DNA sample, after incubation with Tris and EDTA, was submitted to repeated washes in Ultrafree Filter unit. Figure 34 shows the stability of Cd-induced ^{14}C-amino acid DNA crosslinks and ^{109}Cd-binding in Balb/3T3 cells. Repeated washings of AA(s)-DNA complex reduced Cd concentration without reducing AA(s) association once loosely associated AA(s) were washed out. This indicated that the amino acids were tightly bound to DNA, but such strong binding didn't depend upon direct Cd presence.

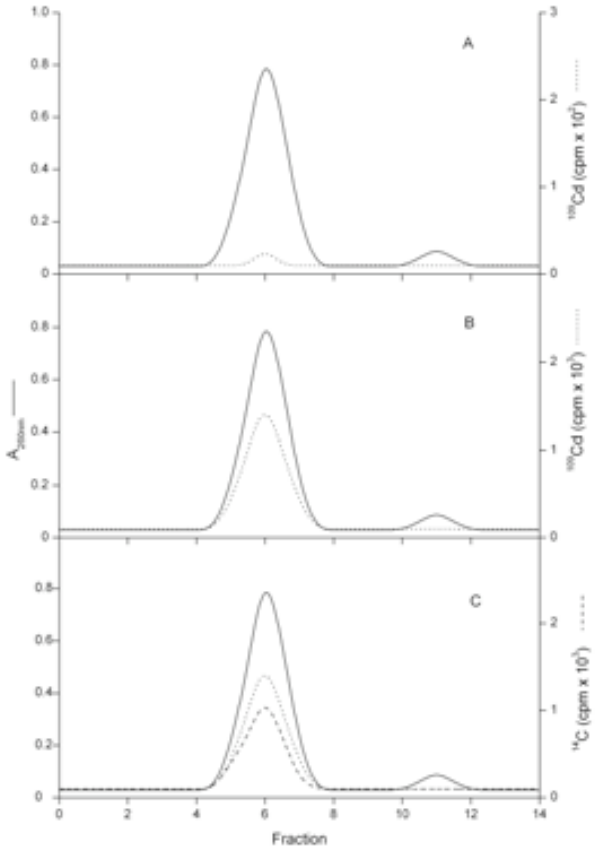

Figure 33. Binding of ^{109}Cd to DNA: previously isolated from Balb/3T3 cells (A); isolated from 1µM ^{109}Cd-treated cells (B); isolated from 1µM ^{109}Cd- and ^{14}C-aminoacids (C).

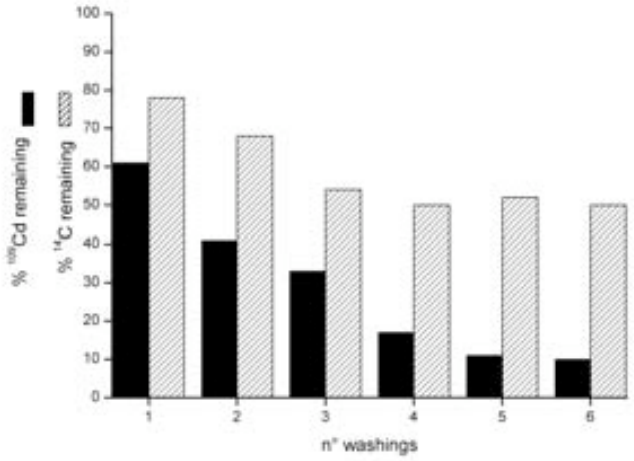

Figure 34. Stability of ^{109}Cd-induced ^{14}C-aminoacids DNA crosslinks in Balb/3T3 cells after 6 washings.

10.2.8 Reactive oxygen species (ROS)

The ROS level were measured in Cd-treated Balb/3T3 cells to examine the involvement of oxidative stress in Cd cytotoxicity (Figure 35). It appears that all the Cd concentrations tested induce an increase in ROS levels in a dose-dependent fashion. After 1h of Cd exposure to 1, 3 and 5µM the increase was 2.1, 2.4 and 3.2-fold higher compared to the corresponding value of unexposed cells.

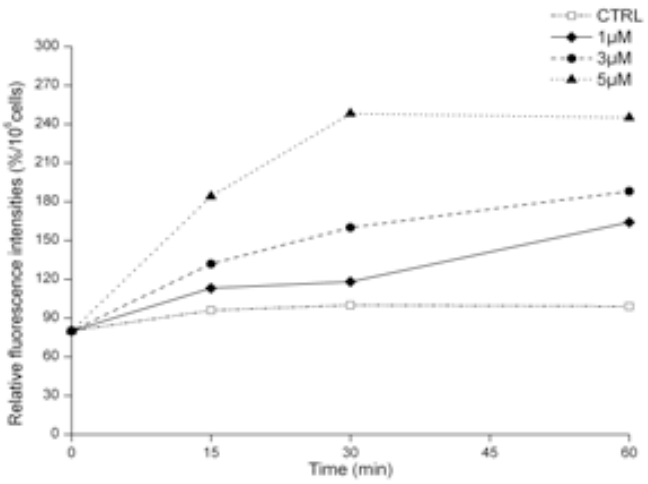

Figure 35. Effect of Cd(II) on ROS generation in Balb/3T3 cells.

10.2.9 Lipid peroxidation

In Figure 36 are presented the effects of increasing concentrations of Cd upon thiobarbituric-acid reacting substances, TAB-RS) production, as an index of lipid peroxidation, in Balb/3T3cells exposed for 72h to 1, 3 and 5 μM of $CdCl_2$.

The three Cd concentration tested induced a dose-dependent formation of TBA-RS related chromogens. Compared to the value of TBA-RS production at 1 μM the effect at 3 and 5 μM increased of 5 and 7 –fold.

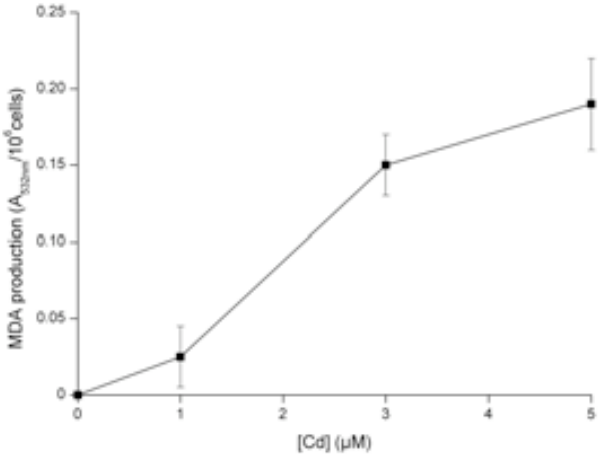

Figure 36. Effect of different concentration of Cd(II) on TBA-RS production in Balb/3T3 cells. Each point is the mean of results from three different incubations and cell preparations.

19.2.10 Inhibition of DNA synthesis

The ^{3}H-thymidine incorporation assay was used to detect the newly synthesized DNA in Balb/3T3 cells (Table 32). A marked increase of radioactivity of 21% was observed in cells treated for 72h with 0.5μM Cd compared to Cd-unexposed control. Then, the incorporation of ^{3}H-thymidine decreased in cells of Cd-exposed groups treated with 1, 3 and 5μM, accounting for 95, 66 and 59% of the radioactivity incorporated compared to the control. This indicate that the stimulation or the inhibit DNA synthesis is dependent on the Cd concentration.

Table 32. Effect of Cd(II) on DNA synthesis in Balb/3T3 cells.

Dose (µM)	^{3}H radioactivity		
	cpm/10^6cells	% of the control	p[a]
Ctrl	5070 ± 48	100	-
0.5	6130± 96	121	S
1	4815 ± 66	95	S
3	3332 ± 81	66	S
5	2990 ± 44	59	S

a: $p<0.05$

10.2.11 Determination of glutathione

Glutathione is considered the most important intracellular thiol involved in the formation of protein-mixed disulfides. Incubations of Balb/3T3 cells with different concentrations of Cd(II) (Table 33) induced significant changes in the cellular glutathione levels. The lowest concentration of Cd tested (0.5µM) produced a 23% increase in intracellular glutathione compared of the control value, while the highest concentrations tested caused a drop of control levels ranging from 6% at 1µM to 46% at 5µM.

Table 33. Levels of glutathione in Balb/3T3 cells exposed or not to CdCl2 for .

Dose (µM)	GSH content (nmoles/mgprotein ± SD)
Ctrl	17.3±1.4
0.5	21± 2.9
1	16.1± 4.2
2	13.2± 2.5
3	9.8± 3.7
5	8.9±3.3

10.3 Chromium

Results reported concern Balb/3T3 cells exposed to $Na_2CrO_4x4H_2O$ (Cr(VI)) or $CrCl_3x6H_2O$ (Cr(III)). They are related to the following studies: cytotoxicity, morphological neoplastic transformation, behaviour in culture medium, uptake, intracellular distribution, binding to cytosolic biomolecules, determination of the oxidation state of Cr in the cytosol and culture medium and binding to DNA.

10.3.1 Cytotoxicity assay (CFE)

Figure 37 shows the cytotoxicity of Cr on Balb/3T3 cells after 72h of exposure to different concentrations of Cr(VI) and Cr(III) ranging from 0.1 to 100µM as determined by CFE assay.

The following remarks can be drawn:

(i) the cytotoxic effect of Cr in cells exposed to Cr(VI) was dose-dependent. A complete inhibition of the CFE was observed at 15µM (IC_{50}=7µM).

(ii) no significant CFE inhibition was observed in Balb/3T3 for all doses of Cr(III) tested.

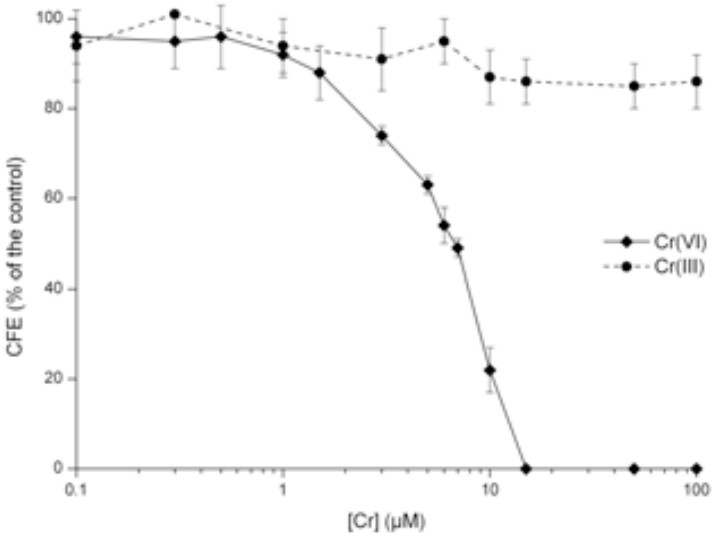

Figure 37. CFE response in Balb/3T3 cells exposed for 72h to different concentrations of Cr(VI) and Cr(III).

10.3.2 Morphological transformation assay

Table 34 reports the results of the concurrent cytotoxicity and morphological transformation assay of Cr on the Balb/3T3 exposed to different concentrations of Cr(VI) amd Cr(III).

The following remarks can be drawn:

(i) Cr(VI) was significantly positive ($p<0.05$) in the assay for the tested doses ranging from 1 to 10μM. Increasing doses caused a dose-related increase of the transformation frequency, from 0.1 at 1μM to 6.9 at 10μM.

(ii) exposure of Balb/3T3 cells to 10 and 50μM Cr(III) failed in inducing type III foci.

Table 34. Concurrent cytotoxicity and morphological transformation induced in Balb/3T3 cell line by exposure to Cr(VI) and Cr(III).

Exposure		CFE (%) ± SD	N° type III foci / N° dishes	N° type III foci positive dishes / N° dishes	Transforming frequency (T_f)	*p*
Metal form	**Dose (μM)**					
H_2O biol.	**0,1% v/v**	100±	0 / 20	0 / 20	-	-
B*(a)*P	**0,1**	8.3 ± 3.1	11 / 20	8 / 20	12.4	< 0.001
Cr(VI)	**1**	88 ± 4.3	2 / 20	1 / 20	0.1	< 0.05
Cr(VI)	**5**	66 ± 4.4	16 / 20	9 / 20	3.8	< 0.01
Cr(VI)	**10**	22 ± 2.1	18/ 20	10 / 20	6.9	< 0.01
Cr(III)	**10**	88 ± 5.3	0 / 20	0 / 20	-	–
Cr(III)	**50**	85 ± 6.6	0 / 20	0 / 21	-	-

10.3.3 Behavior of Cr(VI) in cell-free or cell-containing culture medium

Table 35 reports the data concerning the oxidation state of chromium, determined by Minoia's method (Section 4.1.3), after incubation of 0.1 and 20μM ^{51}Cr(VI) in cell-free culture medium or in the medium after exposure of Balb/3T3 cells to the same concentrations of chromate.

The following remarks can be drawn:

(i) for all times of incubation considered, more than 95% of ^{51}Cr in the cell-free medium was recovered in the organic phase suggesting that the oxidation state +6 was unchanged (Table 35). Ultrafiltration study shows a recovery of ^{51}Cr in the filtrate, suggesting that no binding with proteins occurred (Table 36).

(ii) after 72h an amount of ^{51}Cr, increasing with time, was detected in aqueous phase suggesting that a reduced species of Cr(III) was formed from Cr(VI).

Table 35. Oxidation state of Cr after incubation of 1µM and 10µM $^{51}Cr(VI)$ for 72h with cell-free or cell-containing medium.

Time of incubation (h)	^{51}Cr radioactivity (% of the amount incubated)[a]			
	Organic phase[b]		Aqueous phase[b]	
	1µM	10µM	1µM	10µM
	Cell-free medium			
0.25	98	98	2	2
4	96	95	4	5
24	96	99	4	1
72	98	97	2	3
	Cell-containing medium			
0.25	90	93	10	7
4	61	79	39	21
24	52	67	48	33
72	22	35	88	65

a: mean of 3 determinations, RSD<15%
b: aqueous phase: Cr(III); organic phase: Cr(VI)

Table 36. Ultrafiltration of cell-free medium 15min and 72h after incubation with 1µM and 10µM $^{51}Cr(VI)$.

Fraction	^{51}Cr radioactivity (% of the amount incubated)[a]	
	15min	72h
Cell-free medium	100	100
Ultrafiltrate	99.5	98.7
Membrane	0.5	1.3

a: mean of 3 determinations, RSD<20%

10.3.4 Uptake

Figure 38 shows the curves of the uptake of ^{51}Cr by Balb/3T3 cells exposed for 72h to concentrations of $^{51}Cr(VI)$ ranging from 1 to 8μM while Figure 39 illustrates the timed uptake of ^{51}Cr by the cells exposed to 4μM $^{51}Cr(VI)$.

The following remarks can be drawn:

(i) the rate of ^{51}Cr uptake by cells was dose-dependent for both alive and death cells.

(ii) at the end of the exposure to 1 and 8μM the Cr content of alive cells were 24.2 and 895fgCr/cell while the corresponding values for the dead cells were 55 and 1980fgCr/cell (Figure 38).

(iii) already after 4h the accumulation of Cr in alive and died cells was obvious (Figure 39).

(iv) the amount of total Cr into died cells was 529fgCr/cell. This value was almost unchanged at 24h (511fgCr/cell) lowering to 450fgCr/cell at 72h.

(v) the content of Cr in alive cells at 4h was 67fgCr/cell. This value increased to 333fgCr/cell at 4h, then decreasing to 196fgCr/cell at 72h.

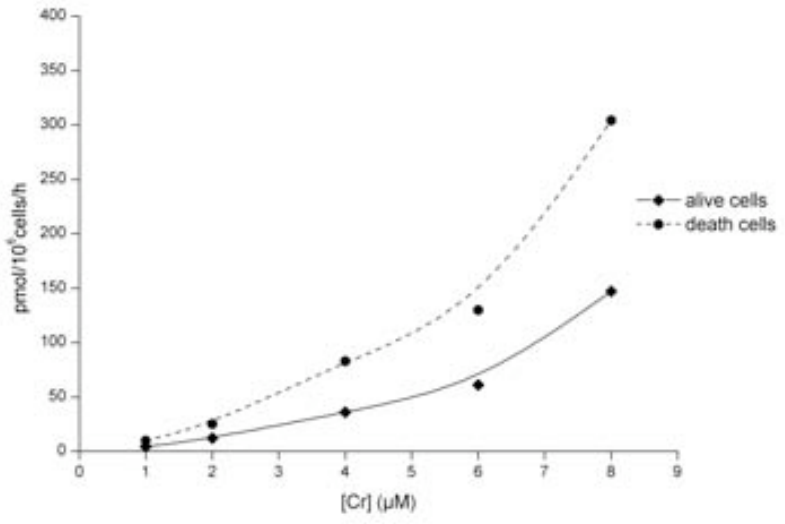

Figure 38. Cr uptake in alive and died Balb/3T3 cells exposed to $^{51}Cr(VI)$for 72h.

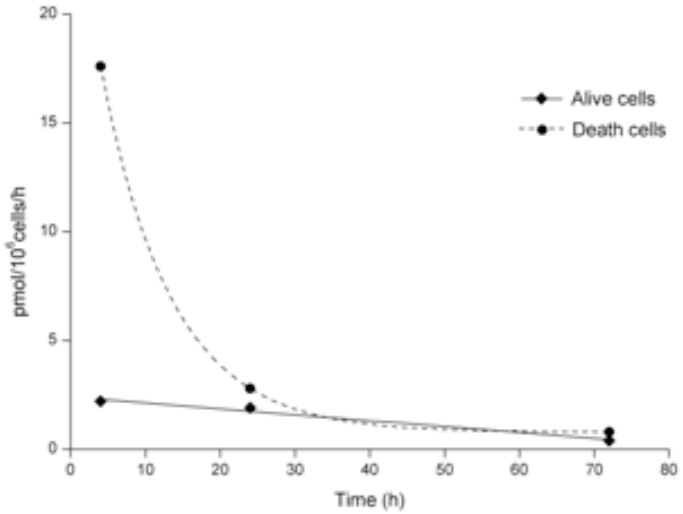

Figure 39. Kinetic of uptake of ^{51}Cr in Balb/3T3 cells exposed to ^{51}Cr(VI) at different time.

10.3.5 Intracellular distribution

The intracellular distribution of absorbed ^{51}Cr was examined after exposure of cells for 72h to 0.1and 7µM of ^{51}Cr(VI) (Table 37).

The following remarks can be drawn:

(i) at 0.1µM 75.3% of the intracellular ^{51}Cr was present in the cytosol. Among cellular organelles the nuclear fraction incorporated the highest amount of ^{51}Cr (15.6% of the homogenate).

(ii) at 7µM the intracellular distribution of ^{51}Cr changed. Compared to 0.1µM the percentage of ^{51}Cr into the cytosol decreased to 26.2% leading to an increase of ^{51}Cr associated to organelles (46.8% in the nuclear and 18,5% in the mitochondrial fractions)

Table 37. Intracellular distribution of ^{51}Cr in Balb/3T3 cells exposed to 0.1 and 7µM for 72h to ^{51}Cr(VI).

Subcellular fraction	^{51}Cr content (% homogenate)[a]	
	0.1µM	7µM
Homogenate	100	100
Nuclei	15.6	48.8
Mitochondria	4.5	18.5
Lysosomes	3.2	2.9
Microsomes	1.4	3.6
Cytosol	75.3	26.2

a: mean of 3 determinations, RSD<10%

Figure 40 illustrates the results of the gel filtration on Sephacryl S200 resin performed on the soluble fraction of Balb/3T3 cells exposed to 0.1 and 7µM of ^{51}Cr(VI) for 72h. Table 38 reports the following results of the ultrafiltration study of the cytosolic ^{51}Cr (^{51}Cr-peak I and II) to verify the "real" binding to proteins.

The following remarks can be drawn:

(i) in both cases, two peaks of ^{51}Cr emerged in the eluate in association with two UV-absorbing peaks.

(ii) however, the relative distribution of the two ^{51}Cr peaks were different at the two doses tested. At 0.1µM most of ^{51}Cr was associated with UV-absorbing peak II, while at 7µM most of the radioactivity was bound to UV-absorbing peak I.

(iii) ultrafiltration of ^{51}Cr-peak I and ^{51}Cr-peak II showed that at 0.1µM most of ^{51}Cr was ultrafiltrated suggesting that ^{51}Cr was unbound to proteins (Table 38). Exposure to 7µM lead to an obvious increase of ^{51}Cr retained on the membrane up to 30% of the ^{51}Cr of peak I.

The relative repartition of ^{51}Cr-peak II between membrane and ultrafiltrate was similar for the two doses tested, more than 95% being retained on the membrane. This suggests a binding of ^{51}Cr to UV-absorbing components of peak II.

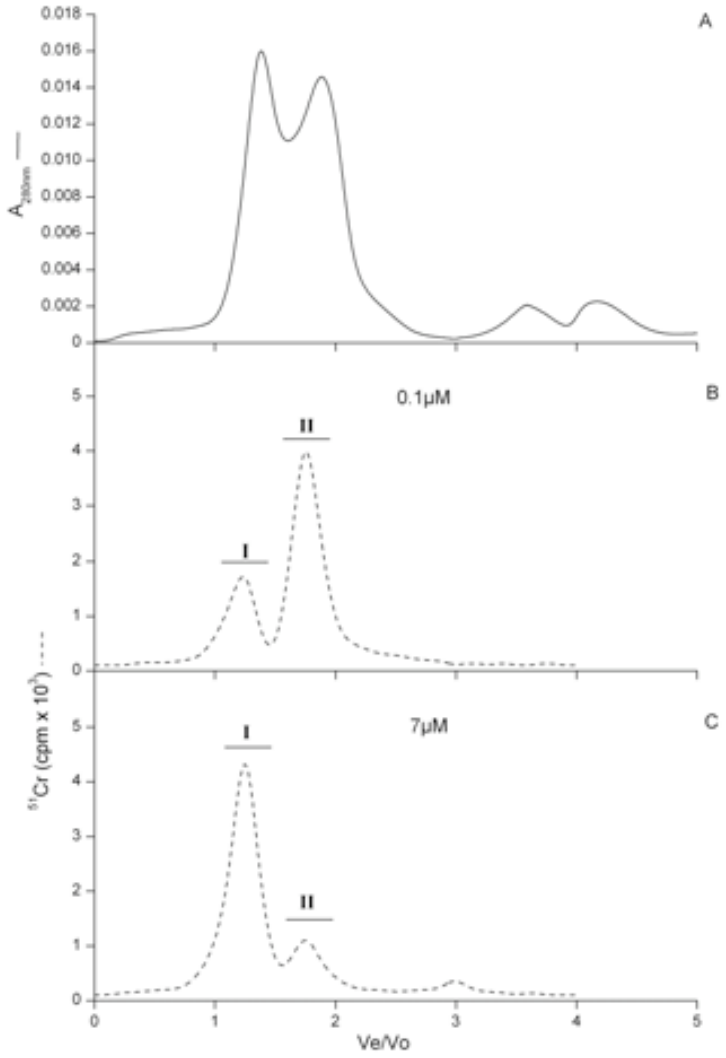

Figure 40. Gel filtration chromatography of ^{51}Cr-cytosol from Balb/3T3 cells exposed to 0.1µM and 7µM ^{51}Cr(VI) for 72h.

Table 38. Ultrafiltration of ^{51}Cr-peak I and ^{51}Cr-peak II as emerged from gel filtration of ^{51}Cr-cytosols of Balb/3T3 exposed to 0.1 and 7µM of ^{51}Cr(VI) for 72h.

Fraction from gel filtration	^{51}Cr (% of the total cytosol)[a]		
	Total cytosol	Membrane	Ultrafiltrate
	0.1µM		
^{51}Cr-peak I	100	5.2	94.8
^{51}Cr-peak II	100	98.1	1.9
	7µM		
^{51}Cr-peak I	100	31.3	68.7
^{51}Cr-peak II	100	95.2	4.8

a: mean of 3 determinations, RSD<20%

10.3.6 Oxidation state of Cr in the cytosol

Table 39 summarizes the data of the determination (Minoia's method, Section 4.1.3) of the oxidation state of Cr recovered in association with the two peaks emerging in the eluates of the gel filtration of ^{51}Cr-cytosol of Balb/3T3 cells exposed to 0.1 and 7μM of ^{51}Cr(VI) (Figure 40).

The following remarks can be drawn:

(i) at 0.1μM 92.9% of ^{51}Cr-peak I was recovered into the organic phase, suggesting that the Cr was in oxidation state +6. This percentage decreased to 60.4% at 7μM exposure.

(ii) at the two doses tested more than 90% of ^{51}Cr-peak II was recovered in the aqueous phase suggesting that almost Cr was in the oxidation state +3.

Table 39. Oxidation state of Cr of ^{51}Cr-peak I and ^{51}Cr-peakII as emerged from gel filtration of ^{51}Cr-cytosol of Balb/3T3 exposed to 0.1μM and 7μM of ^{51}Cr(VI) for 72h.

Fraction	^{51}Cr (% of the fraction)[a]			
	0.1μM[b]		7μM[b]	
	Aq. Phase	Organic Phase	Aq. Phase	Organic Phase
^{51}Cr-peak I	7.8	92.2	39.6	60.4
^{51}Cr-peak II	91.6	8.4	90.7	9.3

a: mean of 3 determinations, RSD<10%
b: aqueous phase: Cr(III); organic phase: Cr(VI)

10.3.7 Binding of Cr to DNA

Table 41 summarizes the results of the isolation by NucleoSpin of ^{51}Cr-DNA adducts from Balb/3T3 cells exposed to 7μM of ^{51}Cr(VI) for 72.

The following remarks can be drawn:

(i) a significant amount of Cr was recovered associated to the total DNA fraction (9.9ng) isolated from cells at the end of exposure.

(ii) the ^{51}Cr-DNA radioactivity was not ultrafiltrable (Table 42) being retained on the membrane. When this fraction was resuspended and chromatographed on Sephadex G25 a peak of ^{51}Cr emerged in association with the absorbing peak of DNA.

Table 41. Binding of ^{51}Cr to DNA from Balb/3T3 cell exposed to 7µM of ^{51}Cr(VI) for 72 as determnated by NucleoSpin method.

Fraction	Cr content[a]	
	ng	%
Cellular homogenate	235.4	100
Eluate	208.3	88.5
Washings	17.2	7.3
DNA fraction	9.9	4.2

a: mean of 3 determinations, RSD<15%

Table 42. Ultrafiltration of the ^{51}Cr-DNA isolated from Balb/3T3 cells exposed to 7µM of ^{51}Cr(VI) for 72h.

Fraction	^{51}Cr (% DNA fraction)[a]	
	ng	%
Total DNA fraction	8.3	100
Membrane	8.2	98.7
Ultrafiltrate	0.1	1.3

a: mean of 3 determinations, RSD<10%

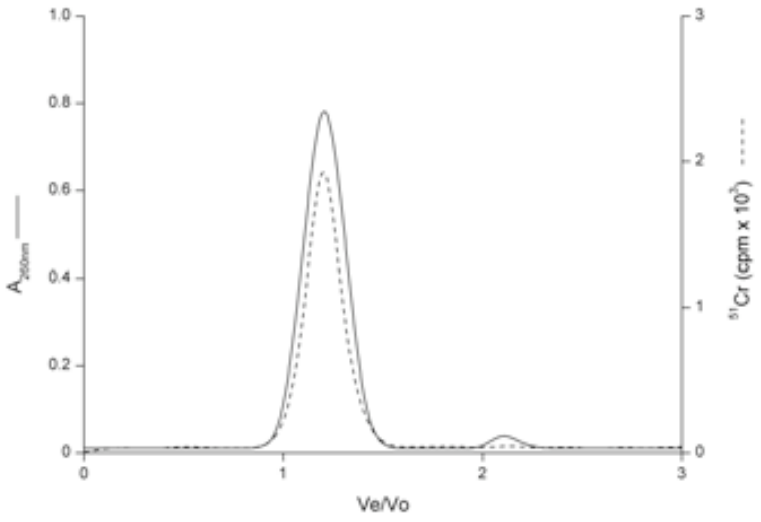

Figure 40. Binding of ^{51}Cr(VI) to DNA isolated from Balb/3T3 cells incubated with 7µM ^{51}Cr(VI).

Table 43. ^{51}Cr-DNA adduct isolated from Balb/3T3 cells exposed to 7µM of ^{51}Cr(VI) for 72h.

Fraction	^{51}Cr (% of the initial radioactivity)[a]
Submitted to solvent extraction (Minoia's method)	100
Aqueous phase[b]	95.2
Organic phase[b]	4.8

a: mean of 3 determinations, RSD<10%
b: aqueous phase: Cr(III); organic phase: Cr(VI)

10.4 Platinum

Hereafter are reported the results on Balb/3T3 cells exposed to inorganic cationic and anionic Pt compounds. They concern the following studies: cytotoxicity, behaviour in culture medium, uptake, intracellular distribution and binding to biomolecules.

10.4.1 Cytotoxicity assay (CFE)

Figures 41 and 42 display the inhibitory effect on CFE in Balb/3T3 cells exposed to different concentrations of Na_2PtCl_6, Na_2PtCl_4, $PtCl_2$ and $PtCl_4$.

The following remarks can be drawn:

(i) the inhibition of CFE was dose-dependent for the four compounds tested. The cationic Pt compounds in the oxidation state +4 ($PtCl_4$) inhibited CFE at much less extent compared to the corresponding divalent compound ($PtCl_2$). On the contrary, the tetravalent hexachloro salt (Na_2PtCl_6) inhibited CFE at higher extent compared to the corresponding divalent tetrachloro salt (Na_2PtCl_4).

(ii) the derived IC_{50} from the curves of Figures 41 and 42 were: 75µM Na_2PtCl_4; 4µ Na_2PtCl_6; 3µM $PtCl_4$ and 0.5µM $PtCl_2$

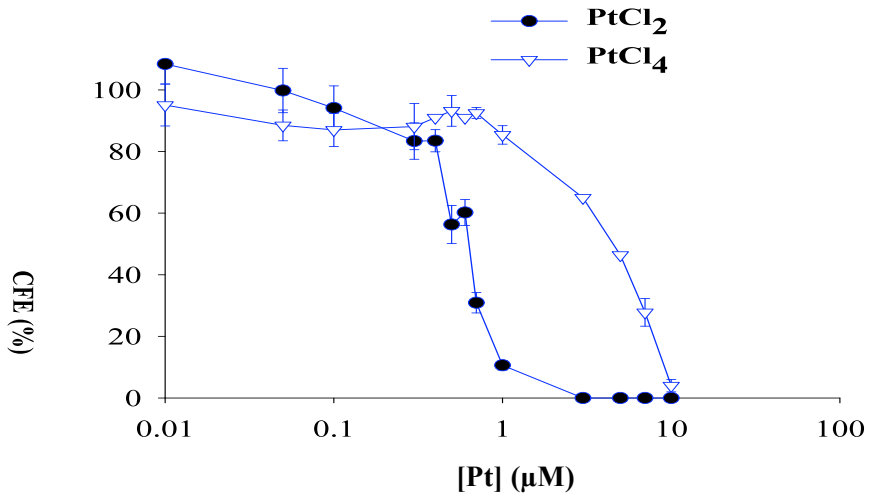

Figure 41. CFE of Balb/3T3 exposed to $PtCl_2$ or $PtCl_4$ for 72h.

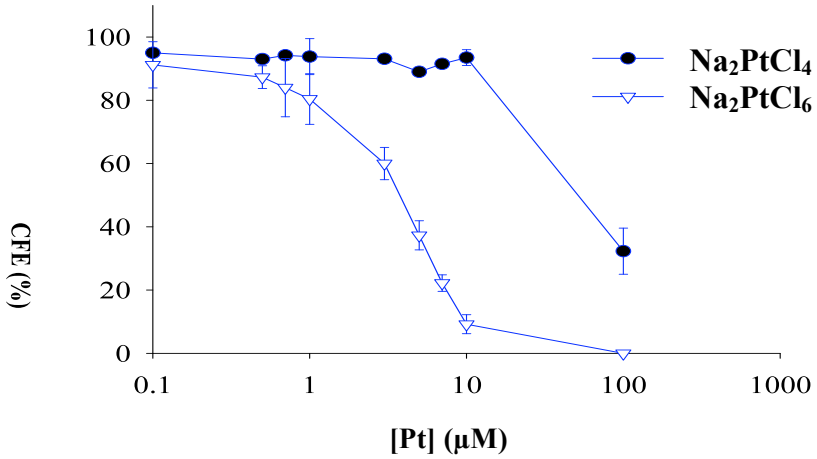

Figure 42. CFE of Balb/3T3 exposed to Na_2PtCl_4 or Na_2PtCl_6 for 72h.

10.4.2 Behaviour in culture medium

Figures 43 shows the elution profiles of $PtCl_2$, PtC_4, Na_2PtCl_4 or Na_2PtCl_6 after 30min incubation in DMEM as obtained by HPLC-ICPMS. Figure 44A displays the elution profile of Na_2PtCl_6 after incubation with histidine while Figure 44B shows the chromatogram of the same salt after 24h of incubation with complete culture medium.

The following remarks can be drawn:

(i) $PtCl_2$: two main peaks, not completely separated, emerged in the eluate (Retention time, Rt=8.8min and 9.03min).

(ii) $PtCl_4$: a main peak with Rt=8.35min was found.

(iii) Na_2PtCl_4: two main peaks were eluted at Rt=7.80min and 8.35min respectively.

(iv) Na_2PtCl_6: two main peaks were eluted at Rt=7.90min and 8.20min respectively.

(v) in the eluate from all four Pt compounds tested a small peak emerged at Rt=13.5min.

(vi) incubation of Na_2PtCl_6 with histidine led to a main peak with Rt=7.90min.

(vii) at 24h post-incubation of Na_2PtCl_6 with DMEM the elution profile drastically changed compared to the corresponding profile at 30min.

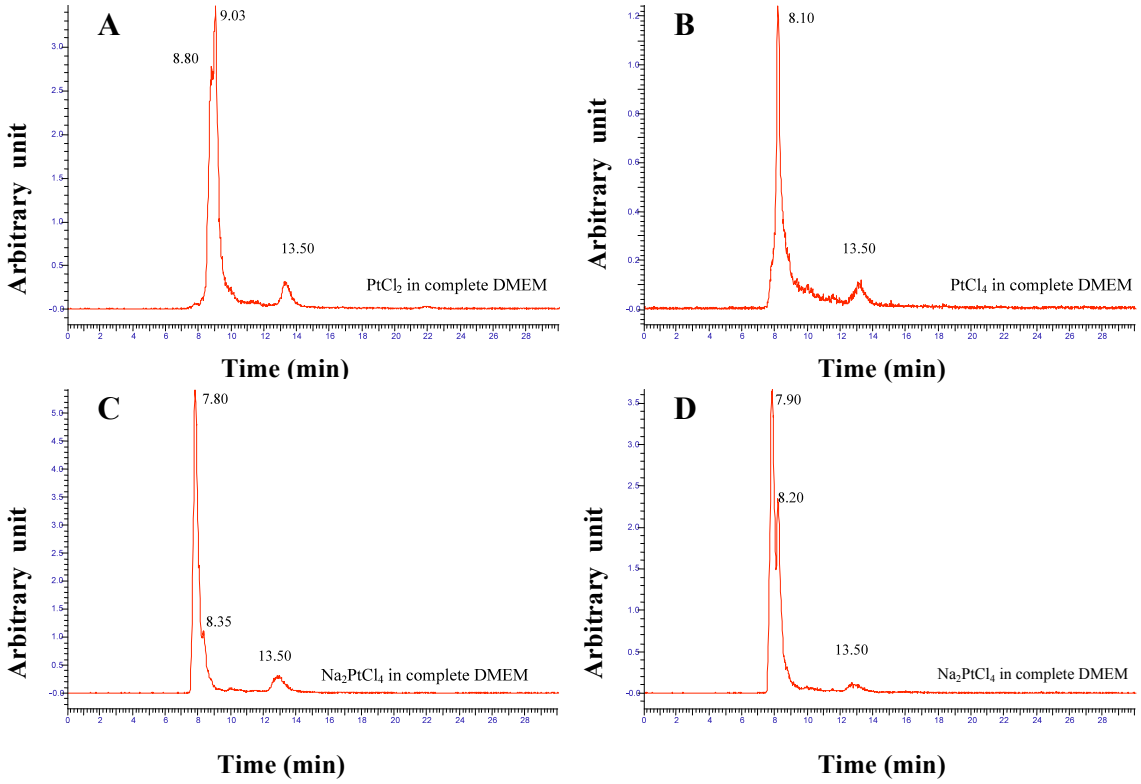

Figure 43. Chromatograms of Pt compounds after 30min incubation with complete DMEM (by ICPMS).

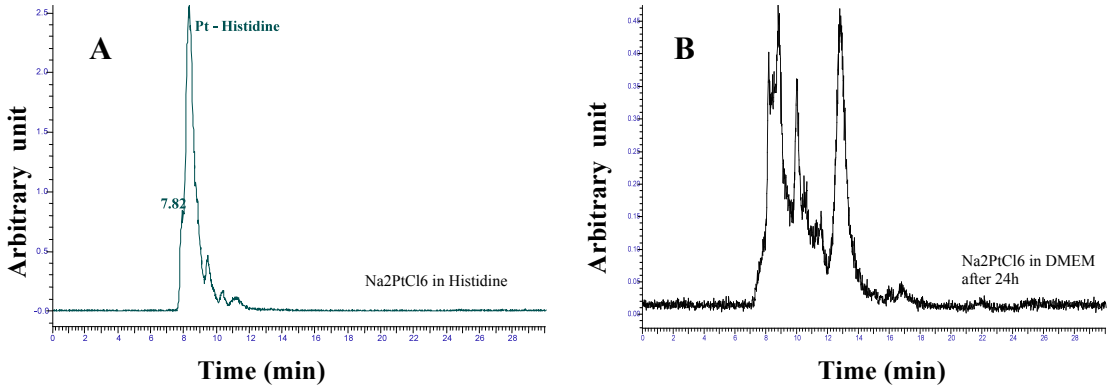

Figure 44. Chromatograms of Na_2PtCl_6 in aqueous solution incubated with histidine for 2h (A) and after incubation with DMEM for 24h (B) (by ICPMS).

Figure 45 shows the signals of DMEM after incubation from 0 to 8days with platinum compounds, in particular reports the NMR spectra concerning the

experiments with $PtCl_2$, the spectra concerning $PtCl_4$, Na_2PtCl_4 and Na_2PtCl_6 are not reported.

The following remarks can be drawn:

(i) $PtCl_4$ shows the disappearance of histidine signals after 1h from the sample preparation, Na_2PtCl_4 and Na_2PtCl_6 after 16h and $PtCl_2$ after 3days. The disappearance of histidine signals can be due to the formation of insoluble Pt-His_2 complex.

(ii) the histidine presence in the insoluble fraction was comfirmed by ^{13}C-NMR characterization, obtaining a characteristic signals of histidine carbons.

(iii) the formation of Pt-His_2 complex was confirmed by mass spectrometry analysis, obtaining the characteristic histidine mass (156.048g/mol) and the corresponding Pt-His_2 complex mass (503.128/mol).

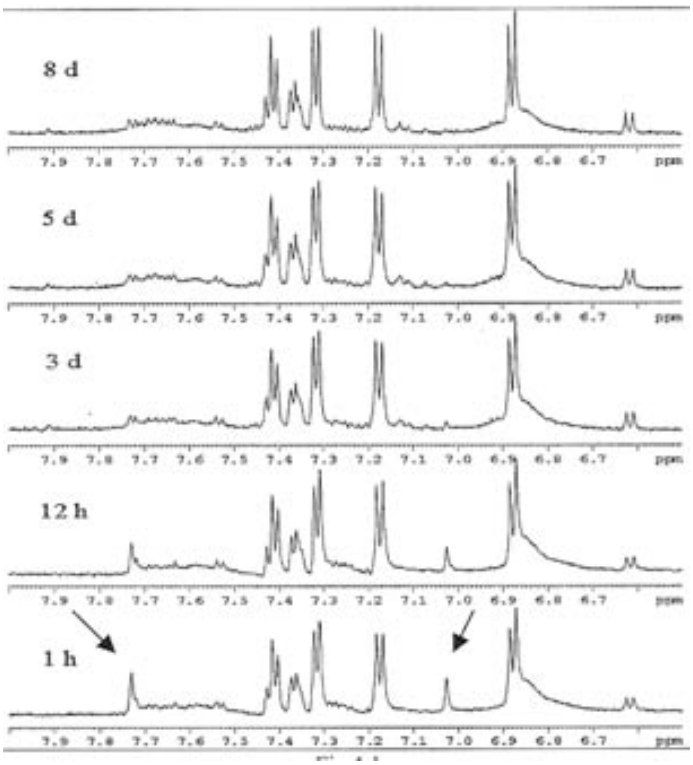

Figure 45. NMR signals of DMEM incubated from 1h to 8days with $PtCl_2$. Arrow: histidine signal.

10.4.3 Uptake

Tables 44 reports the results of the uptake of Pt (fgPt/cell) by Balb/3T3 cells exposed for 3, 24 and 72h to different concentrations of Na_2PtCl_6 and Na_2PtCl_4, while Figure 44 displays the corresponding curves expressed as pmol/10^6cells/h. Table 35 summarizes the corresponding data at 72h for exposure to $PtCl_2$ and $PtCl_4$.

The following remarks can be drawn:

(i) the amount of ^{191}Pt associated with cells exposed to Na_2PtCl_6 was dose-dependent and qualitatively similar for all the doses tested.

(ii) the uptake of Pt by cells was highest during the first hours of exposure (Figure 46). At concentrations <1μM Na_2PtCl_6 the uptake of Pt was linear with the dose. The amounts of Pt associated with the cells exposed to 1μM Na_2PtCl_6 for 72h were of the order of 2.0pmol/10^6cells/h. At higher exposure, the total Pt taken up leveled off of decreased (Figure 46).

(iii) at equimolar concentrations of exposure (0.1μM), the amounts of Pt incorporated were 2.34fgPt/cell (Na_2PtCl_4)); 1.51fgPt/cell (Na_2PtCl_6)) (Table 44); 0.22fgPt/cell ($PtCl_4$) and 0.07fgPt/cell ($PtCl_2$) (Table 45).

Table 44. Uptake of Pt by Balb/3T3 exposed to different concentrations of $Na_2{}^{191}PtCl_6$ and $Na_2{}^{191}PtCl_4$.

Treatment (μM)	Pt (fg·cell^{-1})[a]					
	Na_2PtCl_6			Na_2PtCl_4		
	4h	24h	72h	3h	24h	72h
0.03	-	0.30	0.21			
0.05	0.41	0.69	0.41	0.49	1.15	0.62
0.1	0.96	1.56	1.51	1.04	3.58	2.34
0.5	4.66	12.38	7.29	5.12	15.59	19.25
1	8.02	19.71	25.44			
3	9.93	21.54	28.88			
2	-	-	35.76	10.16	37.13	48.13
5	9.78	20.17	24.75	13.06	59.59	66.01
10	7.11	16.04	26.13	11.92	68.30	-

a: mean of 3-5 determinations, RSD<10%

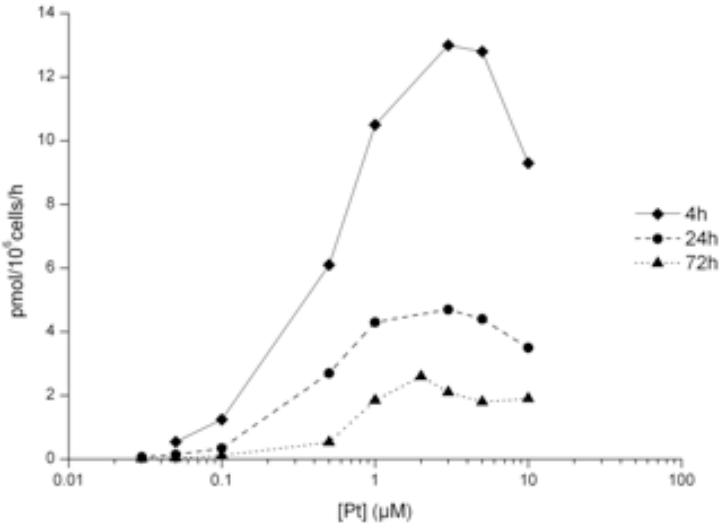

Figure 46. Uptake of Pt by Balb/3T3 cells exposed for 4, 24 and 72h to different concentrations of $Na_2{}^{191}PtCl_6$.

Table 45. Uptake of Pt by Balb/3T3 exposed to $PtCl_4$ and $PtCl_2$ for 72h.

Treatment (µM)	$PtCl_4$[a]		$PtCl_2$[a]	
	pmol/10^6cells/h[b]	fg/cell	pmol/10^6cells/h[b]	fg/cell
0.1	0.016	0.22	0.005	0.07
0.5	-	-	0.038	0.52
0.7	-	-	0.075	1.03
1	0.114	1.57	-	-
3	-	-	-	-
7	1.197	16.46	-	-

a: mean of 3-5 determinations, RSD<15%
b: basal value = <0.001fgPt·cell^{-1}

10.4.4 Intracellular distribution and binding to biomolecules

Table 46 summarizes the results of the intracellular distribution of Pt in Balb/3T3 cells exposed for 4 and 72h to 1 and 10µM of $Na_2{}^{191}PtCl_6$ and $Na_2{}^{191}PtCl_4$.

The following remarks can be drawn:

(i) after 4 and 72h of exposure to 1 and 10µM $Na_2{}^{191}PtCl_4$, 62.4 to 69% of the ^{191}Pt cell-associated was recovered in the cytosol, while 16.6 to 20.4% of radioactivity was found incorporated into the nuclear fraction.

(ii) after 4 and 72h of exposure to 1µM $Na_2{}^{191}PtCl_6$, the ^{191}Pt incorporated into cells followed an intracellular pathway similar to that of Na_2PtCl_4. However, at 10µM $Na_2{}^{191}PtCl_6$ a different pathway of Pt accumulated by cells was observed. The amounts in the cytosol decreased to 55.3% (4h) and to 45.8% (72h). At the same time, the percentages of Pt in the nuclear fraction increased to33.3% and 40.1% at 4 and 72h respectively.

Table 46. Intracellular distribution of Pt in Balb/3T3 cells exposed for 72h to 1µM and 10µM of $Na_2{}^{191}PtCl_6$ or $Na_2{}^{191}PtCl_4$.

Subcellular fraction	Pt content (% of the total uptake)[a]			
	1µM		10µM	
	4h	72h	4h	72h
		Na_2PtCl_4		
Homogenate	100	100	100	100
Nuclei	18.7	20.4	19.2	16.6
Mitoch+Lys	9.2	8.0	11.0	9.5
Microsomes	4.8	5.5	7.4	4.9
Cytosol	67.3	66.1	62.4	69.0
		Na_2PtCl_6		
Homogenate	100	100	100	100
Nuclei	16.4	15.2	33.3	40.1
Mitoch+Lys	8.7	4.9	7.5	9.4
Microsomes	5.1	3.3	4.0	4.7
Cytosol	69.8	76.6	55.3	45.8

a: mean of 3-5 determinations, RSD<10%

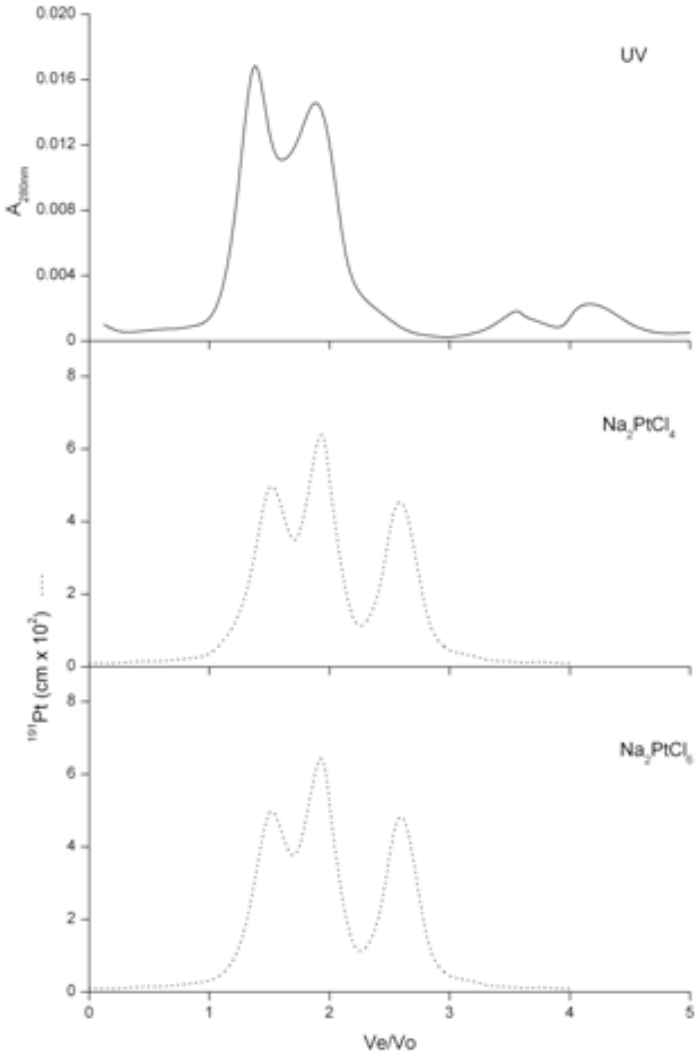

Figure 46. Gel filtration chromatography of the ^{191}Pt-cytosol from Balb/3T3 cells exposed to 1μM $Na_2{}^{191}PtCl_6$ for 72h.

Figure 47 shows the signals of the lysate of Balb/3T3 cells (Figure 46-1) compared to the signal of the lysate of Balb/3T3 previously exposed to 4μM Na_2PtCl_6 (Figure 46-2). It is evident the disappearance of signals at 8.61 and 8.60ppm (glutathione amilic proton signal) in the exposed cells lysate.

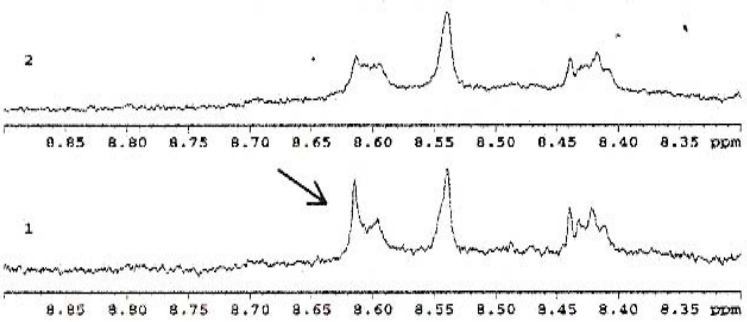

Figure 47. NMR signals of lysate of unexposed Balb/3T3 cells and Balb/3T3 exposed to 4µM Na_2PtCl_6. Arrow: glutathione amilic proton signal.

10.5 Vanadium

Results presented concern Balb/3T3 cells exposed to $NaVO_3$ (V(V)) and $VOSO_4x6H_2O$ (V(IV)). Results are related to the following studies: cytotoxicity, morphological neoplastic transformation, behaviour in culture medium, uptake, intracellular distribution, binding with cytosolic biomolecules and to DNA.

10.5.1 Cytotoxicity assay (CFE)

Figure 48 illustrate the results of the CFE inhibition of V on the Balb/3T3 cells after 72h of exposure to different concentrations of V(V) or V(IV).

Increasing doses from 0.01 to 100µM caused a dose-related increase of cytotoxicity for both V species. However, the effect of V(V) was much more obvious than that of V(IV) being the complete CFE inhibition different of about one order of magnitude (10µM and 100µM for V(V) and V(IV) respectively). The calculated IC_{50} were 5µM and 50µM for V(V) and V(IV) respectively.

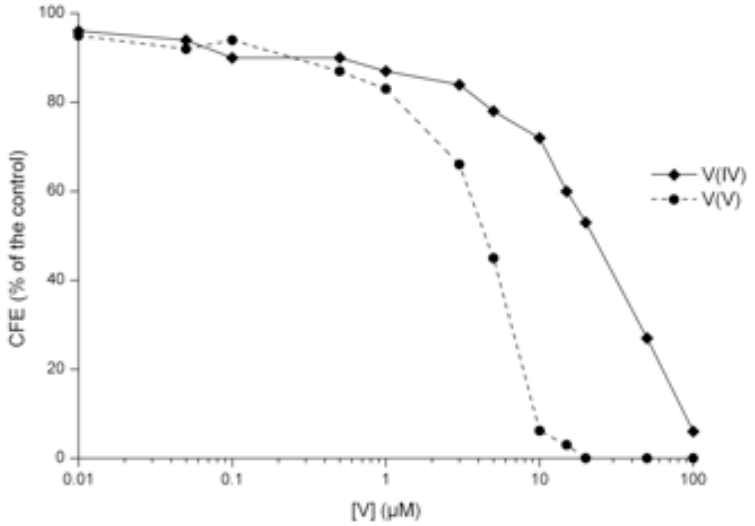

Figure 48. CFE of Balb/3T3 exposed to V(V) or V(IV) for 72h.

10.5.2. Morphological transformation assay

Table 47 summarizes the results of the concurrent cytotoxicity and morphological transformation assay carried out on Balb/3T3 cells exposed to V(V) or V(IV).

The following remarks can be drawn:

(i) V(V) was significantly positive ($p<0.001$) for the tested doses of 5 and 10µM inducing type III foci in a dose-dependent fashion. On the contrary, V(IV) was not significantly positive with a transformation frequency Tf=0.2.

(ii) compared to the control, the Tf was significantly higher in cells simultaneously exposed to 10µM V(V) and 3µM of DEM (Tf=9.9) than in cells exposed to 10µMV(V) alone (Tf=3.3).

Table 47. Cytotoxicity and morphological transformation of Balb/3T3 cells induced dy vanadium salts.

Exposure		CFE (%) ±SD	N° type III foci / N° dishes	N° type III foci positive dishes / N° dishes	Transformation frequency (T_f)	p
V chemical form	Dose (µM)					
$NaVO_3$	10	6 ± 2.2	8 / 18	9 / 18	3.3	<0.00
$NaVO_3$	5	52 ±4.7	8 / 18	5 / 18	1.1	<0.00
$NaVO_3$ + DEM[a]	10	7 ± 2.1	12 / 18	10 / 18	9.9	<0.00
$VOSO_4 \cdot 5\ H_2O$	10	26 ± 3.3	1 / 18	1 / 18	0.2	NS
DEM[a]	3	89 ± 6.4	0 / 18	0 / 18	0.05	NS
H_2O	0.1%	100	0 / 18	0 / 18	0.05	-

a: DEM=diethylmaleate

10.5.3 Behaviour of V in culture medium

Table 48 summarizes the results of the Chelex 100 chromatography of cell-free medium alone of incubated for 4h and 72h with 10µM of $^{48}V(V)$. The same Table 48 shows also the data concerning the medium after incubation of Balb/3T3 cells for 4h

and 72h with both ^{48}V species. Figure 49 shows the ^{48}V profiles from gel filtration of cell-free medium at 4 and 72h incubation.

The following remarks can be drawn:

(i) in all cases considered at 15 min more than 94% of V was recovered in the eluate suggesting that the element was in the oxidation state +5.

(ii) at 4h and 72h of incubation of $^{48}V(V)$ with DMEM alone or as complete medium more than 93% of ^{48}V was still recovered in the eluate, indicating that the original V(V) was still in pentavalent form.

(iii) after incubation with cells, the ^{48}V of the medium recovered in the eluate drastically decreased to 18.7 at 4h reaching 7.7% at 72h. This indicates a biotransformation of the original V(V) to a tetravalent form.

(iv) gel filtration of ^{48}V in cell-free medium culture medium shows two peaks of ^{48}V associated to high molecular weight components (about 10% of total ^{48}V) and a main third peak of ^{48}V eluted in the low molecular weight region (Figure 49).

Table 48. Chelex 100 chromatography of cell-free medium incubated with 10µM $^{48}V(V)$ for 15min, 4 and 72h, and of the medium after exposure of Balb/3T3 cells for 4 and 72h to both ^{48}V species.

DMEM medium	^{48}V(% of V(V) chromatographed)[a]					
	t=15min		4h		72h	
	Chelex	Eluate	Chelex	Eluate	Chelex	Eluate
Alone	1.0	99.0	2.2	98.8	1.9	98.1
Complete (+10%FBS)	1.4	98.6	7.1	92.9	6.2	93.8
Complete after incubation with cells	5.8	94.2	81.3	18.7	90.3	9.7

a: mean of 3 determinations, RSD<20%

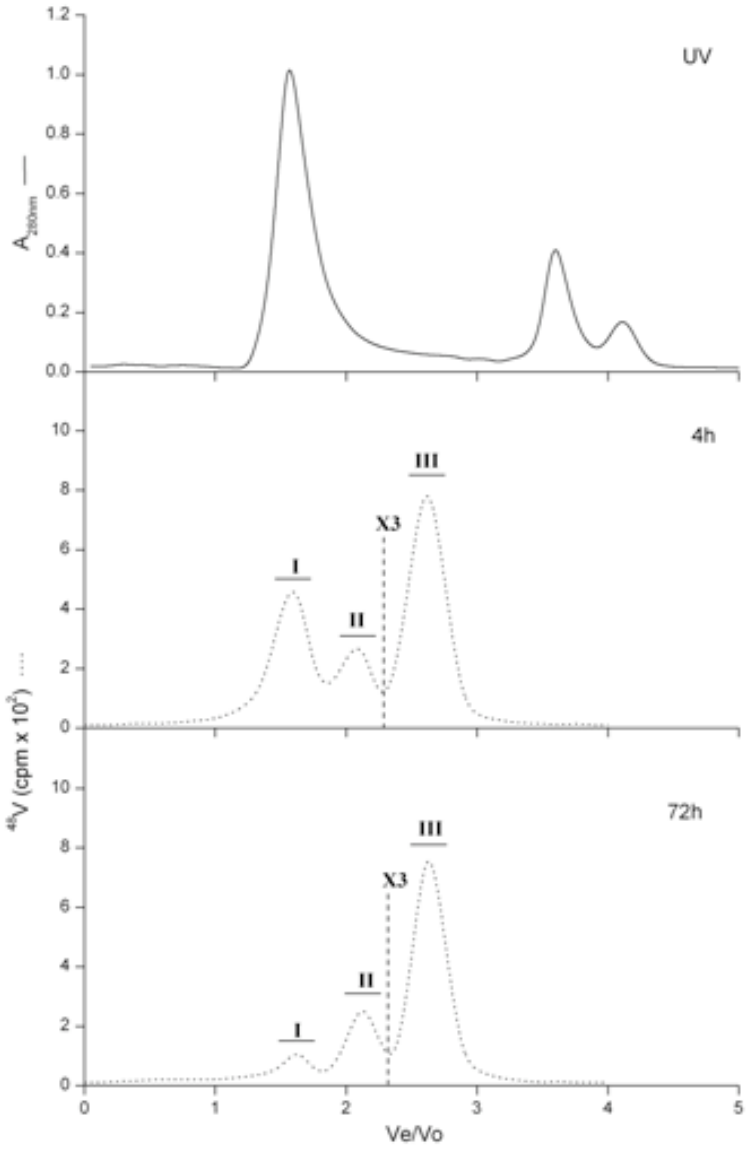

Figure 49. Gel filtration chromatography of ^{48}V after incubation of 10µM ^{48}V(V) with complete DMEM medium for 4 of 72h.

10.5.4 Uptake

Table 49 reports the analytical data (expressed as fg/cell) of ^{48}V incorporated into Balb/3T3 cells after 72h of exposure to different concentrations of V(V) and V(IV) while Figure 50 displays the corresponding incorporation rate expressed in pmol/10^6cells/h.

The following remarks can be drawn:

(i) the amount of ^{48}V associated with the cells was dose-dependent for all doses tested. At V(V) concentrations lower than 1μM the uptake was linear with the dose (Figure 50). At higher exposure the total V taken by the cells decreased, the highest amount incorporated being at 3μM (26.9fg/cell) (Table 49). At such concentration the incorporation rate was 7.8pmol/10^6cells/h). (Figure 50)

(ii) the ^{48}V uptake of V(IV) was quantitatively different compared to V(V), the highest amount incorporated being 79.5fg/cell at 20μM (Table 49) (incorporation rate 23pmol/10^6cells/h, Figure 50).

Table 49. Uptake of V by Balb/3T3 cells exposed for 72h to $^{48}V(V)$ and $^{48}V(IV)$.

Treatment (μM)	V (fg/cell)[a]	
	V(IV)	V(V)
0.01	0.66	0.09
0.05	5.2	0.48
0.1	9.3	1.3
0.5	24.2	7.3
1	32.1	16.9
3	55.3	26.9
5	62.2	22.1
10	72.6	16.6
20	79.5	10.4
50	69.1	-
100	48.4	-

a: mean of 3-5 determinations, RSD<10%

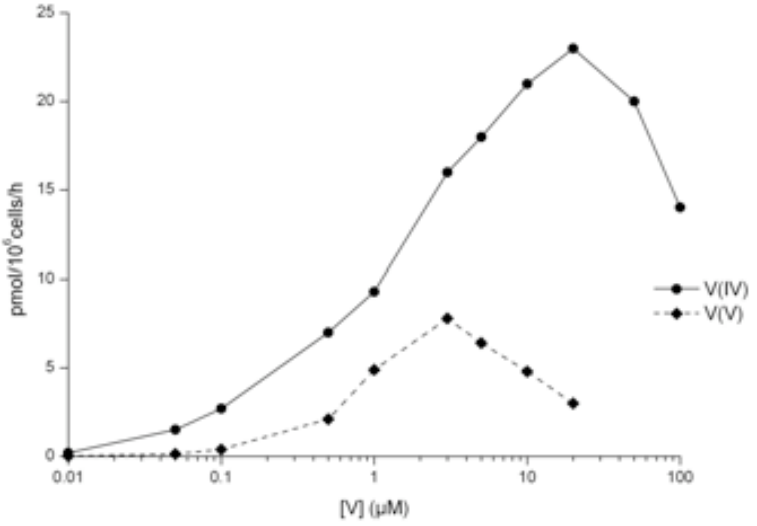

Figure 50. Uptake of V by Balb/3T3 exposed for 72h to ^{48}V(V) or ^{48}V(IV).

10.5.5 Intracellular distribution and binding to biomolecules

Table 50 reports the results of the intracellular distribution of V in Balb/3T3 cells exposed for 72h to V(V) or V(IV) while Figure 51 shows the corresponding gel filtration of ^{48}V-containing cytosol.

The following remarks can be drawn:

(i) at non-toxic dose tested (0.1µM) more than 95% of the ^{48}V was recovered in the cytosol for both V species while less than 5% was associated to cellular organelles (Table 50).

(ii) at 10µM of V(IV) most of the ^{48}V was still found in the cytosol, the intracellular distribution being similar to that at 0.1µM. Differently, incubation of cells with 10µM V(V) led to a decrease of the amount of ^{48}V into cytosol to 76.3% and a corresponding increase of ^{48}V associated to cell organelles to 23.7% (Table 50).

(iii) after exposure of cells to 10µM of ^{48}V(V) or ^{48}V(IV), gel filtration of the ^{48}V-cytosol shows that ^{48}V radioactivity was eluted as three peaks: two in association with UV-absorbing peaks (the first immediately after the void volume; the

second in the region of the chromatogram corresponding to a mol.wt of 70-80KDa); the third ^{48}V peak emerged in the position of the ^{48}V alone (Figure 51).

(iv) although the ^{48}V profiles in the gel filtration chromatogram were qualitatively similar for both V species the relative proportion of the two protein-associated ^{48}V was different being the first ^{48}V peak higher in the case of V(IV) compared to the corresponding peak from V(V) exposure (Figure 51).

Table 50. Intracellular distribution of V in Balb/3T3 cells exposed to $^{48}V(V)$ and $^{48}V(IV)$ for 72h.

Subcellular fraction	V content (% of the total homogenate)[a]			
	$NaVO_3$		$VOSO_4 \cdot 5H_2O$	
	0.1μM	10M	0.1μM	10M
Homogenate	100	100	100	100
Nuclei	2.5	13.6	2.1	1.7
Mitoch + Lys	1.7	9.5	1.3	1.5
Microsomes	0.4	0.6	0.8	0.6
Cytosol	95.4	76.3	95.8	96.2

a: Mean of 3-5 determinations, RSD<30%.

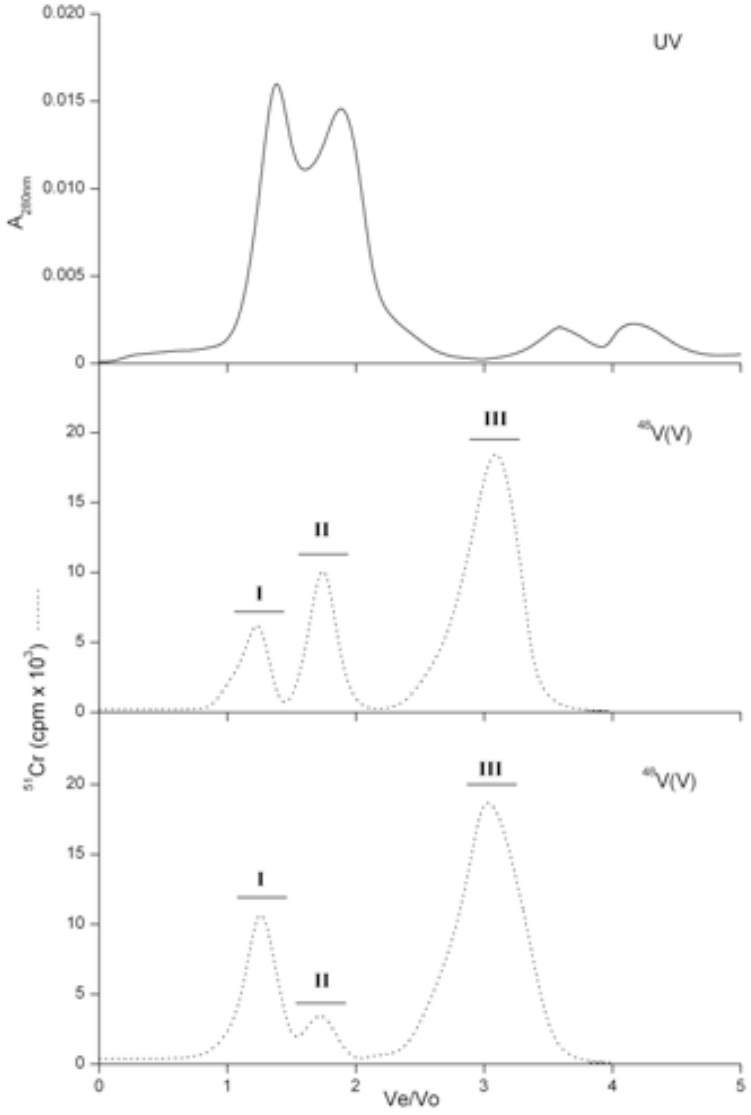

Figure 51. Gel filtration chromatography of ^{48}V-cytosol from Balb/3T3 cells exposed to 10µM ^{48}V(VI) and ^{48}V(VI) for 72h.

10.5.6 Oxidation state of V in the cytosol

Table 51 summarizes the data, obtained bi Chelex 100 chromatography, on the determination of the oxidation state of V associated to the three peaks from gel filtration of ^{48}V-cytosol from cells exposed for 72h to 10µM V(V) or V(IV) (Section 4.1.5).

The following remarks can be drawn:

(i) for both V(V) and V(IV) exposure, more than 96% of the ^{48}V associated with UV-absorbing peak I and peak II was retained on the column suggesting that V was in the oxidation state +4.

(ii) in the treatment with ^{48}V(IV) more than 98% of the ^{48}V eluted as peak III was retained on the Chelex 100 resin (oxidation state +4). However, in case of V(V), this value decrease to 74.6% (oxidation state +4) while 25.4% was recovered in the elute still in oxidation state +5.

Table 51. Chelex 100 chromatography of ^{48}V containing peaks obtained by gel filtration of the ^{48}V-cytosols from Balb/3T3 cells exposed to 10µM of ^{48}V(V) and ^{48}V(IV) for 72h.

Fraction	^{48}V (% of the total fraction)	
	Chelex 100 column[a]	Eluate[a]
	^{48}V(V)	
Peak I	97.3	2.7
Peak II	96.5	3.5
Peak III	74.6	25.4
	^{48}V(IV)	
Peak I	99.9	0.1
Peak II	98.6	1.4
Peak III	99.0	1.0

a: Chelex 100 column=V(IV), eluate=V(V)

10.5.7 Binding of V to DNA

Figure 52 shows the chromatograms from gel filtration on Sephadex G25 resin of a solution of ^{48}V(V) incubated *in vitro* with DNA previously isolated from unexposed Balb/3T3 cells (Figure 52A), and of a ^{48}V-containing DNA fraction isolated from cells exposed to 5µM of V(V) (Figure 52B) by NucleoSpin method (Table 6).

The following remarks can be drawn:

(i) no peak of ^{48}V radioactivity emerged in association with the UV-absorbing peak of DNA after *in vitro* incubation of $^{48}V(V)$ with the nucleic acid (Figure 52A).

(ii) a significant ^{48}V radioactivity was found in DNA fraction isolated by Nucleospin from cells exposed to $^{48}V(V)$ (Table 52). When the DNA fraction was chromatographed on Sephadex G25 the ^{48}V radioactivity was recovered in association with the DNA UV-absorbing peak (Figure 52B).

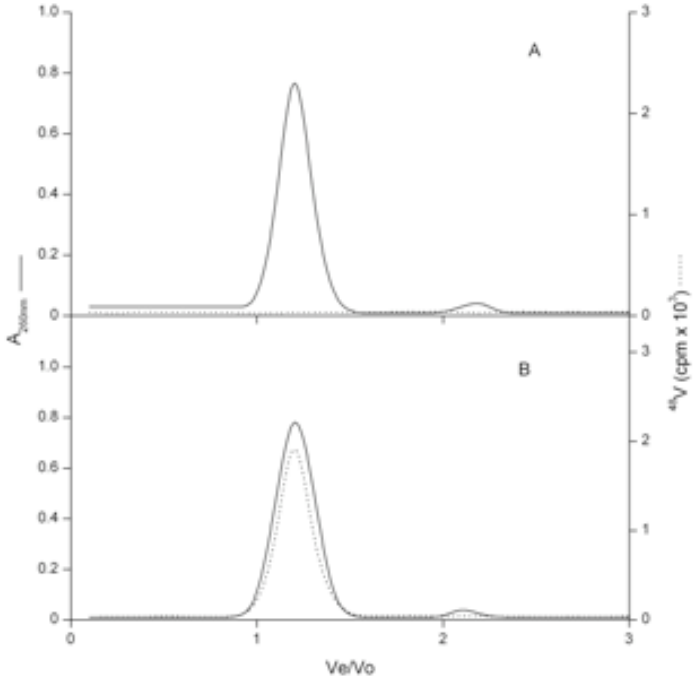

Figure 52. Binding of $^{48}V(V)$ to DNA previously isolated from Balb/3T3 cells (A) or isolated from Balb/3T3 cells incubated with $^{48}V(V)$ (B).

Table 52. Binding of ^{48}V to DNA: (A) after *in vitro* incubation of $^{48}V(V)$ with DNA previously isolated from cells, (B) from exposed Balb/3T3 cells incubated with 5µM $^{48}V(V)$ for 72h.

Fraction	^{48}V content[a]			
	In vitro incubation		DNA from exposed cells	
	ngV/fraction	%	ngV/fraction	%
Homogenate	120	100	120	100
Eluate	103.44	86.2	101.40	84.5
Washings	16.36	13.8	18.48	15.4
DNA fraction	<0.00036	<0.0003	0.12	0.1

a: mean of 3-5 determinations, RSD<15%
b: 5µM $^{48}V(V)$ incubated with 317µg DNA

11. Studies on PC12 cell line

Hereafter are reported the results concerning the studies carried out on Mn(II) and Mn(VII) in PC12 cell line. Results are related to the following studies: behaviour in culture medium, determination of cell viability, uptake, intracellular distribution, effect on reactive oxygen species.

11.1 Manganese

11.1.1 Cell viability (MTT)

Figure 53 shows the results concerning the cell viability inhibition by MTT assay on the PC12 cell line after 24h of exposure to different concentrations of Mn(II) and Mn(VII). The following remarks can be drawn:

(i) a dose-dependent inhibition of cell viability is evident for both species

(ii) the effect of Mn(VII) is higher than the effect induced by the exposure of cells to Mn(II). The calculated IC_{50} were 15 and 150µM for Mn(VII) and Mn(II) respectively.

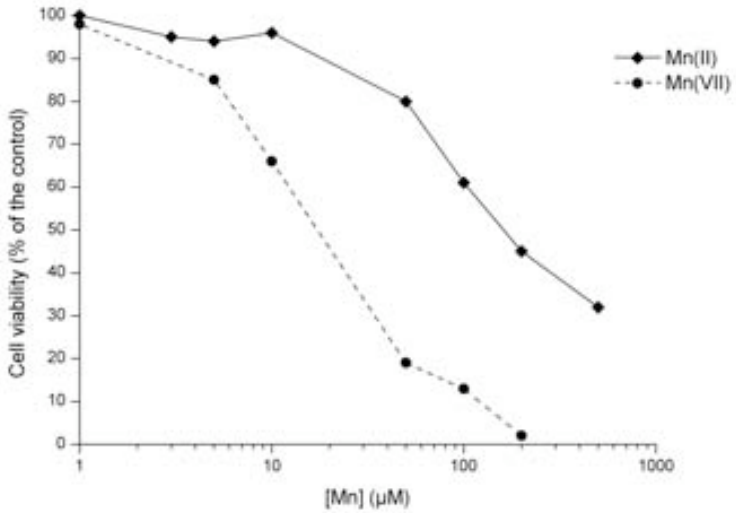

Figure 53. Cell viability by MTT assay of PC12 cells exposed to different concentration of Mn(II) or Mn(VII) for 24h.

11.1.2 Behaviour in culture medium

Figure 54 shows the elution profiles from gel filtration chromatography on Sephadex G-150 resin of RPMI medium (serum free or complete) incubated for 1h with 1µM ^{54}Mn(II).

The following remarks can be drawn:

(i) analysis of the ^{54}Mn in the eluate from chromatography of serum free ^{54}Mn - RPMI 1640 shows only one peak of radioactivity in association with a small UV absorbing peak in the region of low molecular weight (<3KDa).

(ii) the corresponding gel chromatography of complete ^{54}Mn-RPMI 1640 (Section 7.2) reveals two ^{54}Mn peaks in the eluate; a first, accounting approx for 90% of the radioactivity recovered in the eluate, in correspondence of the region of 75-80 KDa, a second (about 10% of the total ^{54}Mn) appearing in the low molecular weight(<3KDa).

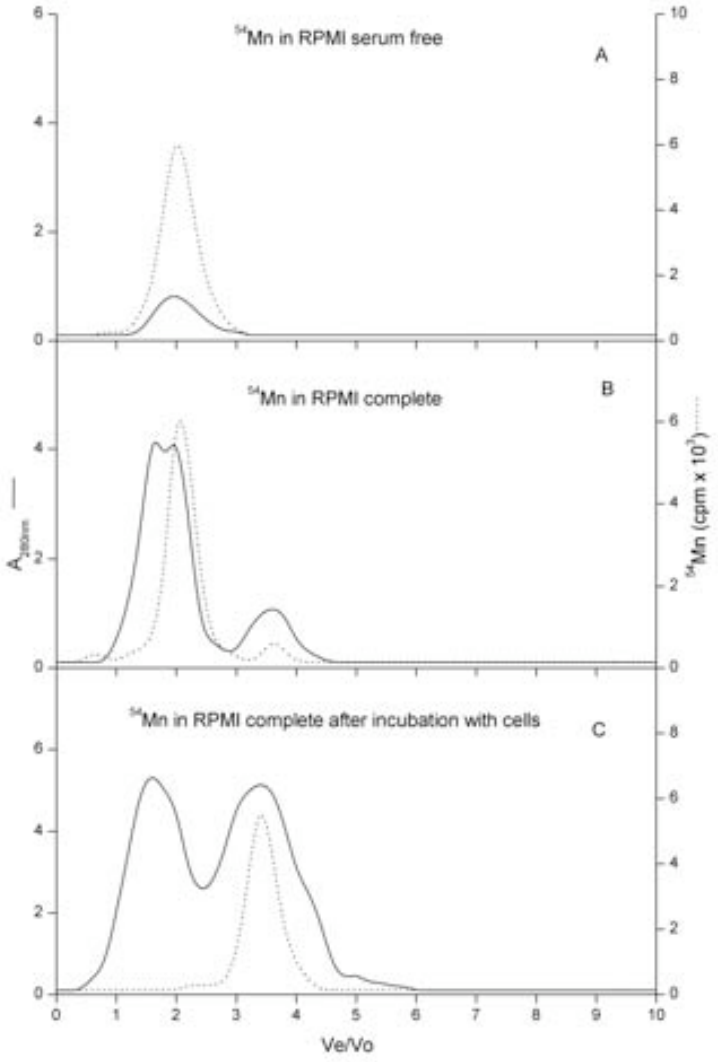

Figure 54. Gel filtration chromatography of RPMI 1640 medium previously incubated for 1h with 1µM ^{54}Mn(II). A: serum free RPMI; (B): complete RPMI; (C): after incubation of PC 12 cells for 1h.

The chemical form o Mn in culture medium was also investigated by NMR.

Figure 55 shows the NMR spectra of serum free RPMI after incubation from 1h to 4days with 100 µM Mn(II).

The following remarks can be drawn:

(i) at 1h the signals appeared larger than normal spectra (normal spectra not showed), probably it is due to the paramagnetic properties of Mn(II).

(ii) after 2days this effect disappears gradually, at 4days the spectra appears similar to the normal diamagnetic spectra showing slim signal, but with disappearance of histidine signals. The last effect is an index of: (a) the formation of a precipitate (e.g. an insoluble Mn-histidine complex), (b) the presence of a paramagnetic species (c) the coexistence of both previous situations.

.

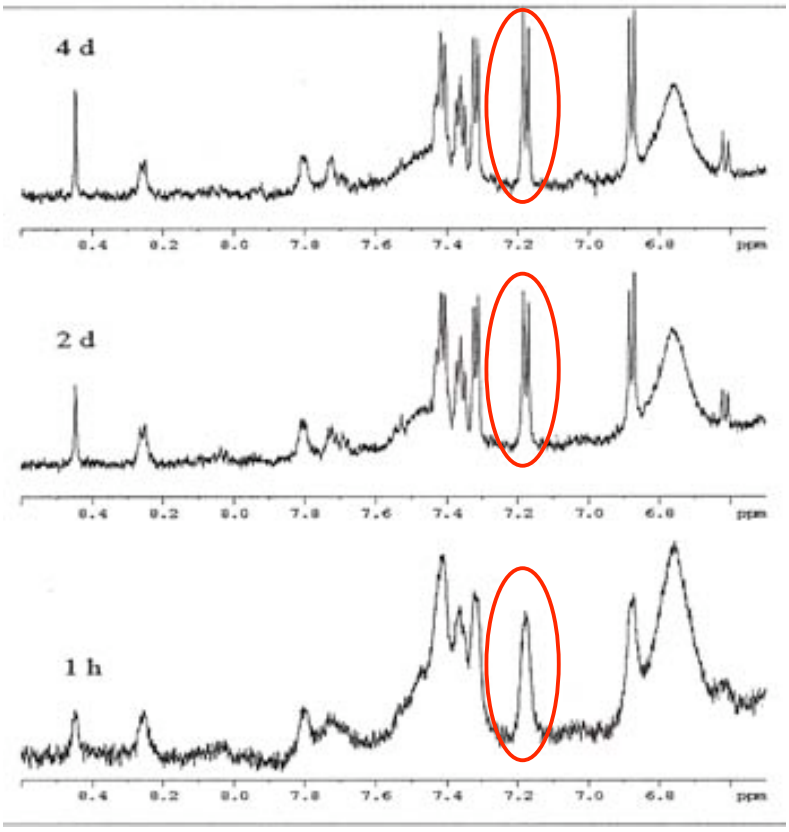

Figura 55. NMR spectra of serum free RPMI incubated from 1h to 4days with 100 µM $MnCl_2$. Circle: histidine signal.

11.1.3 Uptake

^{54}Mn (as $MnCl_2$ or $KMnO_4$) uptake was quantified after incubation for 3 or 24h of PC12 cells with concentrations of $^{54}Mn(II)$ or $^{54}Mn(VII)$ ranging from 0.1 to 500µM.

Figure 56 displays the uptake of ^{54}Mn, expressed as pmol/10^{6}cells/h, by cells exposed to the two chemical forms of Mn.

The following remarks can be drawn:

(i) the rate of ^{54}Mn(II) uptake was maximal at 3h of incubation and for concentration of 10μM. At higher concentrations of exposure a constant value of the uptake was reached up to 100μM and then decreasing at the highest concentration tested (500 μM).

(ii) the trend of the uptake rate of ^{54}Mn(II) at 24h was similar to that at 3h; however, the rate of uptake at 24h was constantly lower than the corresponding values at 3h.

(iii) in the range of the doses tested, the uptake of ^{54}Mn(VII) at 24h was considerably higher than the corresponding uptake of ^{54}Mn(II), although qualitatively the trend was similar to that of the cationic species.

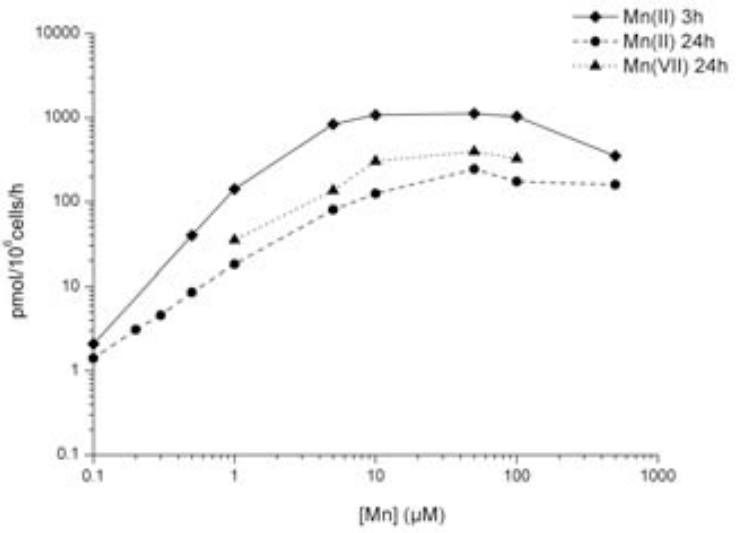

Figure 56. Uptake of Mn by PC12 cells exposed for 3 or 24h to different concentrations of Mn(II) or 24h for Mn(VII).

In order to get information on the biochemical pools of Mn in PC12 cells further experiments on the uptake of Mn were carried out by repeated discontinuous exposure of the cells to Mn differently radiolabelled with ^{54}Mn, ^{52}Mn and ^{56}Mn radiotracers (Figure 57). Table 53 reports the results of such triple labelling experiments.

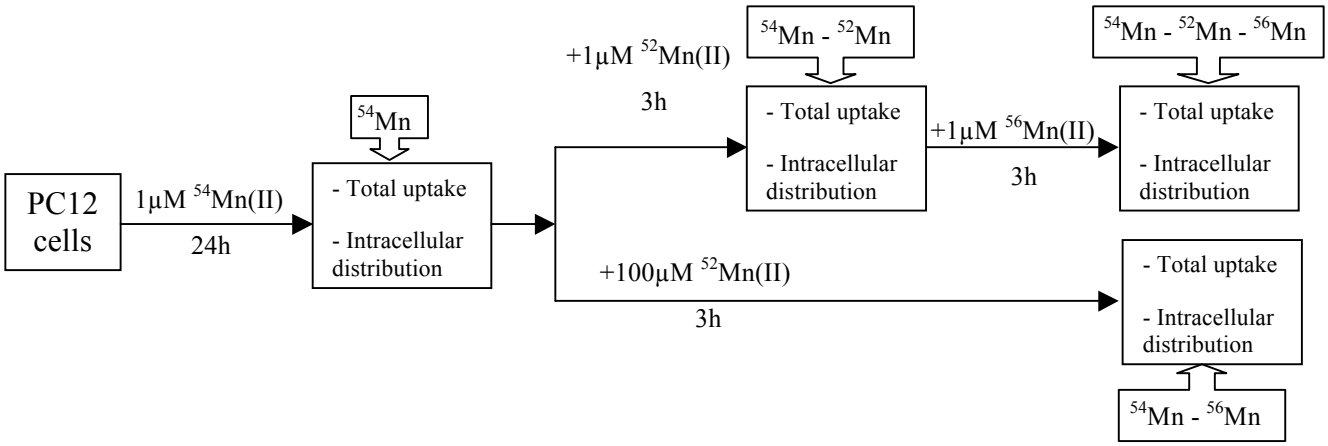

Figure 57. Scheme of the uptake experiments concerning the different Mn isotopes exposure in PC12 cells at different exposure times and concentrations.

Exposure of PC12 cells to 1μM ^{54}Mn(II) for 24h, followed by two repeated exposure to 1μM ^{52}Mn(II) and to ^{56}Mn(II) for 3h led to a total incorporation of Mn similar after the three exposure, ranging from 434.4 to 471.1pmol/10^6cells (Table 53). However, the contribution of the three radiotracers to the total uptake was different. In cells initially exposed to ^{54}Mn(II), a second exposure to ^{52}Mn(II) caused a partial replacement of ^{54}Mn (about 50%) by the "de novo" ^{52}Mn. ^{54}Mn and ^{52}Mn accounted for 58 and 42% of the total uptake respectively. Then, a new exposure of t ^{54}Mn and ^{52}Mn–labelled cells to ^{56}Mn(II) caused a further replacement of both ^{54}Mn and ^{52}Mn by the "de novo" ^{56}Mn, with a contribution to the total uptake of the three radiotracers of 42, 23 and 35%, respectively.

A similar experiment by exposing cells to 1μM Mn(II) for 24h and then to 100μM ^{56}Mn(II) for 3h led in an elevation of the uptake from 434.4 to 3771.2pmol/10^{6}cells. After the second exposure, 39% of the ^{54}Mn was replaced by the "de novo" ^{56}Mn, being the relative contribution of ^{54}Mn and ^{56}Mn to the total uptake of 7 and 93%, respectively.

Table 53. Uptake of different Mn(II) isotopes in PC12 cells at different exposure times and concentrations.

Exposure			Uptake (pmol/10^{6}cells)			
Compound	**Dose (μM)**	**Time (h)**	**Total**	**From $^{54}Mn^{2+}$**	**From $^{52}Mn^{2+}$**	**From $^{56}Mn^{2+}$**
^{54}Mn(II)	1	24	434.4 ± 12.3	434.4 ± 12.3	-	-
+ ^{52}Mn(II)	1	3	471.7 ± 11.5	271.9 ± 10.8	199.7 ± 8.9	-
+ ^{56}Mn(II)	1	3	450.1 ± 14.2	199.6 ± 7.4	135.5 ± 5.7	116-0 ± 4.0
^{54}Mn(II)	1	24	434.4 ± 9.8	434.4 ± 12.3	-	-
+ ^{56}Mn(II)	100	3	4171.2 ± 32.5	268.5 ±. 12.0	-	3902.7 ± 41.9

11.1.4 Intracellular distribution

The subcellular distributon of ^{54}Mn in PC12 cells exposed for 24h to 1, 10, 100μM ^{54}Mn(II) is reported in Table 54.

At very low exposure concentrations the major part of ^{54}Mn incorporatd into cells was present in the nuclear fraction (40.2% of the homogenate), followed by mitochondrial+lysosomal (33.6%) and cytosol (23%) fractions. These proportions progressively changed in the same intracellular fractions at increasing dose exposure. With the exception of microsomal fraction a significant decrease of ^{54}Mn was observed in the other organelle fractions that was matched by an increase in the cytosol in which ^{54}Mn reached the 67.4% of the total homogenate at 100μM.

Table 54. Intracellular repartition Mn in PC12 cells exposed for 72h to different concentrations of ^{54}Mn(II).

Subcellular fraction	^{54}Mn content (% of the homogenate)			
	Carrier-free (0.08µM)	1µM	10µM	100µM
Homogenate	100	100	100	100
Nuclei	40.2 ± 5.3	32.8 ± 3.4	28.8 ± 4.4	22.1 ± 6.0
Mitochondria + Lysosomes	33.6 ± 8.0	16.7 ± 5.0	14.0 ± 5.7	7.6 ± 3.2
Microsomes	3.2 ± 2.2	3.4 ± 1.6	2.2 ± 1.3	2.9 ± 0.8
Cytosol	23.0 ± 4.6	47.1 ± 8.3	55.0 ± 6.8	67.4 ± 9.2

Similarly to the uptake experiments, in order to get information on the biochemical pools and on the movements of Mn at subcellular level and an experiment was carried out by exposing cells firstly to 1µM ^{54}Mn(II) for 24h and then to 1µM ^{52}Mn(II) for 3h, detecting the proportion of the two radiotracers into the subcellular fractions.

After the exposure of ^{54}Mn-labelled cells to equimolar concentrations of ^{52}Mn(II) both radiotracers were found incorporated into all intrcellular fractions in a mean ratio ^{54}Mn/^{52}Mn of 1.54.

Table 55. Intracellular repartition Mn in PC12 cells exposed to 1µM of ^{54}Mn(II) for 24h and then to 1µM of ^{56}Mn(II).

Subcellular fraction	^{54}Mn and ^{52}Mn content (% of the homogenate)			
	Total ^{54}Mn+^{52}Mn	From ^{54}Mn	From ^{52}Mn	R=^{54}Mn/^{52}Mn
Homogenate	100	60.2	39.8	1.67
Nuclei	33.5 ± 4.2	20.2 ± 4.2	13.3 ± 4.2	1.51
Mitochondria + Lysosomes	16.3 ± 5.0	9.9 ± 5.0	6.4 ± 5.0	1.44
Microsomes	5.0 ± 3.6	3.5 ± 3.6	1.5 ± 3.6	2.30
Cytosol	45.2 ± 9.3	26.6 ± 9.3	18.6 ± 9.3	1.43

Table 56 shows the intracellular distribution of ^{54}Mn in PC12 cells exposed for 24h to 1 and 20μM of ^{54}Mn(VII).

The following remarks can be drawn:

(i) the radioactivity was recovered into all subcellular fractions. At 1μM more than 60% of ^{54}Mn of the homogenate was present in the nuclear, mitochondrial and lysosomal fractions while cytosol accounted for 34.2% of cellular ^{54}Mn.

(ii) at 20μM the percentage of ^{54}Mn in the cytosol didn'change significantly. However, although the sum of ^{54}Mn recovered in the nuclear, mitochondrial and lysosomal fractions was the same compared to the corresponding value at 1μM a significant decrease of the radioactivity was found in the nuclear faction that was matched by mitochondrial+lysosomal fraction.

Table 56. Intracellular repartition of Mn in PC12 cells exposed for 24h to different concentrations of ^{52}Mn(VII).

Subcellular fractions	^{52}Mn content (% of the homogenate)	
	1μM	50μM
Homogenate	100	100
Nuclei	33.0 ± 4.6	26.0 ± 3.8
Mitochondria + Lysosomes	28.2 ± 6.8	37.5 ± 8.6
Microsomes	4.6 ± 2.5	2.9 ± 1.5
Cytosol	34.2 ± 5.1	33.6 ± 4.2

The analysis of the eluate profiles of gel filtration chromatography (Figure 58) of the cytosol fractions from cells exposed to equimolar concentration (1μM) of ^{54}Mn (II) for 24h (Figure 58B) shows the presence of two "^{54}Mn pools", in association with high (pool A) and with low (pool B) molecular weight components.

A repeated exposure of these ^{54}Mn-labelled cells to 1µM of ^{52}Mn (II) for 3h reveals an incorporation of the "de novo" ^{52}Mn into the two "^{54}Mn- pools", decreasing at the same time the amount of ^{54}Mn (Figure 58C). A third exposure to 1µM of ^{56}Mn (II) led to the incorporation of the "de novo" ^{56}Mn into "^{54}Mn- and ^{52}Mn-containing pool A and B", with a replacement of part of of ^{54}Mn and ^{52}Mn.

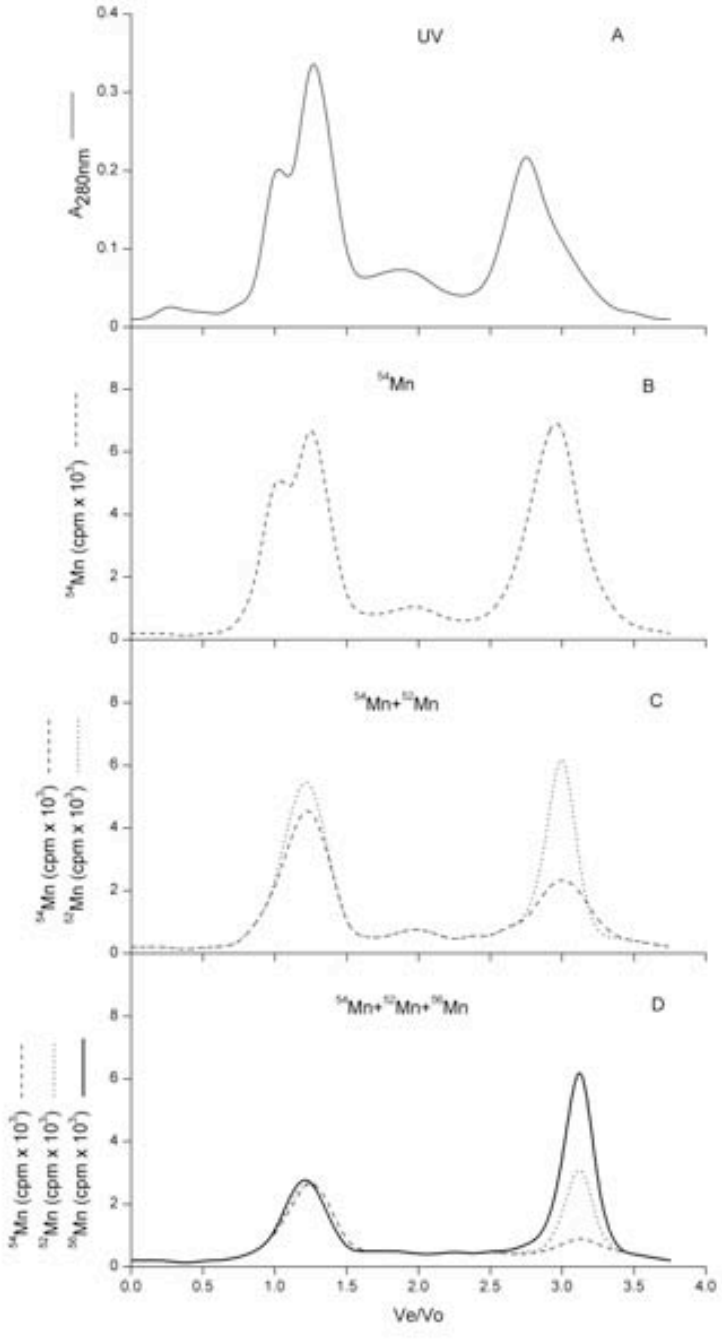

Figure 58. Gel filtration of cytosols from PC12 cells exposed to 1µM ^{54}Mn(II) for 24h (B), then to a second and a third exposure for 3h to 1µM ^{52}Mn(II) (C) and 1µM ^{56}Mn(II) (D).

11.1.4 Reactive oxygen species (ROS)

The ROS levels were measured to examine the involvement of oxidative stress in Mn(II) and Mn(VII) cytotoxicity. Figure 59 shows the effect of 1 and 20µM $MnCl_2$ and $KMnO_4$ on ROS generation in PC12 cells. Mn(VII) induced ROS at significantly greater amounts compared to Mn(II). The heptavalent Mn(VII) induced a 8-fold increase in ROS levels, whereas the divalent Mn(II) induced a 3-fold increase in ROS level compared to the control levels.

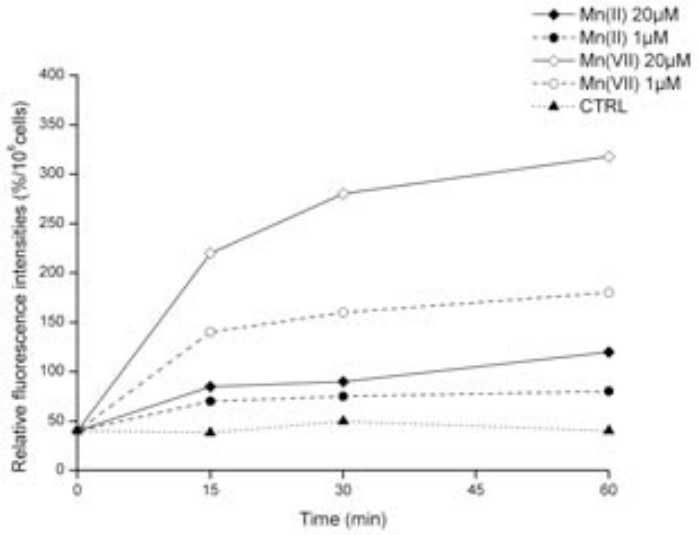

Figure 59. Effect of Mn(II) and Mn(VII) on ROS generation in PC12 cells.

12. Studies on rat brain aggregates

Hereafter are reported the results concerning:

1. uptake and identification of biomethylated forms of As in the extract from brain aggregates, and in culture medium at the end of the exposure.
2. vitality of isolated cell components of brain aggregates exposed to As(III) and uptake of As by the same cells.

12.1 Brain aggregates

Table 57 reports the results of the uptake of As in brain aggregates exposed for 72h to 1-1000μM As(III) while Table 58 shows the corresponding data on the biomethylation in the extract from brain aggregates. Table 58 reports also the data on the speciation of As in culture medium at the end of the experiment.

The following remarks can be drawn:

(i) the highest incorporation of As incorporated into aggregates was observed at 30μM As(III) (5ngAs/aggregate). At 100μM As(III) this value decreased to 1.4ngAs/aggregate which did not significantly changed at higher doses (Table 56).

(ii) in addition to inorganic As, biomethylated MMA(V) and DMA(V) were identified in the extract from brain aggregates. However, while the relative percentage of MMA(V) increased from 2 to 48% with increasing dose exposure that of DMA decreased from 57 to 17% (Table 58). At the end of exposure of brain aggregates biomethylated forms were found released into DMEM. However, other unidentified As species were found (0.11 and 0.57% of the dose, Table 57, as suggested by the amounts of As retained by the resin used in Tam's method (Section 4.1.1).

Table 57. As uptake in rat brain aggregates exposed for 72h to $^{73}As(III)^{a}$.

Dose (µM)	ngAs/µgProteins	ngAs/aggregate
0.1	0.003	2.6
1	0.010	2.5
30	0.020	5.0
100	0.056	1.4
330	0.053	1.3
1000	0.051	1.2

a: mean of 3 determinations, RSD<15%. Basal value=0.001ngAs/µgProteins.

Table 58. Repartition of the chemical forms of As identified in complete DMEM or in the extract of brain aggregates exposed for 72h to $^{73}As(III)$.

Dose (µM)	As content						
	Aggregate (% of extract)			DMEM (% of dose)			
	As_i^{a}	MMA(V)	DMA(V)	As_i^{a}	MMA(V)	DMA(V)	Others
0.1	41	2	57	99.3	0.14	0.49	0.11
30	35	48	17	99.3	0.09	0.03	0.57

a: As_i=total inorganic As

12.2 Isolated cells of brain aggregates

Table 59 shows the results of the uptake of As in individual cell components of brain aggregates (neurons, microglia and astrocytes) exposed to As(III) while Figure 58 illustrates the corresponding data of cell vitality.

The following remarks can be drawn:

(i) qualitatively the incorporation of As in the three types of cells was dose-dependent. However, from the quantitative point of view the ranking of As uptake was astrocytes>neurons>microglia.

(ii) exposure of microglial cells to As did not significantly affect cell vitality. On the contrary, an obvious effect was observed in case of neurons and astrocytes for which at 30µM the vitality was inhibited.

Table 59. Uptake of As by astrocytes, neurons and microglia after exposure for 72h to As(III).

Treatment (µM)	pmolAs/106cells/ha		
	Astrocytes	**Neurons**	**Microglia**
0.1	0.39	0.28	0.06
1	6.19	2.20	0.37
3	11.46	4.44	1.72
10	33.15	8.00	2.65
30	57.13	29.24	11.72

a: mean of 3 determinations, RSD<15%

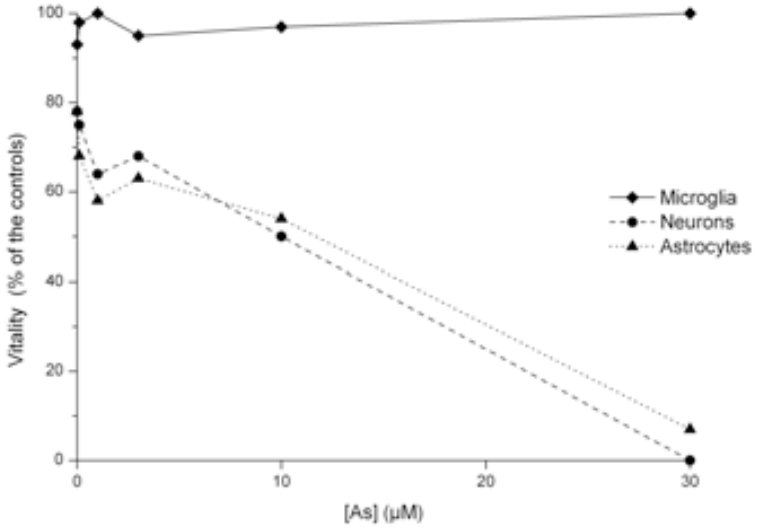

Figure 60. Cell vitality of microglia, neurons and astrocytes exposed to As(III) for 72h.

DISCUSSION

The present research is related to the development and validation of advanced test methods and testing strategies that could be used to reduce, refine and replace the use of animals for the testing of chemicals substances and product by in the *in vitro* system (Hartung et al, 2003). The experimental acticities foresee the use of omics technologies for improved toxicity prediction to meet ethical, political and commercial expectations. In this context, one of the aims is the integration of toxicological aspects of selected inorganic compounds with ECVAM activities.

Hereafter is reported the discussion of the results achieved in the present research in relation to the planned objectives (see Objectives) which are related to metallomics, an emerging aspect in metal toxicology (Szpunar, 2004). In particular, metal compounds considered (As, Cd, Cr, Mn, Pt and V) were chosen taking into account the existing *in vivo* knowledge on their metabolism and mechanisms of toxicity and induced effect which are relevant to environmental and occupational exposure . They were selected as potential models of metal compounds for future validation studies (Sabbioni et al, 1999) concerning the toxicological areas here considered such as neurotoxicity (PC12 cell line and rat brain re-aggregates) and carcinogenic potential (Balb/3T3 cell line).

Carcinogenic potential of As, Cd, Cr, Pt and V compounds

Hereafter a discussion is reported concerning the research on carcinogenic potential of As, Cd, Cr, Pt and V in Blab/3T3 cell line.

Check of chemical purity of metals compounds used in cell transformation assay

A key factor of the *in vitro* study of the carcinogenic potential of metal compounds concern their chemical purity. Elemental impurities of the salts tested, particularly those with the same chemical affinity of the metal under study, could create artifacts regarding the cytotoxic and transforming response, being in same cases the impurities transforming by themselves. It is the case of vanadate which is in the same chemical group of chromate, a well known potent cytotoxic and transforming compound in mammalian cells (Elias et al., 1991). Thus, the knowledge of Cr contamination in V salts to be tested for their carcinogenic potential.

In our work, analysis by NAA, ICPMS and GFAAS of the As, Cd, Cr, Pt and V salts used for carcinogenicity studies showed levels of impurities which were judged too low to induce either cytotoxic and morphological transformation in the Balb/3T3 cell line (Table 20). Consequently, we can exclude that in our experiments the observed type III foci were due to the presence of chemical impurities added to the culture medium with the salts tested, being in any case the estimated contaminations in culture medium less than 0.01μM under our experimental conditions.

Arsenic

The experiments on As compounds related to the cytotoxicity and morphological transformation confirmed previous findings (Bertolero et al., 1987) on strictly

relationships between cytotoxicity/carcinogenic potential and the chemical form of the element to which cells were exposed (Table 22).

Interesting results have been obtained in our work by using a new pentavalent inorganic (AsF) and organic (Ph_4As and MMA(III)) As species. In spite of its inorganic nature, $NaAsF_6$ was not toxic and not transforming in Balb/3T3 cell line (Table 22). In addition in spite of its organic nature Ph_4As was cytotoxic and transforming while MMA(III) was far more cytotoxic than inorganic As(III) but not transforming. These findings are of particular interest because As toxicology considers the inorganic but not the organic As species harmful to various types of mammalian cells (Abernathy et al., 1990). Our findings on inorganic AsF and organic Ph_4As explode this thinking stressing the great importance of speciation of this metalloid in inducing biological effects. In this context, the observation on the uptake of the pentavalent AsF compared to that of the corresponding inorganic pentavalent Na_2HAsO_4 is of particular value. At equimolar concentrations of exposure (5 and 20μM) the amount of As incorporated into cells were of the same order of magnitude for the two species, leading about 3 and 4 times lower than those of the toxic trivalent As(III) (Table 24). Thus, the completely different effects induced by the two pentavalent inorganic species do not seem due to the amount of As present into the cell but rather to a different metabolisation of the two species accumulated by cells. This was confirmed by the experiments on speciation of As accumulated by cells exposed to As(III), As(V) and AsF (Table 25). In all cases, As was mainly incorporated into cytosol (Table 26). However, while for As(II) and As(V) mono- and dimethylated As species were identified in the cytosol and in culture medium at the end of exposure, in case of AsF exposure, no biomethylated species were detected. This suggests that into cells the fluorine-As bonding in of

$NaAsF_6$ is highly stable, compared to the oxygen-As bonding in of Na_2HAsO_4, explaining why AsF is not metabolised and excreted as such in culture medium (Table 26). A further support to this hypothesis is drawn from the experiments of gel filtration of the As-containing cytosol of cells exposed to As(III), As(V) and AsF. In case of As(III) about 10% of As was associated to high molecular components (Figure 20). Similar results was found for As(V), while in the cytosol of cells exposed to AsF no binding of As with proteins was found (data not reported).

Concerning the cytotoxicity and transforming response of Balb/3T3 cells exposed to Ph_4As we underline that at equimolar non-toxic and at toxic concentrations of Ph_4As and As(III) (0.1μM and 5μM) the uptake of the organic species was about 20 and 30 times lower compared to the corresponding values of As(III) and about of the same order of other toxic organic species (MMA(V), DMA(V), TMAO, Asβ, AsCh, Ph_4As) (Table 24).

A particular mention merits the findings on methylarsonous MMA(III). Our results confirm that this compound is a potent toxin (Styblo et al, 2002) and, for the first time, we proved that is not able to induce *in vitro* neoplastic morphological transformation (Table 22). We hypothised that a "metabolic deviation" of MMA(III) from the normal pathway to non toxic DMA(V) may be linked to the carcinogenicity of inorganic As(III). Our results don't support this hypothesis. Interestingly, at 0,1μM MMA(III) exposure, the amount of As accumulated into cells was about 10 times higher compared to that incorporated into Balb/3T3 cells exposed to the transforming inorganic As(III). This finding is in agreement with the hypothesis that biomethylated As metabolites containing trivalent As may activate As as a potent toxin, but no as carcinogen.

Considering that also in Balb/3T3 the biomethylation of As(III) would be a detoxication mechanism and that the bioreduction of As(V) to As(III) by GSH would be part of this process (Bertolero et al., 1987) it is reasonable to assume that the observed cytotoxicity and morphological transformation induced by As(V) in these cells may be related to the ability of the GSH-dependent mechanism to reduce As(V). In order to verify this hypothesis, the cells were exposed to As(V) alone or in combination with diethylmaleate (DEM), a well known cellular GSH-depleting agent (Bertolero et al., 1987). We found that in cells exposed to As(V) and DEM in combination, CFE inhibition and morphological transformation were significantly decreased compared to the corresponding results from cells exposed to As(V) alone (Table 23). This suggests that the final neoplastic transformation of Balb/3T3 cells by As(V) should be strictly related to changes in metabolic patterns of As(V) as a consequence of the lack of its bioreduction to the more toxic As(III) by intracellular GSH. The decreased transformation frequency in GSH-depleted cells confirms an important role for GSH in protecting the cells against the neoplastic action of As(III).
In order to establish if As(III) is a genotoxic or non-genotoxic carcinogen an attempt was done to isolate the adduct As-DNA from cells exposed to As(III). The results were negative (Tables 27 and 28), suggesting that As(III) is a non-genotoxic carcinogen.

Experiments on the effects of As(III) exposure on protein, nucleic acids content of Balb/3T3 cells (Figures 22-24) showed a linear increase of total protein as a function of incubated dose. This suggests a possible stimulation of specific protein synthesis (Figure 21) and is in agreement with the observed: (i) linear increase of RNA that indicates a possible stimulation of gene transcription (Figure 22), (ii) the double total DNA compared to control values (Figure 23) that suggest a possible blocking of the

cell in the S-phase of the cell cycle (after DNA replication), (iii) the RNA/DNA ratio increase with the dose-level (stimulation of gene expression) (Figure 24).

Cadmium

In spite of new and significant information achieved in the last decade on multiple mechanisms of action of Cd in in vitro systems, much more has to be elucidated before the significance of the various pathways leading to the neoplastic morphological transformation will be fully understood.

In the present work we have investigated the influence of some factors on the cytotoxicity and the morphological transformation response in Cd-exposed Balb/3T3 cells. In particular, studies carried out concerned metabolic pathways (uptake, intracellular distribution and analysis of biochemical forms of Cd in the cytosol) and biochemical effects induced by Cd exposure (cellular glutathione (GSH) levels, generation of oxygen reactive species (ROS) and lipid peroxidation, binding to DNA and formation of amino acids crosslinks).

In agreement with previous *in vitro* studies (Saffiotti and Bertolero, 1989) the present research on cytotoxicity and morphological transformation on Cd(II) in Balb/3T3 cells confirms the *in vitro* carcinogenic potential of this metal (Table 29 and Figure 28), in a clear dose-response fashion (Figure 25). Interestingly, the cytotoxic response in cells exposed to Cd(II) in combination with two GSH-depleting agents, BSO or DEM, was significantly more intensive compared to the corresponding values observed in cells exposed to Cd(II) alone (Figure 27). Furthermore, a similar finding was found for the morphological transformation: an increased transformation frequency was observed in cells treated with Cd(II) and DEM compared to cells exposed to Cd alone (Table 29).

This suggests that glutathione may be involved in modulating the cellular Cd(II) cytotoxic and transforming responses in Balb/3T3 cells. In fact, no significant effect of DEM treatment on Cd(II) uptake in Balb/3T3 cells was observed (Figure 29), suggesting that the reduced GSH content in the cells and the observed increase of transforming activity were not due to alterations in Cd-accumulation.

Our study has demonstrated that after 72h the Cd-treated Balb/3T3 cells are able of accumulating Cd(II) from culture medium in a linear fashion up to dose of 2μM Cd(II). Interestingly, this is a dose which doesn't yet induce statistically significant morphological transformation (Table 29). Different modes of transport into cells are possible for metal ions:(i) diffusion (ii) active transport via a receptor or carrier system (Luckkey and Venugopal, 1979). Diffusion is only possible if the metal is present as an uncharged complex. Uptake by diffusion, however, is linear with the solute concentration while uptake via an active mechanism should level off when the metal reaches a certain concentration, as it was observed in our study (Figure 29). Iron proton-metal cotransporter DMT1 and voltage-gated calcium channels have been reported as major carriers involved in Cd uptake in the intestinal epithelium and in neurons (Martelli et al, 2006). Cadmium uptake is further complicated by its possible binding to proteins immediately after entering the cell. Thus, the intracellular free Cd pool can be effectively reduced and the rate of uptake, as determined in our experiments, would depend on which step, transport or binding, is the rate limiting one. Since the present study didn't yield a clarification on what of these factors influenced the uptake of Cd in Balb/3T3 cells, further investigations in this area appear necessary.

The intracellular repartition of Cd between 110000xg cells pellet and supernatant showed the metal was almost present in the cytosolic fraction (Table 30).

Interestingly, more than 97% of the element was recovered in the cytosol of cells treated with doses of Cd(II) not inducing transformation in Balb/3T3 cells (1-2μM, Table 30); on the other hand, exposure to doses inducing morphological transformation led to a decrease in the proportion of Cd in the cytosol to about 90% of the cellular Cd which was matched by an increasing association, about 10% of the cellular Cd, with cell organelles. The increase of Cd in the organelle fraction from cell exposed at transforming (Table 30) is of particular interest in connection with the mechanism(s) responsible for the morphological transformation response. Although this work has not established to what organelle Cd was associated, several in vitro studies have shown that Cd produces a variety of direct and indirect genotoxic effects such as DNA strand breaks, DNA-protein crosslinks, oxidative DNA damage, chromosomal aberrations mostly at high, cytotoxic concentrations (Waalkes, 2003). In addition to a direct DNA damaging activity, Cd was reported to act as cancer promoter (Liu and Templeton, 2007) and to have co-genotoxic activity, probably interfering with DNA repair process (Hartwig and Beyersmann,1987), and perturbing apoptosis (Yuan et al., 2000). In the present study, we found that in Balb/3T3 cells Cd induced generation of oxygen active species ROS, lipid peroxidation, increased synthesis of DNA, binding and crosslinks of amino acids to DNA (Table 32, Figures 33, 34, 35 and 36). Thus, the presence of an “excess” of Cd in cellular compartments such as nuclei, mitochondria, lysosomes and lysosomes may play a role in creating the conditions for the cytotoxicity and transforming responses induced by Cd in Balb/3T3 cells.

We hypothesized that the ability of Balb/3T3 cells to accumulate Cd was related to the presence of a cytoplasmatic metallothionein-like proteins. Metallothioneins are cysteine-rich small proteins, which have been identified in the cytosol and in the

nuclei of higher eukaryotic cells (Hamer, 1986). It was first discovered by Margoshes and Vallee (Margoshes and Vallee, 1957) in equine kidney cortex and was subsequently named metallothionein since about 20% of aminoacids residues were comprised by cysteine. Our chromatographic studies revealed that Balb/3T3 cells incorporated ^{109}Cd into an intracellular cytosolic component (Cd BP) that has an approximate molecular weight of 6KDa, compatible with that of metallothionein (Hamer, 1986) (Figure 30C and D). In contrast, Balb/3T3 cells growth in culture medium, lacking Cd, didn't show Cd-BP species under our experimental conditions (Figure 30A). The protein nature of the identified 6KDa Cd BP in Balb/3T3 cells was assessed by further experiments:

(i) doubly radiolabelled experiments. In ^{109}Cd- and ^{35}Scys-treated cells a simultaneous incorporation of ^{109}Cd and ^{35}S into the 6KDa component was observed (Figures 30C and D), suggesting that a "de novo" bio synthesis of the Cd-BP occurred

(ii) heat stability experiments (Figure 31). A heat treatment of the 6KDa component at 80°C failed to dissociate Cd from the apoprotein (Cherian and Goyer, 1978) (Figure 31C) , while a significant proportion of ^{35}S, initially associated with high molecular weight components of the cytosol, shifted to small molecular weight components, probably due to the heat denaturating effect (Figure 31C).

(iii) UV absorption experiments. The 6KDa Balb/3T3 Cd-binding component exhibited spectral properties characteristic of metallothionein-like proteins, showing little absorbance at 280nm and a significant absorption at 254nm, due to the lack of aromatic aminoacids and the mercaptide bond formation between Cd and the great number of cysteine residues (Hamer, 1986). For the first time these

findings indicate that Cd-exposed Balb/3T3 cells resemble several other cell types with respect to the presence of a metallothionein-like protein (Cd-BP).

Interestingly, at not transforming doses exposure all cytosolic Cd was in the form of Cd-BP, while at higher transforming doses (5 and 7μM) the amount of metal in this form accounted for about 90% of total cytosolic Cd (Table 30), suggesting the presence of other biochemical species of Cd. The chromatographic experiments (Figure 30) confirmed this observation: at 1μM all cytosolic Cd was recovered from gel filtration as Cd-BP (Figure 30C), while at 5μM two other species of Cd were present, the first in association with high molecular weight components (peak1, Figure 30D), the second, smaller, present in the low molecular weight region (peak3, Figure 30D). Although the nature of these biochemical pools of Cd has not been clarified and their possible role in inducing cytotoxicity and morphological transformation is unknown, the appearance of these new Cd species in the cytosol in Cd-exposed transformed cells suggests that the "de-novo" biosynthesis of Cd-BP was saturated. This supports the belief that the formation of Cd-BP would be a process of cellular detoxication of Cd in Balb 3/T3 cells by sequestering the element in the cytoplasm, efficiently reducing at physiological level the cellular concentration of the "free metal", and so acting as protective mechanism against Cd cytotoxicity.

However, metallothionein may not be the only intracellular Cd scavenger. Glutathione, an abundant intracellular thiol with good chelating properties towards Cd, was found in nearly all cell types. This peptide acts as an antioxidant to detoxify a variety of endogenous and exogenous free radicals and its depletion is considered a marker of oxidative stress (Spear and Aust, 1995). Decreased intracellular GSH levels have been implicated in the pathogenesis of a number of degenerative conditions and diseases including cancer (Reed, 1990). Interestingly, BSO and DEM

treatment on 1μM Cd-exposed cells differently affect the levels of ^{35}S-cys incorporation into Cd-BP (Table 31). While BSO significantly increased, DEM decreased the Cd(II)-induced ^{35}S-cys incorporation into Cd-BP. This may be explained by the different way of action of the two GSH-depleting agents. BSO inhibits selectively the activity of γ-glutamilcysteine synthetase, the enzyme catalyzing the first step of glutathione biosynthesis, to block GSH synthetic pathway (Plummer et al., 1981). Its inhibiting effect lasts for a long period of time after removal of BSO from medium. On the contrary, DEM conjugates with GSH to deplete cellular GSH content (Griffith, 1981). Thus, the two GSH-depleting agents potentially have opposite effects on cellular cysteine content: BSO, by inhibiting GSH biosynthesis, "shaves" intracellular cysteine, so potentially enhancing Cd-BP biosynthesis. On the contrary, DEM, by conjugating with and depleting cellular GSH, could spend intracellular cysteine, potentially decreasing Cd-BP synthesis, in case that cysteine content is the rate limiting. This suggests that GSH and Cd-BP may have a differential role in protecting against Cd toxicity and that their additive effects may contribute to enhance cell defense against Cd cytotoxicity in Balb/3T3 cells. Some observations concerning the marked reduction of cytotoxicity of cadmium in cells pretreated with zinc supports this role (Ochi et al., 1988). Such protective effect of zinc was dependent upon duration of pretreatment, being parallel with the increased accumulation of MTs. Protection of cells from cadmium toxicity by zinc pretreatment was as or a little more effective in the cells depleted of GSH as in those not depleted. Thus, GSH appears to be an intrinsic protector against cadmium toxicity, while MTs would serve as an induced cellular defense that is mobilized against heavy metal stress, but takes more than 2h to accumulate in significant amounts. Accordingly, this suggests that also in Balb/3T3 cells GSH and

MTs may have cooperative protective roles against cadmium toxicity, as an initial defense for the former and a second-stage defense for the latter.

The biochemical effects detected in the present study merit some further considerations.

In the present study, the Cd treatment of Balb/3T3 cells increased significantly lipid peroxidation (Figure 36). The process of lipid peroxidation determines the alteration in the structure of cell membrane, being one of the consequences of oxidative stress, a situation that occurs when the production of ROS exceeds that of the antioxidant defense systems. The fact that the lipid peroxidation increased in response to Cd exposure in our cells may either due to enhanced free radical generation (Shukla et al., 1987) or depletion in the antioxidant capacity (Hussain et al., 1987). In Cd-exposed Balb/3T3 cells we found the generation of oxygen active species ROS (Figure 35), suggesting that Cd increased the oxidizing potential of cells undergoing oxidant-mediated damage. However, Cd(II) is not a directly active redox metal , a potential mechanism of oxidative damage-induced genotoxicity for redox active carcinogenic metals such as Cr(VI), Ni(II), Co(II) (Valko et al., 2005). Since Cd(II) does not catalyze Fenton-type reactions because it does not accept or donate electrons under physiological conditions (Waisberg et al., 2003) the mechanism of Cd in inducing ROS in Balb/3T3 cells may have a nongenotoxic epigenetic component. Then, Cd-enhanced ROS in Balb/3T3 may occur via suppression of free radical scavengers (e.g. glutathione) or by inhibition of detoxifying enzymes (e.g. catalase, glutathione peroxidase and superoxide dismutase) (Waisberg et al., 2003) or binding to sulfhydril groups of proteins (Valko et al., 2005). Moreover, other possible indirect mechanism(s) could help to explain the increase of ROS induced by

Cd. For example, the displacement of Fenton metals (Fe and Cu) by Cd from various intracellular sites (Casalino et al, 1997) may increase the concentrations of ionic Cu and Fe, which could cause oxidative stress by Fenton reactions. The fact that desferrioxamine (a iron chelator) prevents the Cd-induced ROS formation and cytotoxicity supports this hypothesis (Pourahmad and O'Brien, 2000). Since ROS can act as signalling molecules (D'Autréaux and Toledano, 2007) our finding on the ROS production in Balb/3T3 cells suggest to study if the increase of ROS induced by Cd is involved in the induction of apoptosis and gene expression by this metal (Fernandez et al., 2003). Furthermore, our finding on the ROS elevation with Cd dose exposure is consistent with the observed increase of Cd in the organelles fractions at transforming doses (Figure 35). In this context, future studies in this area would be focussed on mitochondria, since it has been suggested that mitochondria are the ROS sites for non-redox or poor cycling transition metals (Cd, Hg and As) while lysosomes are sites of cytotoxic ROS formation of redox transition metals (Cu, Cr, Ni and Co) (Pourahmad et al., 2003).

Cadmium is considered a weakly genotoxic agent (Bertin and Averbeck, 2006).Due to the observed presence of Cd-BP in Balb/3T3 it is interesting from the mechanistic point of view to discuss the possible role of Cd-BP in interfering with antioxidant defense mechanisms. A study has reported the ability of Cd, when bound to metallothionein, to induce DNA damage via radicals formed by the metallothionein complex (Muller et al., 1994). On the contrary, other studies suggested that metallothionein gene expression provides protection against Cd genotoxicity (Coogan et al, 1994; Klassens et al., 1999).Our results are in agreement with the second suggestion. In fact, if the binding of Cd to metallothionein induces radicals in a whole cell system, one may expect that the binding of Cd to metallothionein within

the cytosol would generate also radicals that should lead to radical-induced cytotoxicity and not protection as is consistently observed. At present, the induction of metallothionein by Cd is considered a paradox: on the one hand it binds and detoxifies ROS, on the other hand mobilization of Cd from the metallothionein complex increases the toxicity of the element.

We have found that in Cd-treated Balb/3T3 cells Cd doses inducing neoplastic transfomation decrease the levels of cellular GSH (Table 29) which is known to maintain cellular redox homeostasis and to scavenge intracellular ROS by a direct reaction, or via the GSH peroxidase/GSH system, or the activities of superoxide dismutase, glutathione peroxidase and catalase (El-Maraghy, 2001).Thus, in our Balb/3T3 cells the decrease in the activity and/or intracellular levels of antioxidants and the enhancement of ROS caused by Cd, together with the generation of radicals that are produced during normal metabolism, probably damage the DNA and may explain the increase in lipid peroxidation we have observed.

In this work, we have isolated a Cd-DNA adduct from Cd-treated cells (Figure 33B). However, the binding of Cd to DNA per se didn't give information on a possible role of the metal in producing DNA -protein crosslinking, which could occur. For this, we have investigated the crosslinking produced by Cd, analysing the residual ^{14}C-amino acids (AAs) associated to DNA (Figure 33).Since the DNA isolation involved a proteinase k treatment, only AAs that were covalently complexed to DNA were being analysed. This led to the isolation of a Cd-AA(s)-DNA complex (Figure 33C). Interestingly, experiments on the stability of this complex (Figure 34) suggests that AA(s) were tightly bound to the DNA, and that the stability of Cd-DNA complex was enhanced when aminoacids were bound to DNA, having the metal a "promoting action" in producing covalent AA(s)-DNA crosslinks. In general, it is recognised that

some metals can directly bind DNA or form crosslinks between DNA strands or between the surrounding protein and DNA (Waalkes, 2002) and that Cd binds only weekly to DNA in ex-vivo systems, thus eliminating this as a potential mechanism of DNA damage leading to mutation (Waalkes and Poirier, 1984). Our results are in good agreement on this. The binding of Cd to DNA previously isolated from cells is small (Figure 33A) while in DNA isolated from Cd- and AAs-treated cells (Figure 33B) we observed a Cd-AA(s)-DNA complex, presumably an indication of protein-DNA crosslinks, lesions which could act as a possible prelude to mutation.

In conclusion, in spite of new and significant information concerning its multiple mechanisms of action (Hartwig, 1989), much more has to be elucidated before the relative significance of the various pathways leading to Cd carcinogenicity will be known. Thus, the use of an in vitro system recognised as a valid model for testing the carcinogenic potential of chemicals such as Balb/3T3 cell line is a great opportunity to give new mechanistic insights. In this context, at present most of the attention is focussed on the biological responses concerning the various pathways leading to the morphological transformation of Cd and too little attention is paid to the metabolic pathways of the element into the cell. Since this aspect is a fundamental determinant in interpreting mechanistically the toxicological data we must keep well in the mind this multidisciplinary approach when future experiments. in this field will be planned.

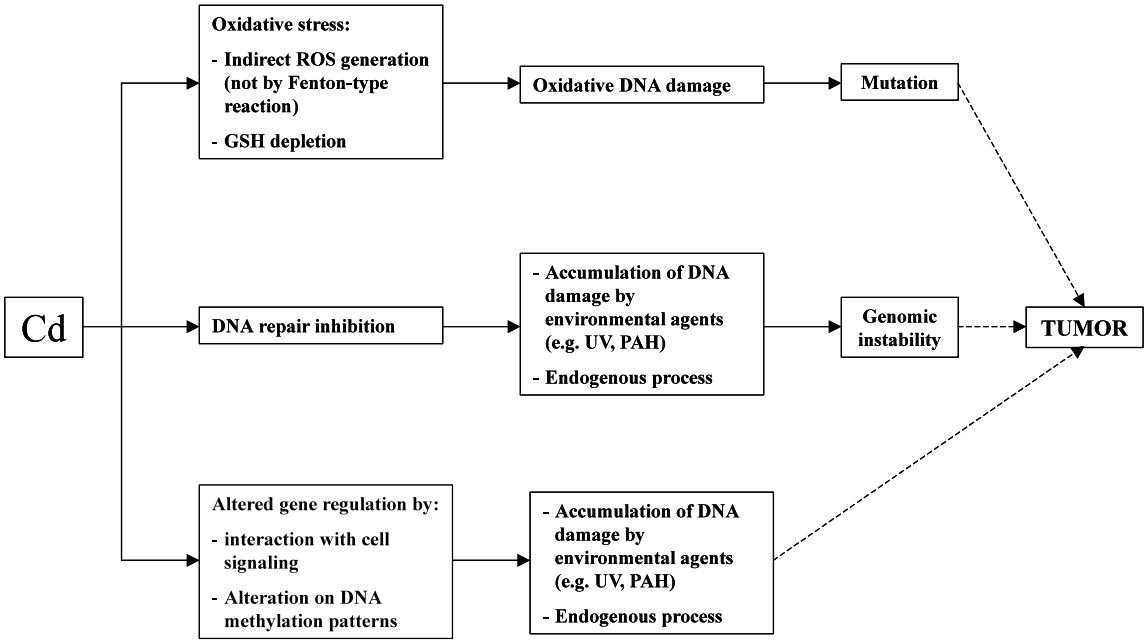

Proposed mechanisms for Cd carcinogenesis to be investigated in Balb/3T3 cell line. From Hartwing and Beyersmann, 1989.

Chromium

The experiments on cytotoxicity and morphological transformation on Cr(VI) and Cr(III) confirmed the carcinogenic potential of Cr(VI) in Balb/3T3 cells and added evidence that Cr(III) was not transforming to the same cell line (Table 34). Interestingly, the experiments on the behaviour of Cr(VI) in cell-free medium showed a high stability of the hexavalent form after 72h incubation (Table 35). This situation changed when cells were exposed to Cr(VI). A considerable amount of Cr was recovered as Cr(III) (Table 35). This suggests that a bioreduction of Cr(VI) by cell components occurred. From our data it is not possible to establish if the observed bioreduction was a consequence of the contact of Cr(VI) in the medium with cell-constituent of the membrane or if it was an intracellular process with a subsequent release of the trivalent species into the medium. Since it is well known that Cr(III) is poorly absorbed and cannot be readily across cellular membranes (Bianchi et al.,

1988) the hypothesis of the bioreduction of hexavalent Cr to trivalent form by surface cell-components seems the most probable.

Our study on the uptake of Cr in Balb/3T3 exposed to Cr(VI) (Figure 38) is an excellent example of a new approach to the study of the cellular uptake of xenobiotics. For the first time, a study on the uptake has taken into account not only the living but also the death cells, an intersting aspect for the interpretation of the cytotoxic effects. We found that the curves of the uptake of Cr in living and died cells approached with time (Figure 39). This suggests a possible presence of a "mechanism of adaptation" of cells to the exposure of Cr(VI), becoming a part of cells resistant to the toxic action of the hexavalent species.

Chromium accumulated by cells exposed to non-toxic (0.1μM) or toxic (7μM) (Figure 40) dose of Cr(VI) was intracellularly distributed in a different way (Table 37). At non-toxic dose more than 75% of Cr was localised in the cytosol, while at toxic dose the highest amount of the element was recovered into the nuclear fraction. This suggests that a redistribution of Cr occurred intracellularly, probably after saturation of the "physiological" binding sites in the cytosol. Gel filtration profiles of the Cr from the cytosol of cells exposed to the non-toxic and toxic doses of Cr(VI) supports this hypothesis (Figure 40). In addition, the experiments on the Cr-bound proteins of the cytosol showed that at non-toxic dose Cr was mainly in the oxidation state +3 while at toxic dose about 60% of Cr still persisted in the oxidation state +6 (Table 39). Furthermore, the isolation of DNA from cells exposed to the toxic dose of Cr(VI) showed the presence of Cr-DNA adduct (Figure 40), in which the oxidation state of Cr was +3 (Table 43).

These findings are in agreement with the litarature data. Cr(VI) is reductively metabolised into cells leading to Cr(III) that forms tight comlexes with DNA,

preference towards the formation of Cr(III)-guanine DNA adduct. During Cr(VI) reduction, genetic lesions occur, including Cr-DNA binary adducts, single-strand breaks, DNA protein crosslinks and oxidised bases (O'Brien et al., 2003).

Platinum

Experiments on inorganic platinum in anionic and cationic form confirmed how the cytotoxic effects observed were dependent on the chemical form of the Pt compound tested (Figure 41 and 42).

The study of Pt compounds in Balb/3T3 cells is an example of the great complexity of how the initial chemical form of a xenobiotic can undergo to complex changes in culture medium with the possibility of binding to the medium components (Figure 30). Thus, the observed different degree of cytotoxicity of the Pt compounds may depend on the changes of the original chemical species generated in culture medium (Figure 44). This raises to important questions: (i) what is the chemical species of Pt penetrating into cells inducing the toxic effects? (ii) is the cytotoxicity results cytotoxic effects induced by more than one Pt species?

Interestingly, after 72h, the ranking of the amount of Pt incorporated into cells exposed to non toxic dose (0.1μM) of the Pt compounds (Tables 44 and 45) was inversely proportional to the corresponding ranking of cytotoxicity ($PtCl_2$>$PtCl_4$>Na_2PtCl_6>Na_2PtCl_4), being 0.007, 0.22, 1.51, 2.34fgPt·cell^{-1} respectively (Tables 44 and 45).

The intracellular distribution of the Pt in cells exposed to non-toxic doses (1μM) of Pt chlorocomplexes (IV) and (VI) shows no obvious differences at 4 and 72h exposure (Table 46). More than 66% of Pt was present in the cytosol. However, at toxic dose of Na_2PtCl_6 (10μM) the cytosolic Pt decreased with a corresponding increase of the element into the nuclear fraction. In addition, gel filtration of the Pt-

containing cytosols from exposure to 1μM of both Pt chlorocomplexes shows similar chromatographic profiles of Pt (Figure 46). These findings and the data concerning the uptake of Na_2PtCl_6 compared to Na_2PtCl_4 is a further demonstration that the oxidation state of Pt plays a critical role in inducing the final biological effects. Moreover, the disappearance of signal at 8.60 and 8.61ppm in the lyaste of Balb/3T3 cells previously trated with Na_2PtCl_6 (Figure 47) is in contrast with the results concerning the interaction of Pt compounds with culture medium (Figure 45) where it was evident that Pt forms insoluble complex with histidine and hence not bioavailable. The toxicity of Na_2PtCl_6 can be explained only with the hypothesis thet uptake is faster than Pt-His_2 complex formation.

Vanadium

Cytotoxicity and morphological transformation on cells exposed to V(V) and V(IV) sodium salts confirmed previous results on the carcinogenic potential of the ammonium salts of V(V), a species leading to the production of morphological transformed Balb/3T3 cells, while the correponding ammonium salt of V(IV) was ineffective in the transformation of the cells (Table 47) (Sabbioni et al., 1991). Table 47 confirmed also that exposure of cells to V(V) sodium salt in combination with DEM lead to unreduced V(V) into cells significantly enhancing the type III foci formation compared to the corresponding results from cells exposed to V(V) alone. This further suggests that the GSH-mediated bioreduction of V(V) to V(IV) is a detoxication mechanism in Balb/3T3 cells against the toxic effects of V(V). Interestingly, new findings on the intracellular distribution of V(V) and V(IV) (Table 50), which were incorporated into cells at different rate (Figure 50 and Table 49), gave further mechanistic insights in connection to the transforming potential of V(V). At non-toxic dose of 0.1μM mainly of the cellular V in Balb/3T3 exposed to

both the V species was present in the cytosol (Table 50). However, at 10μM V(V) (toxic dose) the uptake was not linear with dose exposure (Figure 50) and more than 20% of cellular V shifted from cytosol to cellular organelles, particularly nuclei and mitochondria. In this context, we were able to isolate a V-DNA adduct from exposed cells (Table 52 and Figure 52B). The binding of V to DNA is only apparently in contaddiction with the negative results previously reported on the *in vitro* binding of V(V) to commercial nucleic acid (Sabbioni et al., 1993) by using a method at the equilibrium of (Wood and Cooper, 1970). Also in the present work *in* vitro experiments on the binding of V(V) to Balb/3T3 previously isolated from Balb/3T3 cells gave negative results (Figure 52A). This suggests that the observed binding of V to DNA was cellular-mediated, probably previous bioreduction to the tetravalent form. In addition, at 10μM V(V) and V(IV) differences in the binding to proteins and in the oxidation state of V were observed in the cytosol (Figure 51 and Table 51). The association of V with biomolecules in the cytosol (Figure 51) suggests that two forms of V interact differently with cytosol components from quantitative point of view. This could be explained taking into account the data of the uptake of V in cells exposed to the two V species, about 5 times higher in case of V(IV) compared to V(V) (Table 49). Since the amount of V incorporated into peak II was similar for both V species while was different for peaks II and III, we can conclude that the observed differences of the V profiles in the chromatogram from gel filtration (Figure 51) may be due to a saturation of peak II by tetravalent V.

The simultaneous presence of the two oxidation state +4 and +5 in cells exposed to toxic V(V) species (Table 51) can further reinforces the thinking that the bioreduction of V(V) to V(IV) is a detoxication mechanism. Experiments on the determination of the oxidation state of V in culture medium by using ^{48}V radiotracer

and Sabbioni's method (Section 4.1.2) added new information to the previous findings obtained by electron paramagnetic resonance (EPR) technique. This latter technique is able to detect V in the oxidation state +4 but not in the higher oxidation state (Sabbioni et al., 1993). Exposure to V(V), which is very stable in cell-free culture medium, led to presence in cell-containing medium of V(IV) in a polymeric form (Sabbioni, unpublished results). However, in this work, in the cell-containing medium we found the presence of about 10% of V still in the oxidation state +5 (Table 51). This finding and the demonstration of the presence of pentavalent V into cells after exposure to V(V) is of particular interest. Since the cellular bioreduction of V(V) to (IV) is crucial to prevent the deleterious effects of V(V), the knowledge of the amount of V(V) in the biological systems wuold be a "key point" in assessing a safe limit of V cytotoxicity and morphological transformation. Again, this shows the great potential of the combined use of the *in vitro* bioassay with the nuclear and radioanalytical techniques (Sabbioni and Balls, 1995).

Neurotoxic effects of As and Mn compounds

Hereafter are reported findings concerning the research on neurotoxic effects of As in rat brain re-aggregates and single cells and of Mn in PC12 cell line.

Arsenic

Rat brain re-aggregates exposed to As(III) led to interesting conclusions. Arsenic was able to penetrate the whole aggregate (Table 57) with the formation of biomethylated species (Table 58). The uptake of As into whole aggregates increased at 30μM, then levelled decreasing up at 1000μM. This could be explained considering cell vitality. At 30μM the vitality of neurons and almost astrocytes was inhibited (Figure 60) and almost microglia survived.

In the different types of cell constituents of the aggregates, the uptake of As was mainly measured in the astrocytes (Table 59).

Manganese

Studies on humans have indicated that elevated levels of Mn may put humans at risk of parkinsonism (Olanow, 2004). Manganese exposure is known to produce neurotoxicity in vitro and in animal models. In particular, in vitro studies provide evidence that Mn specifically targets the dopaminergic system. Because of the similarities between the neurological symptoms associated with manganism and Parkinson's disease, most research efforts in the past have focused on model cell systems in which dopamine is the principal neurotransmitter. In this context, PC12 cells are a neuroendocrine cell line able to produce neurotransmitter dopamine (DA) and contain functional DA metabolism pathways (Green and Rein, 1977). These cells are widely used as a model for catecholaminergic neurons. However, *in vitro* studies on Mn in PC12 cells mainly concern the relations between functional changes of dopaminergic system during the development of Mn-induced damage. Little attention has been paid to the metabolic pathways of Mn in the cell in relation to the DA metabolism and the observed adverse cellular effects. This is a serious gap for the mechanistic interpretation of the neurotoxic effects of Mn. In addition, being a transition metal, Mn in living tissues can exist in various oxidation states such as +2, +3, +4, +5, +6, +7, although the last three higher oxidation states are generally unrecognized in biological materials (Keen, 1995). So, the variable valency of Mn is extremely important, emphasizing the potential for Mn to act as prooxidant or an antioxidant in biological medium (Aschner, 1997). The present study was designed to assess the time course metabolic patterns of two Mn chemical forms, such as

cationic divalent Mn(II) and anionic Mn(VII), in PC12 cells in relation to their cytotoxicity.

Our findings show a clear dependence of the uptake and of the cytotoxic effects on the oxidation state of Mn (Figures 53 and 54). In particular, uptake versus Mn concentrations showed saturation-type kinetics. In addition, at equimolar concentrations eptavalent Mn(VII) was taken up by cells at a greater extent than Mn(II) (Figure 54). Thus, the extent of Mn uptake by PC12 seems an important determinant of the different cytotoxicity observed in the case of the two chemical species tested (Figure 53). It has been reported that Mn would be transported into cells via a mechanism similar to that for iron (Heilig et al., 2006), as evidenced by the fact that both Mn and iron, as well as several other divalent transition metals, compete for uptake into a number of different cell systems (Roth et al., 2002). In particular, two distinct but related mechanisms responsible for the transport of Mn and ferrous ion: a transferrin-dependent and a transferrin independent pathway. The transferrin dependent pathway proposes that the transferrin-Mn(III) complex initially binds to the transferrin receptor (TfR) on the cell surface similar to that, which occurs for iron. After attachment of Tf to the TfR, endosomal vesicles that are formed at the cell surface are internalized, subsequently causing a release of the metal from the Tf/TfR complex. Mn(III) released into the vesicles is presumably reduced to Mn(II). This is a serious gap for the mechanistic interpretation of the neurotoxic effects of Mn.

It is subsequently transported across the endosomal membrane via the transport protein, divalent metal transporter 1 (DMT1; also named Nramp2, DCT1 or SLC11A2) (Andrews, 1999). Since Mn(II) forms a relatively weak complex with either a2-macroglobulin or serum albumin, there is also the possibility that transport

of Mn(II) released from this complex can be taken up directly at the cell surface by DMT1, independent of transferrin (Roth et al, 2002). Our dopaminergic cell type PC12 cells also express DMT1 and TfR (Loder and Melikian, 1997). These mechanisms assume that Mn in culture medium is present in different oxidation states , Mn(II) and Mn(III), and that is differently complexed with proteins. Our gel filtration and NMR studies on the behaviour of Mn in RPMI culture medium are in agreement with the proposed mechanisms (Figure 54). Incubation of ionic Mn(II) in culture medium leads to the disappearance of ionic form of Mn with the formation of Mn-complexes with high molecular weights, of the order of albumin/transferrin, and with low molecular weight, including histidine (Figures 54B). These findings are in agreement with the tendency of Mn to form very tight complexes with biocomponents, so that its free concentrations tend to be extremely low (Keen, 1995).

Our results from the intracellular distribution studies lead to completely new information on the metabolic patterns of Mn in PC12 subcellular compartments. Interestingly, in Mn(II)-exposed cells the relative distribution of the element among cell organelles and cytosol is clear dose-dependent (Table 54). At physiological non toxic doses of exposure a considerable percentage of cellular Mn was present in the nuclei, mitochondria and lysosomes (more than 70% of the Mn accumulated by cells). Increasing dose exposure shows a clear progressive decrease of the percentage of the element in the nuclei, mitochondria and lysosomes. The decrease in the proportion of Mn in these fractions is matched by an increasing in association with cytosl. A recent study has underlined the presence of significant amount in the nuclei of Mn(II)-treated RBE4, Z310, and N27 cells (Kalia et al, 2008). The same work reports also a recovery of 27% and 69% of Mn in nuclei and cytoplasm of Mn(II)-

treated PC12cells, respectively. Since such cells were exposed to 100μM, our results at this dose exposure (Table 54) are in good agreement with Kalia's findings.

In our PC12 cells exposed to1μM of Mn(VII) the intracellular distribution of Mn (Table 56) resembles that of the element in cells treated with the same dose of Mn(II) (Table 54). However, a substantial difference was found at exposure concentration of the order of the IC_{50} (20μM) of Mn(VII). The amount in the cytosol remained constant, while the percentage of Mn in the nuclei decreased, matched by an increase in the mitochondria+lysosomes. This picture was different compared to the intracellular distribution of Mn(II)-treated cells (Table 54).

The dynamic behavior of manganese exposures in biological systems is evidenced by several recent studies indicating that the oxidation state of manganese added to cell lysates or intact mitochondria rapidly changes, likely as a consequence of the complex physicochemical and ligand binding properties of the local environment (Gunter et al., 2004) .In order to study the dynamic movements of Mn incorporated into Mn(II)-exposed cells unique experiments by a triple radiolabelling approach have been carried out at cellular and subcellular level (Tables 53 and 55 and Figures 57 and 58). Such experiments have shown the presence of "different biochemical pools of Mn" in PC12 cells exposed firstly to ^{54}Mn(II) for 24h, then to ^{52}Mn (II) and again to ^{56}Mn(II) for 3h. The partial replacement of ^{54}Mn (first exposure) by ^{52}Mn (second exposure) and of ^{54}Mn+^{52}Mn by ^{56}Mn (third exposure) suggests that the internalized Mn is differently bound to cellular components: a "tightly bound pool" and a "labile pool". The first pool would be responsible for the retention of Mn in the cell while the second pool would represent the mobile pool of Mn. This approach seems of particular interest because the establishment of the role of such pools could

be of great interest in explaining mechanistically the cytotoxic effects of Mn in PC12 cells.

Our study suggests a close relation among uptake, intracellular distribution and cytotoxic effects of Mn(II) and Mn(VII) in PC12 cells, confirming the importance of speciation as a key factor in inducing the biological response. In particular, in addition to the common Mn(II) species we have considered a chemical eptavalent form of Mn. Although the higher oxidation state +7 of Mn in the cell is not demonstrated and probably is not physiologic, the $KMnO_4$ considered was used as "extreme tool" of speciation due its strong oxidising property which is useful from the point of view of mechanistic understanding.

The findings of our experiments on the ROS generation further give evidence of this (Figure 59). It was reported that Mn induces oxidative stress-mediated apoptosis in catecholaminergic PC12 cells (Hirata et al. 1998), although another evidence indicate that Mn(II), unlike that of iron, is a potent antioxidant and that the oxidative stress doesn't contribute to initiate Mn cytotoxicity (Roth et al, 2000). In the preset work the production of ROS was significantly higher in Mn(VII)-treated cells compared to Mn(II)-exposed cells (Figure 59). Thus, as whole our data support that the oxidation state/chemical speciation of manganese exposure could be an important factor mediating cellular uptake and toxicity.

CONCLUSIONS

Analytical aspect of metallomics. The analytical challenges to metallomics must reach a specificity of analytical response regard to a particular element species and sensitivity allowing an analysis to be carried out with microsamples.

This research shows how the use of unique and peculiar nuclear, radioanalytical and advanced spectrochemical techniques, particularly ICPMS, is a powerful analytical tool in metalllomics research.

***In vitro* metallomics.** The introduction of *in vitro* models such as Balb/3T3 and PC12 cell lines as well as rat brain aggregates, which are relevant at ECVAM for *in vitro* testing of carcinogenic potential and neurotoxicity of chemicals, allowed important findings about qualitative and quantitative metallomics. There is no doubt that *in vitro* metallomics will play a fundamental role in future investigations on the molecular bases of many metal-dependent biochemical processes.

Metallomics, a multidisciplinary task. The present research confirms the complex multidisciplinary character of speciation of metallomes, requiring a real cooperation among different scientists including biochemists, toxicologists, analytical chemists, metallorganic chemists, radiochemists, etc.

BIBLIOGRAPHY

Abernathy C.O., Liu J.P., Longfellow D., et al.; Arsenic health effects, mechanisms of actions and research issues. *Envirom. Health Persp*. 1990, 107: 593-597.

Al-Nasiry S., Geusens N., Hanssens M., Luyten C., Pijnenborg R. The use of Alamar Blue assay for quantitative analysis of viability, migration and invasion of choriocarcinoma cells. *Hum Reprod*. 2007, 22(5): 1304-9.

Andrews N.C. The iron transporter DMT1. *Int J Biochem Cell Biol*. 1999, 31: 991-994.

Aschner M. Astrocyte metallothioneins (MTs) and their neuroprotective role. *Ann N Y Acad Sci.* 1997, 825: 334-47.

Baker M.A., Cerniglia G.J., Zaman A.. Microtiter plate assay for the measurement of glutathione and glutathione disulfide in large numbers of biological samples. *Anal Biochem*. 1990, 190:360-5.

Bianchi V., Levis A.G. Review of genetic effects and mechanisms of action of chromium compounds. *Sci. Total Environ.* 1988, 71:99-172.

Birattari C., Bonardi M., Groppi L., Gallorini M., Sabbioni E. and Stroosnijder M.F. Cyclotron production of "very high specific activity" platinum radiotracers in no carrier added form. *Cyclotron and their applications 2001, Sixteenth International Conference.* 2001: 52-54.

Bertolero F., Pozzi G., Sabbioni E. & Saffiotti U. Cellular uptake and metabolic reduction of pentavalent to trivalent arsenic as determinants of cytotoxicity and morphological transformation. *Carcinogenesis*. 1987, 8: 803-808.

Beuge J.A. and Aust S., Microsomal lipid peroxidation. *Methods Enzymol*. 1978, 51: 302-310.

Bertin G. and Averbeck D.. Cadmium: cellular effects, modifications of biomolecules, modulation of DNA repair and genotoxic consequences (a review).*Biochimie*. 2006, 88: 1549-1559

Casalino E., Sblano C. and Landriscina C. Enzyme activity alteration by cadmium administration to rats: the possibility of iron involvement in lipid peroxidation. *Arch Biochem Biophys*. 1997, 346: 171-179.

Cherian M.G. and Goyer R.A. Role of metallothioneins in disease *Ann.Clin. Lab. Sci*. 1978, 8: 91-94.

Combes R., Balls M., Current R., Fischbach M., Fusenig N., Kirkland D., Lasne C., Landolph J., LaBoeuf R., Marquardt H., McCormick J., Muller L., Rivedal E., Sabbioni E., Tanaka N., Vasseur P. & Yamasaki H.. Cell transformation assay as predictors of human carcinogenicity. The report and recommendations of ECVAM, Workshop 39. *ATLA*. 1999, 27: 745-767.

Coogan T.P., Bare R.M., Bjornson E.J. and Waalkes M.P. Enhanced metallothionein gene expression is associated with protection from cadmium-induced genotoxicity in cultured rat liver cells. *J Toxicol Environ Health*. 1994, 41: 233-245.

Cullen, W.R., McBride, B.C., and Reglinski J. The reaction of methylarsenicals withthiols. *Some biological implications*. *J. Inorg. Biochem*. 1984, 21:179-194.

D'Autréaux B. and Toledano M.B. ROS as signalling molecules: mechanisms that generate specificity in ROS homeostasis. *Nat. Rev. Mol. Cell. Biol.* 2007, 8: 813-824.

Di Paolo J.A.. Quantitative in vitro transformation of Syrian golden hamster embryo cells with the use of frozen stored cells. *J. of the National Cancer Institute*. 1980, 64: 1485-1489.

Donaldson J., La Bella F.S. and Gesser D. Enhanced autooxidation of dopamine as a possible basis of manganese neurotoxicity. *Neurotoxicology*. 1991, 2: 53–64.

Elias Z., Poirot O., Baruthio F. and Daniere M.C.. Role of solubilized chromium in the induction of morphological transformation of Syrian hamster embryo (SHE) cells by particulate chromium(VI) compounds. *Carcinogenesis*. 1991, 12/10: 1811-1816.

El-Maraghy S.A., Gad M.Z., Fahim A.T., Hamdy M.A. Effect of cadmium and aluminum intake on the antioxidant status and lipid peroxidation in rat tissues. *J Biochem Mol Toxicol.* 2001, 15: 207-214.

Eskes, C., Honegger, P., Juillerat-Jeanneret, L. and Monnet-Tschudi, F. (). Microglial reaction induced by noncytotoxic methylmercury treatment leads to neuroprotection via interaction with astrocytes and IL-6 release. *Glia*. 2002, 37: 43-52.

Farina M. Applicazione di tecniche analitiche avanzate in studi *in vitro* di metalli in tracce mediante colture cellulari. *Thesis degree*, Università degli Studi di Pavia, 2003.

Fernández E.L., Gustafson A.L., Andersson M., Hellman B. and Dencker L. Cadmium-induced changes in apoptotic gene expression levels and DNA damage in mouse embryos are blocked by zinc. *Toxicol Sc*i. 2003, 76: 162-170.

Greene S. Validation and *in vitro* neurotoxicity. Division of Toxicological Research, US Food and Drug Administration, Laurel, MD 20708, USA. *Clin. Exp. Pharmacol. Physiol.* 1995, 22: 747-755.

Greene L.A., Tischler A.S. Establishment of a noradrenergic clonal line of rat adrenal pheochromocytoma cells which respond to nerve growth factor**.** *Proc Natl Acad Sci U S A*. 1976, 73: 2424-8.

Griffith O.W. Depletion of glutathione by inhibition of biosynthesis. *Methods Enzymol*. 1981, 77: 59-63.

Gunter T.E., Miller L.M., Gavin C.E., Eliseev R., Salter J., Buntinas L., Alexandrov A., Hammond S. and Gunter K.K. Determination of the oxidation states of manganese in brain, liver, and heart mitochondria. *J. Neurochem*., 2004, 88: 266–280.

Hamer D.H. Metallothionein. *Annu Rev Biochem*. 1986,55: 913-51.

Haraguchi H. Metallomics as integrated biometal science. *JAAS*. 2004, 19: 5-14.

Hartung T., Bremer S, Casati S., Coecke S, Corvi R., Fortaner S., Gribaldo L, Halder M., Hoffmann S., Roi-Janusch A., Prieto P., Sabbioni E., Scott L., Worth A. and Zuang V. ECVAM's response to the changing political environment for alternatives: consequences of the European Union chemicals and cosmetics policies. *ATLA*. 2003, 31: 473-481.

Hartung T., Bremer S, Casati S., Coecke S, Corvi R., Fortaner S., Gribaldo L, Halder M., Hoffmann S., Roi-Janusch A., Prieto P., Sabbioni E., Scott L., Worth A. and Zuang V. A Modular Approach to the ECVAM Principles on Test Validity. *ATLA*. 2004, 32: 497-472.

Hartwig A. and Beyersmann D. Comutagenicity and inhibition of DNA repair by metal ions in mammalian cells. *Biol Trace Elem Res.* 1989, 21: 359-65.

Heilig E.A., Thompson K.J., Molina R.M., Ivanov A.R., Brain J.D. and Wessling-Resnick M. Manganese and iron transport across pulmonary epithelium. *Am J Physiol Lung Cell Mol Physiol*. 2006, 290: 247-259.

Hirata Y., Adachi K. and Kiuchi K. Activation of PNK pathway and induction of apoptosis by manganese in PC12 cells. *J Neurochem*. 1998, 71: 1607-1615.
IARC/NCI/EPA Working-Group, Cellular and molecular mechanisms of cell transformation and standardization of transformation assays of established cell lines for the prediction of carcinogenic chemicals: overview and recommended protocols. Cancer Research. 1985, 45: 2395-2399.

Honegger P. and Matthieu J.M. Aggregating brain cell cultures: a model to study meylination and demeylination. In: Cellular and Molecular Biology of Meylination. Jeserich G, Althaus HH, Waehneldt TV, ed. Berlin:Springer Verlag. 1985, 155–170.

Honegger P. and Monnet-Tschudi F. Aggregating neural cell cultures. In: S. Fedoroff and A. Richardson, Editors. *Protocols for Neural Cell Culture* (third ed.). Humana Press. Ottawa, 2001, 199-218.

Hussain T., Shukla G.S., Chandra S.V. Effects of cadmium on superoxide dismutase and lipid peroxidation in liver and kidney of growing rats: in vivo and in vitro studies: Pharmacol Toxicol. 1987; 60: 355-358.

IARC. Monograph on the evaluation of carcinogenic risk to humans. Chromium, nickel and welding. IARC, International Agency for Research on Cancer, Lyon. 1990, 49.

Kakunaga T. A quantitative system for assay of malignant transformation by chemical carcinogens using a clone derived from Balb/3T3. *Int. J. of Cancer*. 1973, 12: 463-473.

Kalia K., Jiang W., Zheng W. Manganese accumulates primarily in nuclei of cultured brain cells. *Neurotoxicology*. 2008, 29: 466-470.

Keen C.L. Overview of manganese toxicity. In Proceedings of the Workshop on the Bioavailability and Oral Toxicity of Manganese, (Velazquez S, EPA Liaison). US EPA. Environmental Criteria and Assessment Office 1995: 3-11.

Kinsner A., Pilotto V., Deininger S., Brown G.C., Coecke S., Hartung T. and Bal-Price A. Inflamatory neurodegeneration induced by lipoteichoic acid from *Staphylococcus aureus* is mediated by glia activation, nitrosative and oxidative stress and caspase activation. *Journal of Neurochemistry*. 2005, 95: 1132-1143.

Kinsner A., Boveri M., Hareng L., Brown G.C., Coecke S., Hartung T. and Bal-Price A. Highly purified lipoteichoic acid induced pro-inflammatory signalling in primary culture of rat microglia through Toll-like receptor 2: selective potentiation of nitric oxide production by muramyl dipeptide. *Journal of Neurochemistry*. 2006, 99: 596-607.

Klaassen C.D., Liu J., Choudhuri S. Metallothionein: an intracellular protein to protect against cadmium toxicity. *Annu Rev Pharmacol Toxicol*. 1999, 39: 267-94.

Leist M,, Gantner F., Bohlinger I., Tiegs G., Germann P.G., Wendel A. Tumor necrosis factor-induced hepatocyte apoptosis precedes liver failure in experimental murine shock models. Am J Pathol. 1995, 146: 1220-34.

Lin T.P., Labosky P.A., Grabel L.B. Kozak C.A. and J. Pitman L. The Pem homeobox gene is X-linked and exclusively expressed in extraembryonic tissues during early murine development. *Dev. Biol*. 1994, 166: 170-179.

Liu Y. and Templeton D. Cadmium activates CaMK-II and initiates CaMK-II-dependent apoptosis in mesangial cells .*FEBS Letters*. 2007, 581: 1481–1486.

Luckey T.D. and Venugopal B. Modes of intake and absorption, in Metal Toxicity in Mammals 1. Physiological and Chemical basis for Metal Toxicity, Plenum Press ed. 1979, chapter 2, 39-43.

Loder M.K. Melikian HEAstrocyte metallothioneins (MTs) and their neuroprotective role. *Ann N Y Acad Sci.* 1997, 825: 334-47.

Margoshes M. and Valleee B.L. A cadmium binding protein from equine kidney cortex. *J. Am. Che. Soc*. 1957, 79: 1813-14

Martelli A., Rousselet E., Dycke C., Bouron A. and Moulis J.M.. Cadmium toxicity in animal cells by interference with essential metals.*Biochimie*. 2006, 88: 1807-1814.

Mazzotti F., Sabbioni E., Ghiani M., Cocco B., Ceccatelli R. and Fortaner S. In vitro assessment of cytotoxicity and carcinogenic potential of chemicals: evaluation of cytotoxicity induced by 58 metal compounds in Balb/3T3 cell line. *ATLA*. 2001, 29: 601-611.

Minoia C., Mazzuccotelli A., Cavalleri A. And Minganti V. Electrothermal atomisation atomic-absortion spectrophotometric determination of chromium(VI) in urine by solvent extration separation with liquid anion exchangers. *Analyst*. 1983, 108: 481-484.

Minoia C., Pietra R., Sabbioni E., Ronchi A., Gatti A., Cavalleri A. and Manzo L. Trace element reference values in tissues from inhabitants of the European Community. III The control of preanalytical factors in the biomonitoring of trace elements in biological fluids. *Sci. Tot. Environ*. 1992, 120: 63-79.

Monnet-Tschudi F., Zurich M.G., Honegger P. Aggregate cell cultures for neurotoxicity testing: the importance of cell-cell interactions. *Dev Animal Vet Sciences*.1997, 27: 641–649.

Mosmann T. Rapid colorimetric assay for cellular growth and survival: Application to proliferation and cytotoxicity assays. *J.immunol.Methods*. 1983, 65: 55-63

Müller T., Schuckelt R. and Jaenicke L. Evidence for radical species as intermediates in cadmium/zinc-metallothionein-dependent DNA damage *in vitro.Environ Health Perspect*. 1994, 102: 27-9.

O'Brien T.J., Ceryak S., Patierno S.R. Complexities of chromium carcinogenesis: role of cellular response, repair and recovery mechanisms. *Mutation Research.* 2003, 533: 3-36.

Ochi T., Otsuka F., Takahashi K., Ohsawa M. Glutathione and metallothioneins as cellular defense against cadmium toxicity in cultured Chinese hamster cells. *Chem Biol Interact.* 1988, 65: 1-14.

Olanow C.W. Manganese-induced parkinsonism and Parkinson's disease. *Ann N Y Acad Sci.* 2004, 1012: 209-223.

Pietra R., Sabbioni E., Gallorini M., Orvini M. Enviromental, toxicological and biomedical research on trace metals: radiochemical separation for neutron activation analysis. *Journal of Radioanalytical and nuclear Chemistry*. 1986, 102: 69-98.

Plummer J.L., Smith B.R., Sies H. and Bend, J.R. Chemical depletion of glutathione *in vivo*. *Methods Enzymol*. 1981, 77: 50–59.

Ponti J., Munaro B., Fischbach M., Hoffmann S. and Sabbioni E. An opyimised analysis for the Balb/3T3 cell transformation assay and its application to metal compounds. *Int. J. Immunopathol Pharm.* 2007, 20: 673-684.

Pourahmad J, O'Brien PJ. A comparison of hepatocyte cytotoxic mechanisms for Cu^{2+} and Cd^{2+}. *Toxicology*. 2000, 143: 263-273.

Pourahmad J., O'Brien P.J., Jokar F., Daraei B. Carcinogenic metal induced sites of reactive oxygen species formation in hepatocytes. *Toxicol In Vitro.* 2003, 17: 803-10.

Ravindra K., Bencs L. and Van Grieken R. Platinum group elements in the environment and their health risk. *Sci. Total Environ.* 2004, 318: 1-43.
Reed D.J. Glatathione: toxicological implications. *Ann. Rev. Pharmacol. Toxicol.* 1990, 30: 603-631.

Roth J.A., Walowitz J. and Browne R.W. Manganese-inducedrat pheochromocitoma (PC12) cell death is independent of caspase activation. *J Neurosci Res.* 2000, 61: 162-171.

Roth J.A., Horbinski C., Higgins D., Lein P. and Garrick M.D. Mechanisms of manganese-induced rat pheochromocytoma (PC12) cell death and cell differentiation. *Neurotoxicology*. 2002, 23: 147-145.

Sabbioni E. and Marafante E. Accumulation of cadmium in rat liver cadmium binding protein following single and repeated cadmium administration. *Environ Physiol. Biochem.* 1975, 5: 465:473.

Sabbioni E. and Marafante E. Identification of lead-binding components in rat liver: in vivo study. *Chem. Biol. Interactions*. 1976, 15: 1-20.

Sabbioni E. Neutron Activation Analysis: general principles and application to the analysis of biological fluids, Ispra-Course Analytical Techniques for Heavy Metals in Biological Fluids, Ispra, November 27-December 1, 1978.

Sabbioni E., Edel J., Goetz L. And Pietra R. Enviromental and biochemical trace-metal speciation studies by radiotracers and neutron activation analysis. *Biol. Trace Element Res.* 1987, 12: 199-209.

Sabbioni E., Bonardi M., Tanet G., Da Kang L., Gallorini M., Weckermann B. and Castiglioni M. Metallobiochemistry of current environmental levels of trace metals: a new method of cyclotron production o f ^{48}V for toxicological studies. *Journal of Radioanalytical and Nuclear Chemistry*. 1989, 134:199-208

Sabbioni E., Pozzi G., Pintar A., Casella L.and Garattini S. Cellular retention, cytoxicity and morphological transformation by vanadium(IV) and vanadium(V) in BALB/3T3 cell lines. *Carcinogenesis*. 1991, 12: 47-52.

Sabbioni E., Pozzi G., Devos S., Pintar A., Casella L. and Fishbach M. The intensità of vanadium(V)-indiced cytotoxicity and morphological transformation in Balb/3T3 cells is dependent on glutathione-mediated bioreduction to V(IV). *Carcinogenesis*. 1993, 14(12): 2565-2568.

Sabbioni E. and Balls M. Use of cell culture and nuclear and radioanalitical techniques for environmental, occupational and biomedical toxicology research at the JRC-Ispra. In the World Congress on Alternatives and Animal Use in Life Sciences; education research testing (Goldberg A.M. Fanzutphen L.F. ed.), 101-108. *Alternative methods in toxicology and the Life Sciences*. 1995: 11 Mary Ann Libert Inc. Publishers, NY.

Sabbioni E., Balls M., Pietra R. and Fortaner S.. The IMETOX project (In Vitro Metal TOXicology). *ATLA*. 1999, 27: 107.

Saffiotti U., Bertolero F., Bignami M., Cortesi F., Ficarella C. & Kaighn M.E. Studies on chemically induced neoplastic transformation and mutation in the Balb/3T3 Cl A31-1-1 cell line in relation to the quantitative evaluation of carcinogens. *Toxicology and Pathology*. 1984, 12: 383-390.

Saffiotti U., Bertolero F. Neoplastic transformation of BALB/3T3 cells by metals and the quest for induction of a metastatic phenotype. *Biol Trace Elem Res*. 1989, 21: 475-82.

Shukla G.S., Hussain T., Chandra S.V. Possible role of regional superoxide dismutase activity and lipid peroxide levels in cadmium neurotoxicity: in vivo and in vitro studies in growing rats. *Life Sci*. 1987; 41: 2215-2221.

Smith M.T., Thor H., Hartizell P. and Orrenius S. The measurement of lipid peroxidation in isolated hepatocytes. *Biochem :Pharmacol*. 1982, 31: 19:26.

Spear N. and Aust S. Effects of glutathione on Fenton reagent-dependent radical production and DNA oxidation. *Arch Biochem Biophys.* 1995, 324: 111-116.

Stredrick D.L., Stokes A.H., Worst T.J., Freeman W.M., Johnson E.A., Lash L.H., Aschner M., Vrana K.E. Manganese-induced cytotoxicity in dopamine-producing cells. *Neurotoxicology*. 2004, 25:543-53.

Styblo M., Drobna Z., Jaspers I., Lin S. and Thomas D.J. The role of biomethylation in toxicity and carcinogenicity of arsenic: a research update. *Environ. Health Perspect.* 2002, 110: 767-771.

Suzuki K.T. Metabolomics of arsenic based on speciation studies. *Analytical Chimica Acta*. 2005, 540: 71-76.

Szpunar J. Metallomics: a new frontier in analytical chemistry. *Anal Bioanal Chem*. 2004, 378: 54-56.

Tam K.H., Charbonneau S.M., Bryce F., Lacroix G. Separation of arsenic metabolites in dog plasma and urine following intravenous injection of 74As. *Anal Biochem*. 1978, 1;86(2):505-11.

Templeton D.M., Ariese F., Cornelis R., Muntau H., Van Leeuwen H.P. and Lobinski R. Guidelines for terms related to chemical speciation and fractionation of elements. Definitions, structural aspects, and methodological aspects. *Pure Appl. Chem.* 2000, 72: 1453-1470.

Teng K.K., Angelastro J.M., Cunningham M.E., Farinelli S.E. and Greene L.A. Cultured PC12 cells: a model for neuronal function, differentiation and survival. *Cell Biology: A Laborotory Handbook (2nd Ed.)*. 1998, 1: 244-250.

Valko M., Morris H., Cronin M.T.D. Metals, Toxicity and Oxidative Stress. *Current Med Chem.* 2005, 12: 1161-1208.

Vescovi A., Facheris L., Faffaroni A., Malanca G. and Parati E.A. Dopamine metabolism alteration in a manganese-treated pheochromocytoma cell line (PC12). *Toxicology*. 1991, 67: 129-142.

Zurich M.G., Honegger P., Schilter B., Costa L.G., Monnet-Tschudi F. Involvement of glial cells in the neurotoxicity of parathion and chlorpyrifos. *Toxicol Appl Pharmacol*. 2004, 201: 97–100.

Yuan C., Kadiiska M., Achanzar W.E., Mason R.P. and Waalkes M.P. Possible role of caspase-3 inhibition in cadmium-induced blockage of apoptosis.*Toxicol Appl Pharmacol*. 2000, 164: 321-9.

Waalkes M.P. and Poirier L.A. In vitro cadmium-DNA interactions: cooperativity of cadmium binding and competitive antagonism by calcium. *Toxicol. Appl. Pharmacol*. 1984. 75: 539-546.

Waalkes M.P. Metal carcinogenesis, in Sarkar B. Handbook of Heavy Metals in the Environment, Marcel Dekker, New York, 2002, 121-146.

Waalkes M.P. Cadmium carcinogenesis. *Mutat Res*. 2003, 533: 107-120.

Waisberg M., Joseph P., Hale B., Beyersmann D. Molecular and cellular mechanisms of cadmium carcinogenesis. *Toxicology*. 2003, 192: 95-117.

WHO. Environmental Health Criteria 224, Arsenic and arsenic compounds, WHO Geneve. 2001.

WHO. Environmental Health Criteria, Vanadium pentoxide and other inorganic vanadium compounds, WHO, Concise International Chemical Assessment 29, Geneve. 2001.

Wood G.C. and Cooper P.F. The application of gel filtration to the study of protein-binding of small molecules. *Chromatog. Rev*. 1970, 12: 88-107.